ISSN: 2667-419X

ESKİŞEHİR TECHNICAL UNIVERSITY JOURNAL OF SCIENCE AND TECHNOLOGY
B– Theoretical Sciences

ESKİŞEHİR TEKNİK ÜNİVERSİTESİ BİLİM VE TEKNOLOJİ DERGİSİ
B– Teorik Bilimler

Volume/Cilt 13 Number/Sayı 1 – February / Şubat 2025

ESKİŞEHİR TEKNİK ÜNİVERSİTESİ BİLİM VE TEKNOLOJİ DERGİSİ
B- TEORİK BİLİMLER

Eskişehir Technical University Journal of Science and Technology B- Theoretical Sciences

Volume: 13 / Number: 1 – February / 2025

Eskişehir Technical University Journal of Science and Technology B - Theoretical Sciences (formerly Anadolu University Journal of Science and Technology B – Theoretical Sciences) is an **peer-reviewed** and **refereed international journal** by Eskişehir Technical University. Since 2010, it has been regularly published and distributed biannually and it has been published biannually and **electronically only since 2016**.

Manuscripts submitted for publication are analyzed in terms of scientific quality, ethics and research methods in terms of its compliance by the Editorial Board representatives of the relevant areas. Then, the abstracts of the appropriate articles are sent to two different referees with a well-known in scientific area. If the referees agree to review the article, full text in the framework of the privacy protocol is sent. In accordance with the decisions of referees, either directly or corrected article is published or rejected. Confidential reports of the referees in the journal archive will be retained for ten years. All post evaluation process is done electronically on the internet. Detailed instructions to authors are available in each issue of the journal.

"Anadolu Üniversitesi Bilim ve Teknoloji Dergisi B- Teorik Bilimler (Anadolu University Journal of Science and Technology B - Theoretical Sciences)" published within Anadolu University started to be published within Eskişehir Technical University which was established due to statute law 7141, in 2018. Hence, the name of the journal is changed to "Eskişehir Teknik Üniversitesi Bilim ve Teknoloji Dergisi B- Teorik Bilimler (Eskişehir Technical University Journal of Science and Technology B - Theoretical Sciences)".

The Journal's Other Variant Title: **Estusicence-Theory;** aproved by ISSN National Centre for Türkiye on April 30, 2024.

Indexed by **ULAKBIM Tr Dizin**

ISSN: 2667-419X

ESKİŞEHİR TEKNİK ÜNİVERSİTESİ BİLİM VE TEKNOLOJİ DERGİSİ
B- TEORİK BİLİMLER

Eskişehir Technical University Journal of Science and Technology B- Theoretical Sciences

Volume: 13 / Number: 1 – February / 2025

CONTACT / İLETİŞİM

Eskişehir Technical University, Graduate School of Sciences
26555 Eskişehir, TURKEY
Phone: +90-222-213 7485
e-mail : btdb@eskisehir.edu.tr

ESKİŞEHİR TEKNİK ÜNİVERSİTESİ BİLİM VE TEKNOLOJİ DERGİSİ
B- TEORİK BİLİMLER
Eskişehir Technical University Journal of Science and Technology B- Theoretical Sciences

Volume/Cilt: 13 / Number/Sayı: 1 – February / Şubat 2025

ESKİŞEHİR TEKNİK ÜNİVERSİTESİ BİLİM VE TEKNOLOJİ DERGİSİ
B- TEORİK BİLİMLER

Eskişehir Technical University Journal of Science and Technology B- Theoretical Sciences

Volume/Cilt: 13 / Number/Sayı: 1 – February / Şubat 2025

ABOUT

Eskişehir Technical University Journal of Science and Technology B- Theoretical Sciences (formerly Anadolu University Journal of Science and Technology B- Theoretical Sciences) is an peer-reviewed and refereed international journal by Eskişehir Technical University. Since 2010, it has been regularly published and distributed biannually and it has been published biannually and electronically only since 2016.

- **The journal accepts TURKISH and ENGLISH manuscripts.**
- **The journal is indexed by ULAKBIM TR DIZIN.**

AIM AND SCOPE

The journal publishes research papers, reviews and technical notes in the fields of theoretical sciences such as Physics, Biology, Mathematics, Statistics, Chemistry and Chemical Engineering, Environmental Sciences and Engineering, Civil Engineering, Electrical and Electronical Engineering, Computer Science and Informatics, Materials Science and Engineering, Mechanical Engineering, Mining Engineering, Industrial Engineering, Aeronautics and Astronautics, Health Sciences, Pharmaceutical Sciences, and so on.

PEER REVIEW PROCESS

Manuscripts are first reviewed by the editorial board in terms of its its journal's style rules scientific content, ethics and methodological approach. If found appropriate, the manuscript is then send to at least two referees by editor. The decision in line with the referees may be an acceptance, a rejection or an invitation to revise and resubmit. Confidential review reports from the referees will be kept in archive. All submission process manage through the online submission systems.

OPEN ACCESS POLICY

This journal provides immediate open access to its content on the principle that making research freely available to the public supports a greater global exchange of knowledge.

The journal doesn't have Article Processing Charge (APC) or any submission charges.

PRICE POLICY

Eskişehir Technical University Journal of Science and Technology B - Theoretical Sciences, peer-reviewed, scientific, free of charge open-access-based journal. The author is not required to pay any publication fees or article processing charges (APCs) for peer-review administration

and management, typesetting, and open-access. Articles also receive Digital Object Identifiers (DOIs) from the CrossRef organization to ensure they are always available.

ETHICAL RULES
You can reach the Ethical Rules in our journal in full detail from the link below:
https://dergipark.org.tr/en/pub/estubtdb/policy

Ethical Principles and Publication Policy

Policy & Ethics
Assessment and Publication

As a peer-reviewed journal, it is our goal to advance scientific knowledge and understanding. We adhere to the guideline and ethical standards from the Committee on Publication Ethics (COPE) and the recommendations of ICMJE (International Committee of Medical Journal Editors) regarding all aspects of publication ethics and cases of research and publication misconduct to ensure that all publications represent accurate and original work and that our peer review process is structured without bias. We have outlined a set of ethical principles that must be followed by all authors, reviewers, and editors.

All manuscripts submitted to our journals are pre-evaluated in terms of their relevance to the scope of the journal, language, compliance with writing instructions, suitability for science, and originality, by taking into account the current legal requirements regarding copyright infringement and plagiarism. Manuscripts that are evaluated as insufficient or non-compliant with the instructions for authors may be rejected without peer review.

Editors and referees who are expert researchers in their fields assess scientific manuscripts submitted to our journals. A blind peer review policy is applied to the evaluation process. The Editor-in-Chief, if he/she sees necessary, may assign an Editor for the manuscript or may conduct the scientific assessment of the manuscript himself/herself. Editors may also assign referees for the scientific assessment of the manuscript and make their decisions based on reports by the referees. The Editor-in-Chief makes the final decision regarding the publishing of the manuscript.

Editors and referees who are expert researchers in their fields assess scientific manuscripts submitted to our journals. A blind peer review policy is applied to the evaluation process. The Editor-in-Chief, if he/she sees necessary, may assign an Editor for the manuscript or may conduct the scientific assessment of the manuscript himself/herself. Editors may also assign referees for the scientific assessment of the manuscript and make their decisions based on reports by the referees. Articles are accepted for publication on the understanding that they have not been published and are not going to be considered for publication elsewhere. Authors should certify that neither the manuscript nor its main contents have already been published or submitted for publication in another journal.

The Journal; Implements the Publication Policy and Ethics guidelines to meet high-quality ethical standards for authors, editors and reviewers:

Duties of Editors-in-Chief and co-Editors

The crucial role of the journal Editor-in-Chief and co-Editors is to monitor and ensure the fairness, timeliness, thoroughness, and civility of the peer-review editorial process. The main responsibilities of Editors-in-Chief are as follows:

• Selecting manuscripts suitable for publication while rejecting unsuitable manuscripts,
• Ensuring a supply of high-quality manuscripts to the journal by identifying important,
• Increasing the journal's impact factor and maintaining the publishing schedule,
• Providing strategic input for the journal's development,

Duties of Editors

The main responsibilities of editors are as follows:

• An editor must evaluate the manuscript objectively for publication, judging each on its quality without considering the nationality, ethnicity, political beliefs, race, religion, gender, seniority, or institutional affiliation of the author(s). Editors should decline any assignment when there is a potential for conflict of interest.
• Editors must ensure the document(s) sent to the reviewers does not contain information of the author(s) and vice versa.
• Editors' decisions should be provided to the author(s) accompanied by the reviewers' comments and recommendations unless they contain offensive or libelous remarks.
• Editors should respect requests (if well reasoned and practicable) from author(s) that an individual should not review the submission.
• Editors and all staff members should guarantee the confidentiality of the submitted manuscript.
• Editors should have no conflict of interest with respect to articles they reject/accept. They must not have a conflict of interest with the author(s), funder(s), or reviewer(s) of the manuscript.
• Editors should strive to meet the needs of readers and authors and to constantly improve the journal.

Duties of Reviewers/Referees

The main responsibilities of reviewers/referees are as follows:

• Reviewers should keep all information regarding papers confidential and treat them as privileged information.
• Reviews should be conducted objectively, with no personal criticism of the author.
• Reviewers assist in the editorial decision process and as such should express their views clearly with supporting arguments.
• Reviewers should complete their reviews within a specified timeframe (maximum thirty-five (35) days). In the event that a reviewer feels it is not possible for him/her to complete the review of the manuscript within a stipulated time, then this information must be communicated to the editor so that the manuscript could be sent to another reviewer.
• Unpublished materials disclosed in a submitted manuscript must not be used in a reviewer's personal research without the written permission of the author. Information contained in an unpublished manuscript will remain confidential and must not be used by the reviewer for personal gain.

• Reviewers should not review manuscripts in which they have conflicts of interest resulting from competitive, collaborative, or other relationships or connections with any of the authors, companies, or institutions connected to the papers.
• Reviewers should identify similar work in published manuscripts that has not been cited by the author. Reviewers should also notify the Editors of significant similarities and/or overlaps between the manuscript and any other published or unpublished material.

Duties of Authors
The main responsibilities of authors are as follows:

• The author(s) should affirm that the material has not been previously published and that they have not transferred elsewhere any rights to the article.
• The author(s) should ensure the originality of the work and that they have properly cited others' work in accordance with the reference format.
• The author(s) should not engage in plagiarism or in self-plagiarism.
• On clinical and experimental humans and animals, which require an ethical committee decision for research in all branches of science;
All kinds of research carried out with qualitative or quantitative approaches that require data collection from the participants by using survey, interview, focus group work, observation, experiment, interview techniques,
Use of humans and animals (including material/data) for experimental or other scientific purposes,
• Clinical studies on humans,
• Studies on animals,
• Retrospective studies in accordance with the law on the protection of personal data, (Ethics committee approval should have been obtained for each individual application, and this approval should be stated and documented in the article.)
Information about the permission (board name, date, and number) should be included in the "Method" section of the article and also on the first/last page.
During manuscript upload, the "Ethics Committee Approval" file should be uploaded to the system in addition to the manuscript file.
In addition, in case reports, it is necessary to include information on the signing of the informed consent/ informed consent form in the manuscript.
• The author(s) should suggest no personal information that might make the identity of the patient recognizable in any form of description, photograph, or pedigree. When photographs of the patient were essential and indispensable as scientific information, the author(s) have received consent in written form and have clearly stated as much.
• The author(s) should provide the editor with the data and details of the work if there are suspicions of data falsification or fabrication. Fraudulent data shall not be tolerated. Any manuscript with suspected fabricated or falsified data will not be accepted. A retraction will be made for any publication which is found to have included fabricated or falsified data.
• The author(s) should clarify everything that may cause a conflict of interests such as work, research expenses, consultant expenses, and intellectual property.
• The author(s) must follow the submission guidelines of the journal.
• The author(s) discover(s) a significant error and/or inaccuracy in the submitted manuscript at any time, then the error and/or inaccuracy must be reported to the editor.
• The author(s) should disclose in their manuscript any financial or other substantive conflicts of interest that might be construed to influence the results or interpretation of their manuscript. All sources of financial support should be disclosed under the heading of "Acknowledgment" or "Contribution".

• The corresponding author should ensure that all appropriate co-authors and no inappropriate co-authors are included in the paper and that all co-authors have seen and approved the final version of the paper and have agreed to its submission for publication. All those who have made significant contributions should be listed as co-authors. Others who have participated in certain substantive aspects of the research should be acknowledged or listed under the heading of "Author Contributions".
• The corresponding author(s) must ensure that all appropriate co-authors are not included in the manuscript, that author names are not added or removed and that the authors' address information is not changed after the review begins and that all co-authors see and approve the final version of the manuscript at every stage of the manuscript. All significant contributors should be listed as co-authors. Other individuals who have participated in significant aspects of the research work should be considered contributors and listed under "Author Contribution".

Cancellations/Returns

Articles/manuscripts may be returned to the authors in order to increase the authenticity and/or reliability and to prevent ethical breaches, and even if articles have been accepted and/or published, they can be withdrawn from publication if necessary. The Editor-in-Chief of the journal has the right to return or withdraw an article/manuscript in the following situations:

• When the manuscript is not within the scope of the journal,
• When the scientific quality and/or content of the manuscript do not meet the standards of the journal and a referee review is not necessary,
• When there is proof of ruling out the findings obtained by the research, (When the article/manuscript is undergoing an assessment or publication process by another journal, congress, conference, etc.,)
• When the article/manuscript was not prepared in compliance with scientific publication ethics,
• When any other plagiarism is detected in the article/manuscript,
• When the authors do not perform the requested corrections within the requested time (maximum twenty-one (21) days),
• When the author does not submit the requested documents/materials/data etc. within the requested time,
• When the requested documents/materials/data etc. submitted by the author are missing for the second time,
• When the study includes outdated data,
• When the authors make changes that are not approved by the editor after the manuscript was submitted,
• When an author is added/removed, the order of the authors is changed, the corresponding author is altered, or the addresses of the authors are changed in the article that is in the evaluation process,
• When a statement is not submitted indicating that approval of the ethics committee permission was obtained for the following (including retrospective studies):
• When human rights or animal rights are violated,

ETHICAL ISSUES

Plagiarism

The use of someone else's ideas or words without a proper citation is considered plagiarism and will not be tolerated. Even if a citation is given, if quotation marks are not placed around words taken directly from other authors' work, the author is still guilty of plagiarism. Reuse of the author's own previously published words, with or without a citation, is regarded as self-plagiarism.

All manuscripts received are submitted to iThenticate®, which compares the content of the manuscript with a database of web pages and academic publications. Manuscripts are judged to be plagiarized or self-plagiarized, based on the iThenticate® report or any other source of information, will be rejected. Corrective actions are proposed when plagiarism and/or self-plagiarism is detected after publication. Editors should analyze the article and decide whether a corrected article or retraction needs to be published.
Open-access theses are considered as published works and they are included in the similarity checks.
iThenticate® report should have a maximum of 11% from a single source, and a maximum of 25% in total.

Conflicts of Interest

Eskişehir Technical University Journal of Science and Technology A - Applied Sciences and Engineering should be informed of any significant conflict of interest of editors, authors, or reviewers to determine whether any action would be appropriate (e.g. an author's statement of conflict of interest for a published work, or disqualifying a referee).

Financial

The authors and reviewers of the article should inform the journal about the financial information that will bring financial gain or loss to any organization from the publication of the article.
*Research funds; funds, consulting fees for a staff member; If you have an interest, such as patent interests, you may have a conflict of interest that needs to be declared.

Other areas of interest

The editor or reviewer may disclose a conflict of interest that, if known, would be embarrassing (for example, an academic affiliation or rivalry,a close relationship or dislike, or a person who may be affected by the publication of the article).

Conflict of interest statement

Please note that a conflict of interest statement is required for all submitted manuscripts. If there is no conflict of interest, please state "There are no conflicts of interest to declare" in your manuscript under the heading "Conflicts of Interest" as the last section before your Acknowledgments.

AUTHOR GUIDELINES

All manuscripts must be submitted electronically.
You will be guided stepwise through the creation and uploading of the various files. There are no page charges. Papers are accepted for publication on the understanding that they have not been published and are not going to be considered for publication elsewhere. Authors should certify that neither the manuscript nor its main contents have already been published or submitted for publication in another journal. We ask a signed **Copyright Form** to start the evaluation process. After a manuscript has been submitted, it is not possible for authors to be added or removed or for the order of authors to be changed. If authors do so, their submission will be cancelled.

Manuscripts may be rejected without peer review by the editor-in-chief if they do not comply with the instructions to authors or if they are beyond the scope of the journal. After a manuscript has been accepted for publication, i.e. after referee-recommended revisions are complete, the author will not be permitted to make any changes that constitute departures from the manuscript that was accepted by the editor. Before publication, the galley proofs are always sent to the authors for corrections. Mistakes or omissions that occur due to some negligence on our part during final printing will be rectified in an errata section in a later issue.

This does not include those errors left uncorrected by the author in the galley proof. The use of someone else's ideas or words in their original form or slightly changed without a proper citation is considered plagiarism and will not be tolerated. Even if a citation is given, if quotation marks are not placed around words taken directly from another author's work, the author is still guilty of plagiarism. All manuscripts received are submitted to iThenticateR, a plagiarism checking system, which compares the content of the manuscript with a vast database of web pages and academic publications. Manuscripts judged to be plagiarised or self-plagiarised, based on the iThenticateR report or any other source of information, will not be considered for publication.

Uploading Articles to the Journal

Authors should prepare and upload 2 separate files while uploading articles to the journal. First, the Author names and institution information should be uploaded so that they can be seen, and then (using the additional file options) a separate file should be uploaded with the Author names and institution information completely closed. When uploading their files with closed author names, they will select the "Show to Referee" option, so that the file whose names are closed can be opened to the referees.

Preparation of Manuscript

Style and Format: Manuscripts should be **single column** by giving one-spaced with 2.5-cm margins on all sides of the page, in Times New Roman font (font size 11). Every page of the manuscript, including the title page, references, tables, etc., should be numbered. All copies of the manuscript should also have line numbers starting with 1 on each consecutive page.

Manuscripts must be upload as word document (*.doc, *.docx vb.). Please avoid uploading ***texts in *.pdf format.***

Manuscripts should be written in Turkish or English.

Symbols, Units and Abbreviations: Standard abbreviations and units should be used; SI units are recommended. Abbreviations should be defined at first appearance, and their use in the title and abstract should be avoided. Generic names of chemicals should be used. Genus and species names should be typed in italic or, if this is not available, underlined.

Please refer to equations with capitalisation and unabbreviated (e.g., as given in Equation (1)).

Manuscript Content: Articles should be divided into logically ordered and numbered sections. Principal sections should be numbered consecutively with Arabic numerals (1. Introduction, 2. Formulation of problem, etc.) and subsections should be numbered 1.1., 1.2., etc. Do not number the Acknowledgements or References sections. The text of articles should be, if possible, divided into the following sections: Introduction, Materials and Methods (or Experimental), Results, Discussion, and Conclusion.

Title and contact information

The first page should contain the full title in sentence case (e.g., Hybrid feature selection for text classification), the full names (last names fully capitalised) and affiliations (in English) of all authors (Department, Faculty, University, City, Country, E-mail), and the contact e-mail address for the clearly identified corresponding author.

Abstract
The abstract should provide clear information about the research and the results obtained, and should not exceed 300 words. The abstract should not contain citations and must be written in Times New Roman font with font size 9.

Keywords
Please provide 3 to 5 keywords which can be used for indexing purposes.

Introduction
The motivation or purpose of your research should appear in the "Introduction", where you state the questions you sought to answer, and then provide some of the historical basis for those questions.

Methods
Provide sufficient information to allow someone to repeat your work. A clear description of your experimental design, sampling procedures, and statistical procedures is especially important in papers describing field studies, simulations, or experiments. If you list a product (e.g., animal food, analytical device), supply the name and location of the manufacturer. Give the model number for equipment used.

Results
Results should be stated concisely and without interpretation.

Discussion
Focus on the rigorously supported aspects of your study. Carefully differentiate the results of your study from data obtained from other sources. Interpret your results, relate them to the results of previous research, and discuss the implications of your results or interpretations.

Conclusion
This should state clearly the main conclusions of the research and give a clear explanation of their importance and relevance. Summary illustrations may be included.

Acknowledgments
Acknowledgments of people, grants, funds, etc. should be placed in a separate section before the reference list. The names of funding organizations should be written in full.

Conflict of Interest Statement

The authors are obliged to present the conflict of interest statement at the end of the article after the acknowledgments section.

CRediT Author Statement

Write the authors' contributions in detail using the specified CRediT notifications. Authors may have contributed in more than one role. The corresponding author is responsible for ensuring that descriptions are accurate and accepted by all authors.

CRediT Notifications	Explanation
Conceptualization	Ideas; formulation or evolution of overarching research goals and aims
Methodology	Development or design of methodology; creation of models
Software	Programming, software development; designing computer programs; implementation of the computer code and supporting algorithms; testing of existing code components
Validation	Verification, whether as a part of the activity or separate, of the overall replication/ reproducibility of results/experiments and other research outputs
Formal analysis	Application of statistical, mathematical, computational, or other formal techniques to analyse or synthesize study data
Investigation	Conducting a research and investigation process, specifically performing the experiments, or data/evidence collection
Resources	Provision of study materials, reagents, materials, patients, laboratory samples, animals, instrumentation, computing resources, or other analysis tools
Data Curation	Management activities to annotate (produce metadata), scrub data and maintain research data (including software code, where it is necessary for interpreting the data itself) for initial use and later reuse
Writing – Original Draft	Preparation, creation and/or presentation of the published work, specifically writing the initial draft (including substantive translation)
Writing – Review & Editing	Preparation, creation and/or presentation of the published work by those from the original research group, specifically critical review, commentary, or revision – including pre-or post-publication stages
Visualization	Preparation, creation and/or presentation of the published work, specifically visualization/ data presentation
Supervision	Oversight and leadership responsibility for the research activity planning and execution, including mentorship external to the core team
Project administration	Management and coordination responsibility for the research activity planning and execution
Funding acquisition	Acquisition of the financial support for the project leading to this publication

References

AMA Style should be used in the reference writing of our journal. If necessary, at this point, the reference writings of the articles published in our article can be examined.

Citations in the text should be identified by numbers in square brackets. The list of references at the end of the paper should be given in order of their first appearance in the text or in alphabetical order according to the surname of the fist author. All authors should be included in reference lists unless there are 10 or more, in which case only the first 10 should be given, followed by 'et al.'. Do not use individual sets of square brackets for citation numbers that appear together, e.g., [2, 3, 5–9], not [2], [3], [5]–[9]. Do not include personal communications, unpublished data, websites, or other unpublished materials as references, although such material may be inserted (in parentheses) in the text. In the case of publications in languages other than English, the published English title should be provided if one exists, with an annotation such as "(article in Turkish with an abstract in English)". If the publication was not published with an English title, cite the original title only; do not provide a self-translation. References should be formatted as follows (please note the punctuation and capitalisation):

Journal articles

Journal titles should be abbreviated according to ISI Web of Science abbreviations.

Guyon I. and Elisseeff A. An introduction to variable and feature selection. J Mach Learn Res, 2003; 3: 1157-1182.

Izadpanahi S, Ozcınar C, Anbarjafari G and Demirel H. Resolution enhancement of video sequences by using discrete wavelet transform and illumination compensation. Turk J Elec Eng & Comp Sci., 2012; 20: 1268-1276.

Books

Haupt RL. and Haupt S.E. Practical Genetic Algorithms. 2nd ed. New York, NY, USA: Wiley, 2004.

Kennedy J and Eberhart R. Swarm Intelligence. San Diego, CA, USA: Academic Press, 2001.

Chapters in boks

Poore JH, Lin L, Eschbach R and Bauer T. Automated statistical testing for embedded systems. In: Zander J, Schieferdecker I, Mosterman PJ, editors. Model-Based Testing for Embedded Systems. Boca Raton, FL, USA: CRC Press, 2012. pp. 111-146.

Conference proceedings

Li RTH and Chung SH. Digital boundary controller for single-phase grid-connected CSI. In: IEEE 2008 Power Electronics Specialists Conference; 15–19 June 2008; Rhodes, Greece. New York, NY, USA: IEEE. pp. 4562-4568.

Theses

Boynukalın Z. Emotion analysis of Turkish texts by using machine learning methods. MSc, Middle East Technical University, Ankara, Turkey, 2012.

Tables and Figures

All illustrations (photographs, drawings, graphs, etc.), not including tables, must be labelled "Figure." Figures must be submitted in the manuscript.

All tables and figures must have a caption and/or legend and be numbered (e.g., Table 1, Figure 2), unless there is only one table or figure, in which case it should be labelled “Table” or “Figure” with no numbering. Captions must be written in sentence case (e.g., Macroscopic appearance of the samples.). The font used in the figures should be Times New Roman with 9 pt. If symbols such as ×, μ, η, or ν are used, they should be added using the Symbols menu of Word.

All tables and figures must be numbered consecutively as they are referred to in the text. Please refer to tables and figures with capitalisation and unabbreviated (e.g., “As shown in Figure 2…”, and not “Fig. 2” or “figure 2”).

The resolution of images should not be less than 118 pixels/cm when width is set to 16 cm. Images must be scanned at 1200 dpi resolution and submitted in jpeg or tiff format. Graphs and diagrams must be drawn with a line weight between 0.5 and 1 point. Graphs and diagrams with a line weight of less than 0.5 point or more than 1 point are not accepted. Scanned or photocopied graphs and diagrams are not accepted.

Figures that are charts, diagrams, or drawings must be submitted in a modifiable format, i.e. our graphics personnel should be able to modify them. Therefore, if the program with which the figure is drawn has a “save as” option, it must be saved as *.ai or *.pdf. If the “save as” option does not include these extensions, the figure must be copied and pasted into a blank Microsoft Word document as an editable object. It must not be pasted as an image file (tiff, jpeg, or eps) unless it is a photograph.

Tables and figures, including caption, title, column heads, and footnotes, must not exceed 16 × 20 cm and should be no smaller than 8 cm in width. For all tables, please use Word’s “Create Table” feature, with no tabbed text or tables created with spaces and drawn lines. Please do not duplicate information that is already presented in the figures.

Article Corrections and Uploading to the System

Authors should upload the desired edits for their articles without destroying or changing the Template file of the article, by selecting and specifying the relevant edits as Colored, and also submit the Clean version of the article in 2 separate files (using the Additional file option if necessary). * In case of submitting a corrected article, a separate File in Reply to the Referees must be prepared and the "Reply to the Referees" option in the Add additional file option should be checked and uploaded. If a separate file is not prepared in response to the referees, the Author will definitely be asked to upload the relevant file again and the evaluation will be in the pending phase.

ESKİŞEHİR TECHNICAL UNIVERSITY JOURNAL OF SCIENCE AND TECHNOLOGY
B - Theoretical Sciences

ESKİŞEHİR TEKNİK ÜNİVERSİTESİ BİLİM VE TEKNOLOJİ DERGİSİ
B – Teorik Bilimler

Volume/Cilt**: 13 / Number/**Sayı**: 1 – February /** Şubat **2025**

CONTENTS / İÇİNDEKİLER

Sayfa / Page

ARAŞTIRMA MAKALESİ / RESEARCH ARTICLE

ESKİŞEHİR TEKNİK ÜNİVERSİTESİ BİLİM VE TEKNOLOJİ DERGİSİ
B- TEORİK BİLİMLER

Eskişehir Technical University Journal of Science and Technology B- Theoretical Sciences

Estuscience – Theory, 2025, 13 [1] pp. 1-6 , DOI:10.20290/estubtdb.1487804

RESEARCH ARTICLE

A COUNTEREXAMPLE TO ELAYDI'S CONJECTURE

İsmail Alper GÜVEY [1,*]

[1] Department of Mathematics, Faculty of Science and Letters, Aksaray University, Aksaray, Türkiye
ismailalper.guvey@aksaray.edu.tr - 0009-0008-6165-643X

Abstract

In this work, we define a chaotic map that contradicts Elaydi's conjecture. Firstly, we present some important concepts used in this paper and define a continuous map f on $[0,2]$, which is connected according to the usual topology on $\mathbb{R}$. Moreover, we show that f is chaotic on $[0,2]$ by using topological conjugacy with the 'tent map'. Finally, we conclude that $f^2 = f \circ f$ is not chaotic on $[0,2]$. In addition, this example also shows that topological transitivity does not imply total transitivity.

Keywords

Chaos,
Topologically Transitive,
Totally Transitive,
Topological Conjugacy

Time Scale of Article

Received :21 May 2024
Accepted : 07 December 2024
Online date : 28 February 2025

1. INTRODUCTION

Chaotic dynamical systems are often used in image encryption, cryptology, fractal geometry, etc. [1-3]. Devaney presented the definition of a chaotic map, which is widely used in mathematics [4]. The definition of a chaotic map consists of three conditions: topological transitivity, the density of the set of periodic points, and sensitive dependence on initial conditions. Topological transitivity indicates that the system exhibits complex behavior, while the density of the set of periodic points suggests that the system exhibits regular behavior. Additionally, sensitive dependence on initial conditions indicates that the system is unpredictable.

Many researchers examined the relations between chaos conditions [5-8]. Banks and his colleagues showed that topological transitivity and the density of the set of periodic points imply sensitive dependence on initial conditions in a non-finite metric space with a continuous map [5]. Vellekoop and Berglund showed that topological transitivity is sufficient for chaos on intervals [6]. Değirmenci and Koçak investigated the relationship between topological transitivity and dense orbit [7]. Chaos conditions were adapted to product spaces by Değirmenci and Koçak [8]. The question may arise whether, for a metric space X and a chaotic map $f: X \to X$, the map f^m, which is the composition of f with itself m times for all $m \in \mathbb{Z}^+$, is also chaotic. In [9] (p. 143), Elaydi put forward the following claim: "Let $f: X \to X$ be a continuous map on a metric space X (an interval I) which is chaotic. Show that if X is connected, then f^m is chaotic for all $m \in \mathbb{Z}^+$."

The aim of this paper is to define a chaotic map that contradicts Elaydi's conjecture. Firstly, we present some important concepts used in this paper and define a continuous map f on $[0,2]$, which is connected

*Corresponding Author: ismailalper.guvey@aksaray.edu.tr

according to the usual topology on $\mathbb{R}$. Moreover, we show that f is chaotic on $[0,2]$ by using topological conjugacy with the 'tent map'. Finally, we conclude that $f^2 = f \circ f$ is not chaotic on $[0,2]$. In addition, this example also shows that topological transitivity does not imply total transitivity.

2. PRELIMINARIES

Let X be a topological space and $f: X \to X$, then (X, f) is called *discrete dynamical system* [4]. For any $a \in X$, the set $Orb_f(a) = \{a, f(a), f^2(a), f^3(a), \dots, f^m(a), \dots\}$ is called *orbit* of a under f [4]. A point $p \in X$ is called a *periodic point* of f if there is a positive integer m such that $f^m(p) = p$ [4]. The smallest such m is called *prime period* of p [4]. The set $Per(f) = \{p \in X : f^m(p) = p,\ m \in \mathbb{Z}^+\}$ is called the *set of periodic points of* f [4].

Definition 2.1. ([4]) Let (X, f) be a discrete dynamical system. f is called *topologically transitive* if for every non-empty open subsets $U, V \subset X$, there exists a $m \in \mathbb{Z}^+$ such that $f^m(U) \cap V \neq \emptyset$.

Definition 2.2. ([10]) Let (X, f) be a discrete dynamical system. f is called *totally transitive* if $f^m: X \to X$ is topologically transitive for all $m \in \mathbb{Z}^+$.

From the definition of total transitivity, it is easy to see that every totally transitive map is topologically transitive. However, as we will see, the reverse is not always true.

Definition 2.3. ([4]) Let (X, f) be a discrete dynamical system where X is a metric space. f is called s*ensitive dependent on initial conditions* if for $r > 0$ following hold, for all $x \in X$ and for every open neighborhood U of x, there exists a $m \in \mathbb{Z}^+$ and $y \in U$ such that, $d\left(f^m(x), f^m(y)\right) \geq r$.

Definition 2.4. ([4]**)** Let (X, f) be a discrete dynamical system, where X is a metric space. The map f is called *chaotic* (sense of Devaney) if f is topologically transitive, $Per(f)$ is dense in X, and f is sensitive dependent on initial conditions.

Theorem 2.5. ([5]**)** Let (X, f) be a discrete dynamical system, where X is a non-finite metric space and f is continuous. If f is topologically transitive and $Per(f)$ is dense in X, then f is sensitive dependent on initial conditions, i.e., f is a chaotic map.

Theorem 2.6. ([6]**)** Let (I, f) be a discrete dynamical system, where $I \subset \mathbb{R}$ is an interval and f is continuous. If f is topologically transitive, then $Per(f)$ is dense in I, i.e., f is a chaotic map.

The notion of topological conjugacy is used for the equivalence of the dynamics of the maps.

Definition 2.7. ([4]) Let (X, f) and (Y, g) be two discrete dynamical systems. If a homeomorphism $h: X \to Y$ exists such that $h \circ f = g \circ h$, then f and g are said to be *topologically conjugate* maps, and (X, f) and (Y, g) are said to be *topologically equivalent dynamical systems.*

Theorem 2.8. ([4,10]) Let (X, f) and (Y, g) be topologically equivalent dynamical systems, where X, Y are non-finite metric spaces and f, g are continuous maps. Then,
(i) $Per(f)$ is dense in X iff $Per(g)$ is dense in Y.
(ii) f is topologically transitive iff g is topologically transitive.
(iii) f is totally transitive iff g is totally transitive.
(iv) f is chaotic on X iff g is chaotic on Y.

3. COUNTEREXAMPLE

We define $f: [0,2] \to [0,2]$ by

$$f(x) = \begin{cases} 2x + 1, & 0 \leq x \leq \frac{1}{2} \\ -2x + 3, & \frac{1}{2} \leq x \leq \frac{3}{2} \\ 2x - 3, & \frac{3}{2} \leq x \leq 2. \end{cases} \quad (1)$$

To show f is a chaotic map, it is sufficient to show that f is topologically transitive by Theorem 2.6, because f is defined on an interval and f is continuous. Graphs of f and f^2 are shown in Figure 1.

(a) **(b)**

Figure 1. (a) Graph of f; (b) Graph of f^2.

We use the famous 'tent map' and a map which is topologically conjugate to it to achieve our aim. The tent map is defined by $T: [0,1] \to [0,1]$,

$$T(x) = \begin{cases} 2x & , \ 0 \leq x \leq \frac{1}{2} \\ 2 - 2x \, , & \frac{1}{2} \leq x \leq 1. \end{cases} \quad (2)$$

T is a well-known chaotic map in the theory of chaotic dynamical systems [4,10]. In addition, T is a totally transitive map, i.e., T^m is topologically transitive for all $m \in \mathbb{Z}^+$ [10]. We will use transitivity of T and T^2 (see Figure 2).

(a) **(b)**

Figure 2. (a) Graph of T; (b) Graph of T^2.

Define $R: [0,1] \to [0,1]$ by

$$R(x) = \begin{cases} -2x + 1 \, , & 0 \leq x \leq \frac{1}{2} \\ 2x - 1 \, , & \frac{1}{2} \leq x \leq 1. \end{cases} \quad (3)$$

Example 3.1. The tent map T defined in (2) is topologically conjugate to the map R defined in (3) via homeomorphism $h: [0,1] \to [0,1]$, $h(x) = 1 - x$. Let $x \in \left[0, \frac{1}{2}\right]$, then $(h \circ R)(x) = 2x = (T \circ h)(x)$. If $x \in \left[\frac{1}{2}, 1\right]$, then $(h \circ R)(x) = 2 - 2x = (T \circ h)(x)$. Hence, $(h \circ R)(x) = (T \circ h)(x)$ for all $x \in [0,1]$. Finally, T and R are topologically conjugate maps.

Result 3.2 According to Theorem 2.8, the dynamical behavior of T and R are same. Since T is chaotic and totally transitive, R is also chaotic and totally transitive.

(a) **(b)**

Figure 3. (a) Graph of R; (b) Graph of R^2.

Example 3.3. The map f defined in (1) is chaotic on $[0,2]$. By Theorem 2.6, it is sufficient to show that f is topologically transitive. Consider the restricted maps of f^2 as $g_1 = f^2|_{[0,1]}$ and $g_2 = f^2|_{[1,2]}$. Note that, the map g_1 is equal to R^2 (see Figure 1 (b) and Figure 3 (b)). Since R is totally transitive, by Result 3.2, R^2 is topologically transitive. Hence, g_1 is topologically transitive. We show that g_2 and T^2 are topologically conjugate via homeomorphism $k: [0,1] \to [1,2]$, $k(x) = x + 1$. Explicit forms of $g_2: [1,2] \to [1,2]$ and $T^2: [0,1] \to [0,1]$ are

$$g_2(x) = \begin{cases} 4x - 3, & 1 \le x \le \frac{5}{4} \\ -4x + 7, & \frac{5}{4} \le x \le \frac{3}{2} \\ 4x - 5, & \frac{3}{2} \le x \le \frac{7}{4} \\ -4x + 9, & \frac{7}{4} \le x \le 2 \end{cases}$$

and

$$T^2(x) = \begin{cases} 4x, & 0 \le x \le \frac{1}{4} \\ -4x + 2, & \frac{1}{4} \le x \le \frac{1}{2} \\ 4x - 2, & \frac{1}{2} \le x \le \frac{3}{4} \\ -4x + 4, & \frac{3}{4} \le x \le 1 \end{cases}$$

respectively. We will show that $(k \circ T^2)(x) = (g_2 \circ k)(x)$ for all $x \in [0,1]$. Let $x \in [0,1]$.
If $x \in \left[0, \frac{1}{4}\right]$, then $(k \circ T^2)(x) = 4x + 1$. Since $x + 1 \in [1, \frac{5}{4}]$, $(g_2 \circ k)(x) = g_2\,(x + 1) = 4x + 1$.
If $x \in [\frac{1}{4}, \frac{1}{2}]$, then $(k \circ T^2)(x) = -4x + 3$. Since $x + 1 \in [\frac{5}{4}, \frac{3}{2}]$, $(g_2 \circ k)(x) = g_2(x + 1) = -4x + 3$.
If $x \in [\frac{1}{2}, \frac{3}{4}]$, then $(k \circ T^2)(x) = 4x - 1$. Since $x + 1 \in [\frac{3}{2}, \frac{7}{4}]$, $(g_2 \circ k)(x) = g_2(x + 1) = 4x - 1$.
If $x \in [\frac{3}{4}, 1]$, then $(k \circ T^2)(x) = -4x + 5$. Since $+1 \in \left[\frac{7}{4}, 2\right]$, $(g_2 \circ k)(x) = g_2(x + 1) = -4x + 5$.
Hence, $(k \circ T^2)(x) = (g_2 \circ k)(x)$ for all $x \in [0,1]$, i.e., T^2 and g_2 topologically conjugate maps. Since T is totally transitive, T^2 is topologically transitive. By Theorem 2.8, g_2 is topologically transitive. Let U and V be non-empty open subsets of $[0,2]$. We will show that f is topologically transitive, i.e., we obtain a $m \in \mathbb{Z}^+$ such that $f^m(U) \cap V \neq \emptyset$. We investigate five cases.

Case 1: If $U, V \subset [0,1]$, since g_1 is topologically transitive, there exists a $n \in \mathbb{Z}^+$ such that $g_1^n(U) \cap V \neq \emptyset$. Hence, $f^{2n}(U) \cap V \neq \emptyset$.

Case 2: If $U, V \subset [1,2]$, since g_2 is topologically transitive, there exists a $k \in \mathbb{Z}^+$ such that $g_2^k(U) \cap V \neq \emptyset$. Hence, $f^{2k}(U) \cap V \neq \emptyset$.

Case 3: Let $\subset [0,1]$, $V \subset [1,2]$. Since f is continuous, $f^{-1}(V) \subset [0,1]$ is an open set. By Case 1, there exists a $n \in \mathbb{Z}^+$ such that $f^{2n}(U) \cap f^{-1}(V) \neq \emptyset$. If $x \in f^{2n}(U) \cap f^{-1}(V)$, then $x \in f^{2n}(U)$ and $x \in f^{-1}(V)$. Therefore, $f(x) \in f^{2n+1}(U)$ and $f(x) \in V$ (since f is onto, $f\left(f^{-1}(V)\right) = V$). Hence, $f^{2n+1}(U) \cap V \neq \emptyset$.

Case 4: Let $\subset [1,2]$, $V \subset [0,1]$. Since f is continuous, $f^{-1}(V) \subset [1,2]$ is an open set. By Case 2, there exists a $k \in \mathbb{Z}^+$ such that $f^{2k}(U) \cap f^{-1}(V) \neq \emptyset$. If $x \in f^{2k}(U) \cap f^{-1}(V)$, then $x \in f^{2k}(U)$ and $x \in f^{-1}(V)$. Therefore, $f(x) \in f^{2k+1}(U)$ and $f(x) \in V$ (since f is onto, $f\left(f^{-1}(V)\right) = V$). Hence, $f^{2k+1}(U) \cap V \neq \emptyset$.

Case 5: If U or V are open sets containing 1, the desired result can be similarly obtained from Case 1,2.

Therefore, f is topologically transitive. Consequently, by Theorem 2.6, f is chaotic on $[0,2]$.

Result 3.4. f^2 is not a chaotic map. Let $U \subset [0,1]$ and $V \subset [1,2]$ be non-empty open subsets. Since $(f^2)^m(U) \subset [0,1]$ for all $m \in \mathbb{Z}^+$ (see Figure 1 (b)), $(f^2)^m(U) \cap V = \emptyset$. Therefore, f^2 is not topologically transitive, i.e., by Definition 2.4, f^2 is not chaotic. Although we construct a chaotic and continuous map f on $[0,2]$, which is connected, f^m is not chaotic on $[0,2]$ for $m = 2$. Hence, this situation contradicts Elaydi's conjecture in [9] (p. 143). Moreover, f is an example of a map that is topologically transitive but not totally transitive.

ACKNOWLEDGEMENTS

I would like to thank the referees for their valuable comments and suggestions, which helped very much in improving the paper. I would also like to thank The Scientific and Technological Research Council of Türkiye (TÜBİTAK) for their support.

CONFLICT OF INTEREST

The author stated that there are no conflicts of interest regarding the publication of this article.

CRediT AUTHOR STATEMENT

İsmail Alper Güvey: Conceptualization, Formal analysis, Investigation, Visualization, Writing – Original Draft.

REFERENCES

[1] Zhang B, Liu L. Chaos-based image encryption: Review, application, and challenges. Mathematics 2023; 11(11): 2585.

[2] Smaoui N, Kanso A. Cryptography with chaos and shadowing. Chaos, Solitons & Fractals 2009; 42 (4): 2312-2321.

[3] Aslan N, Koparal FD, Saltan M, Özdemir Y, Demir B. A family of chaotic dynamical systems on the Cantor dust $C \times C$. Filomat 2023; 37 (6): 1915-1925.

[4] Devaney RL. An Introduction To Chaotic Dynamical Systems. New York, NY, USA: Addison Wesley, 1989.

[5] Banks J, Brooks J, Cairns G, Davis G, Stacey P. On Devaney's Definition of Chaos. Am Math Mon 1992; 99 (4): 332-334.

[6] Vellekoop M, Berglund R. On Intervals, Transitivity = Chaos. Am Math Mon 1994; 101 (4): 353-355.

[7] Değirmenci N, Koçak Ş. Existence of a dense orbit and topological transitivity: When are they equivalent? Acta Math Hungar 2003; 99 (3): 185-187.

[8] Değirmenci N, Koçak Ş. Chaos in product maps. Turk J Math 2010; 34 (4): 593-600.

[9] Elaydi SN. Discrete Chaos. 2nd ed. Boca Raton, FL, USA: Chapman & Hall/CRC, 2007.

[10] Grosse-Erdman KG, Manguillot AP. Linear Chaos. London, UK: Springer, 2011.

ESKİŞEHİR TEKNİK ÜNİVERSİTESİ BİLİM VE TEKNOLOJİ DERGİSİ
B- TEORİK BİLİMLER

Eskişehir Technical University Journal of Science and Technology B- Theoretical Sciences

Estuscience – Theory, 2025, 13 [1] pp. 7-23 , DOI:10.20290/estubtdb.1501639

RESEARCH ARTICLE

ANALYSIS BY DFT, ADME AND DOCKING STUDIES OF N'-(4-HYDROXY-3-METHOXYBENZYLIDENE)NAPHTHO[2,3-B]FURAN-2-CARBOHYDRAZIDE

Kenan GÖREN [1, *], Mehmet BAĞLAN [2], Ümit YILDIKO [3]

[1] Department of Chemistry, Kafkas University, Kars 36100, Turkey
kenangoren49@gmail.com - *0000-0001-5068-1762*

[2] Department of Chemistry, Kafkas University, Kars 36100, Turkey
mehmetbaglan36@gmail.com - *0000-0002-7089-7111*

[3] Department of Bioengineering, Kafkas University, Kars 36100, Turkey
yildiko1@gmail.com - *0000-0001-8627-9038*

Abstract

In this study, N'-(4-hydroxy-3-methoxybenzylidene)naphtho[2,3-b]furan-2-carbohydrazide (HMFC) compound containing Schiff base was theoretically examined. The HMFC molecule was calculated theoretically using the 6-311G(d,p), B3LYP/B3PW91 basis sets and methods. The energy gap of the molecule, the lowest unoccupied molecular orbital (LUMO), and the highest occupied molecular orbital (HOMO) values were calculated using the identical set and two distinct methods. The HMFC compound's molecular stability was examined by applying the natural bond orbital (NBO) study. The Nonlinear optical Properties (NLO) of HMFC molecule, thermodynamic parameters, and Molecular Electrostatic Potential Maps (MEP) were calculated. Molecular docking study of the HMFC compound was performed by downloading two different enzyme codes (PDB ID: 1T46 and PDB ID: 3SXR) from PDB (Protein Data Bank) and examining in silico the cancer-associated proteins to analyze the potential anticancer activity. In the docking analysis, it showed a score of -7.356 kcal/mol for the 1T46 enzyme code in the compound, while it showed a score of -6.866 kcal/mol for the 3SXR enzyme code. Whether the HMFC molecule has drug properties was analyzed using the absorption, distribution, metabolism, and excretion (ADME) approach.

Keywords

Molecular Docking Analyses,
Natural Bond Orbital Analyses,
Molecular Electrostatic Potential Maps,
Nonlinear Optical Properties

Time Scale of Article

Received :15 June 2024
Accepted : 25 November 2024
Online date : 28 February 2025

1. INTRODUCTION

In 1864, Hugo Schiff described the condensation of an amine with an aldehyde to produce a Schiff base. Schiff bases, having the existence of the imine group, are used to clarify the transformation process of the racemization reaction in biological systems [1]. Its azomethine linkage (>C=N-) gives it anticancer, antibacterial, antifungal, and herbicidal activities, among other effects, in biological systems. because of their potent antiviral, antifungal, and antibacterial qualities, several Schiff derivatives are useful therapeutic medications [2]. The structure-activity link between biomolecules and pharmacological molecules is also often understood using Schiff bases and their analogs as model compounds. Schiff bases are considered interesting medicinal compounds for the creation of novel drugs because of their many biological uses, particularly in the case of hydrazone derivatives [3-5]. Schiff bases have been extensively studied by many researchers due to their antibacterial, antiviral, antimalarial, anti-inflammatory, and antioxidant properties. Moreover, it has been documented that Schiff bases coupled

*Corresponding Author: kenangoren49@gmail.comx

with benzothiazole provide unique physiologically active molecular hybrids with noteworthy chemotherapeutic effects [6]. For instance, Schiff bases are essential to the advancement of coordination science since they readily create stable structures with the majority of metals and anticancer medications. Schiff-based chemicals tend to become more anti-cancer when they form complexes with metal ions [7].

The popularity of DFT-based methods is due to their wider range of applications and significantly cheaper computational cost compared to more accurate wave function-based methods [8]. These methods can yield findings that are sufficiently precise for a wide range of chemical systems (both in regard to size and complexity). Particularly in this regard, LR-TD-DFT20 has been shown to be a potent and adaptable method for treating aroused states [9].

Computer-aided quantum chemical calculations are performed using molecular modeling programs to help experimental research or to forecast the outcomes to be attained without completing experimental experiments [10]. The creation of effective programs that can compute molecular parameters including dipole moment, total energy, optimal shape, and vibration wave numbers is the main goal of these programs. These computations are based on quantum mechanics [11]. Atoms and molecules were subjected to the principles of quantum mechanics as soon as quantum theory was developed. In theory, quantum theory allows one to compute any molecule's chemical property. While there are numerous applications for prediction through computation, experimental approaches are still a valuable means of determining a compound's structure and chemistry [12].

The main purpose of this study, the Schiff base derivative N'-(4-hydroxy-3-methoxybenzylidene)naphtho[2,3-b]furan-2-carbohydrazide (HMFC) molecule was theoretically investigated using the 6-311G(d,p), B3LYP/B3PW91 basis sets and methods. The DFT method was used to calculate the chemical descriptors HOMO-LUMO gap, and HOMO-LUMO, which are regarded as markers of the examined compounds' chemical reactivity. A study on molecular docking has been carried out against the molecule to shed more light on its biological application; The study reports on their binding affinity to the pathogen's protein and shows their capacity to bind with the protein through a comparative docking score. Finally, ADME analysis was performed in the study. ADME analysis findings suggest that these compounds may possess intriguing features for use in pharmaceuticals, which might make them useful as active components in novel pharmaceuticals. According to the ADME research, it has an excellent absorption profile of 79.99%, and the field that produces safe and effective medications may find use for the literature study's findings.

2. MATERIALS AND METHODS

The 6-311G(d,p), B3LYP/B3PW91 basis sets and methods were the basis sets and methods used in study for all DFT calculations performed in Gaussian 09 software. We used a semi-empirical conformational analysis method. The initial step of computer analysis was to optimize the final molecule's form. It specifically calls for low energy sensitivity to modifications in molecules caused due to the nuclear location shifting of the molecule. The best molecular structure geometries, vibration frequencies, and energies of HMFC chemical were determined using the DFT method in Gaussian 09 software. The DFT method has been used to generate the Lee's-Yang-Parr correlation function using the 6-311G(d,p) basis set-based computer package [13]. The visualization and input files have been prepared and imported using GaussView 6.0.16 and ChemBio Ultra Drive 3D. To identify the specific binding location and mechanism of the ligand on the protein, molecular docking research was conducted using the Maestro Molecular Modeling platform (version 11.8) [14] of the Schrödinger, LLC model and waited for the wizard module to get data on protein preparation. In the meantime, a crystal structure formed from the separation of all water molecules. The protein ion balance was restored by returning to this module and selecting the flexible protein-binding active site. Designed to serve as the foundation of the receptor network module, network boxes enable adaptable docking by creating networks at the

locations where proteins bind. Receptor connection modules are built on network boxes, which enable flexible docking through the formation of networks at protein binding sites. The lowest energy arrangement represents the strongest affinity for binding. Ultimately, the ADME analysis of HMFC molecule in this work was conducted using the online database SwissADME (http://www.swissadme.ch).

3. RESULTS AND DISCUSSION

3.1. Structure Details and Analysis

Using the Density Function Theory (DFT) method and polarizing functions added to eliminate the polarization effect, the approximate geometry of this molecule in gas phase was drawn using the GaussView 6.0.16 molecular imaging program. The electron density in excited ionic molecules is higher than that of the ground-state molecule. Geometry optimization with restricted closed shell calculations, in which each electron pair is forced to occur in a single orbit, was used to determine the space settlements and space structure of the atoms in the compound using the 6-311G(d,p) basis set, which includes diffuse functions added to model the dispersed state [15, 16]. As a result, theoretical calculations were made for bond lengths (Å), bond angles (°), and dihedral angles (°). Table 1 presents the structure's bond length and bond angles as determined using the 6-311G(d,p), B3LYP/B3PW91 basis sets and methods. With values of 1.37 and 1.41 Å to C-O, the C-C bond lengths for B3PW91 and B3LYP are 1.36-1.53 Å and 1.37-1.54 Å, respectively. The aromatic ring's C-H lengths are around 1.08 Å in value. The range of all C-C-C angles is 101° to 122°. We noticed that some dihedral angles produced negative angle-degree outcomes when atoms were used as dihedral bonds in the Gaussian 09 software. These calculated values were assigned values based on where the atoms were located inside the bonds. We saw very slight variations in the dihedral bond values between the two methods. When we compared the theoretical results obtained with two different methods, we observed that they were close to each other and compatible.

Table 1. Theoretically optimized geometric parameters of the molecule HMFC

Bond Lengths	**B3PW91/ 6-311G(d,p)**	**B3LYP/ 6-311G(d,p)**	**Bond Lengths**	**B3PW91/ 6-311G(d,p)**	**B3LYP/ 6-311G(d,p)**
C4-C5	1.43121	1.43462	**N17-C18**	1.28282	1.28450
C4-C7	1.41993	1.42297	**C18-C19**	1.47151	1.47486
C7-C8	1.43121	1.36663	**C21-C22**	1.38644	1.38833
C8-C9	1.36533	1.41309	**C22-O25**	1.34960	1.35526
C8-O11	1.37052	1.37659	**C23-O26**	1.36379	1.36976
C9-C13	1.50489	1.50849	**O26-C27**	1.41803	1.42564
C12-C13	1.53899	1.54601	**O25-H42**	0.96607	0.96718
C12-C14	1.53700	1.54201	**N16-H37**	1.01553	1.01460
C14-N16	1.36833	1.37178	**C18-H38**	1.08899	1.08826
N16-N17	1.35853	1.36760	**C24-H41**	1.08227	1.08032
Bond Angles	**B3PW91/ 6-311G(d,p)**	**B3LYP/ 6-311G(d,p)**	**Bond Angles**	**B3PW91/ 6-311G(d,p)**	**B3LYP/ 6-311G(d,p)**
C6-C5-C10	122.66744	122.76053	**N16-N17-C18**	118.45382	118.55801
C7-C8-O11	124.77683	124.73284	**N17-C18-C19**	131.07090	131.58017
C9-C8-O11	112.17530	112.19842	**C21-C22-O25**	120.58918	120.44303
C9-C12-C13	101.77366	102.01231	**C23-C22-O25**	120.05667	113.64148
C12-C14-N16	113.39116	113.39530	**C23-O26-C27**	118.28394	118.55989
Planar Bond Angles	**B3PW91/ 6-311G(d,p)**	**B3LYP/ 6-311G(d,p)**	**Planar Bond Angles**	**B3PW91/ 6-311G(d,p)**	**B3LYP/ 6-311G(d,p)**
C1-C6-C5-C10	-179.94428	-179.95212	**C12-C14-N16-N17**	177.78572	177.90167
C5-C10-C9-C13	-177.84628	-178.05155	**C14-N16-N17-C18**	178.90535	178.52697
C4-C7-C8-O11	179.54733	179.61311	**C21-C22-C23-O26**	-179.99596	-178.95493
C8-O11-C12-C14	-105.99149	-108.06229	**C22-C23-O26-C27**	-178.22383	-178.05634

3.2. Mulliken Atomic Charges

The most popular and traditional technique for load analysis is the Mulliken load distribution. Numerous applications contribute to its extensive use [17]. The idea behind this method, which derives from the linear integration of orbitals in atoms, is to distribute the wave functions to the atoms in the same proportion as the locations where two orbitals meet. This distribution, however, does not accurately depict each element's electronegativity [18, 19]. Because it offers a wealth of information about a molecule's polarity, electronic structure, dipole moment of atomic molecules, charge distribution on atoms, acceptor pairs and donors that facilitate charge transfer in the structure, and different chemical structure properties, the Mulliken charge distribution method is a commonly used method [20]. Because the nearby element O15 possesses a notably electronegative property, the C14 carbon atom's mulliken atomic charge value was determined to be larger than that of different chemical structures. Table 2 displays further calculated Mulliken atomic charge measurements for the compound using the 6-311G(d,p), B3LYP/B3PW91 basis sets and methods. Some C atoms were found to be negatively charged, whereas other C atoms were found to be positively charged. Figure 1 compares some C atom values using the different methods. In the Figure 2 has been given the optimized geometry of the molecule HMFC using the B3PW91/6-311G(d,p) method and basis set. Because the nearby element O15 possesses a notably electronegative property, the C14 carbon atom's mulliken atomic charge value was determined to be larger than that of different chemical structures. Table 2 displays further calculated Mulliken atomic charge measurements for the compound using the 6-311G(d,p), B3LYP/B3PW91 basis sets and methods. Some C atoms were found to be negatively charged, whereas other C atoms were found to be positively charged. Figure 1 compares some C atom values using the different methods. Figure 2 has been given the optimized geometry of the molecule HMFC using the B3PW91/6-311G(d,p) method and basis set. When we compared the theoretical results obtained with two different methods, we observed that they took values far from each other and were not compatible.

Table 2. Mulliken atomic charges of the molecule HMFC

ATOMS	B3PW91/ 6-311G(d,p)	B3LYP/ 6-311G(d,p)	ATOMS	B3PW91/ 6-311G(d,p)	B3LYP/ 6-311G(d,p)
C5	-0.070	-0.059	**N16**	-0.298	-0.275
C6	-0.073	-0.065	**N17**	-0.200	-0.188
C7	-0.052	-0.043	**O25**	-0.405	-0.394
C8	0.205	0.205	**O26**	-0.386	-0.378
C9	-0.179	-0.162	**H28**	0.113	0.102
C10	-0.014	-0.014	**H29**	0.113	0.102
C12	-0.129	-0.086	**H30**	0.100	0.090
C13	-0.104	-0.081	**H31**	0.103	0.093
C14	0.379	0.350	**H32**	0.115	0.101
C18	0.106	0.092	**H33**	0.101	0.093
C19	-0.204	-0.175	**H34**	0.161	0.148
C21	-0.104	-0.091	**H35**	0.161	0.146
C22	0.180	0.173	**H36**	0.162	0.142
C23	0.148	0.143	**H37**	0.232	0.217
C24	-0.122	-0.108	**H38**	0.132	0.119

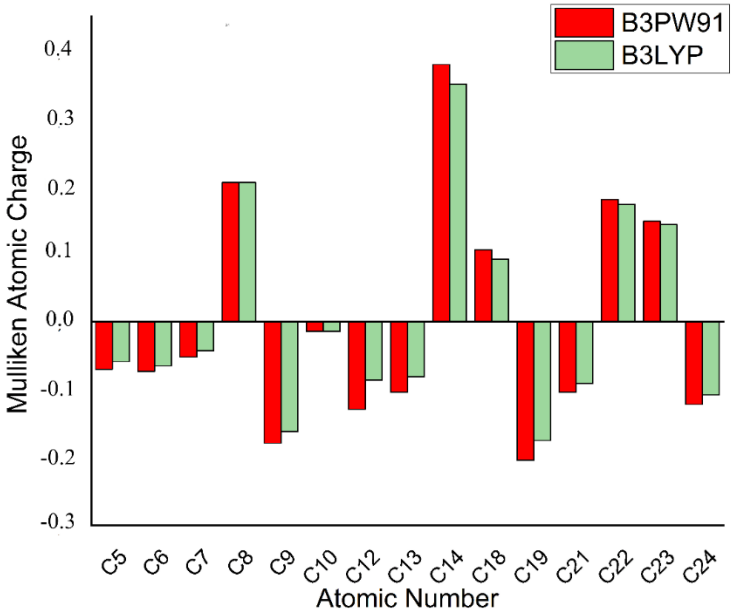

Figure 1. Mulliken atomic charge comparison for molecule HMFC

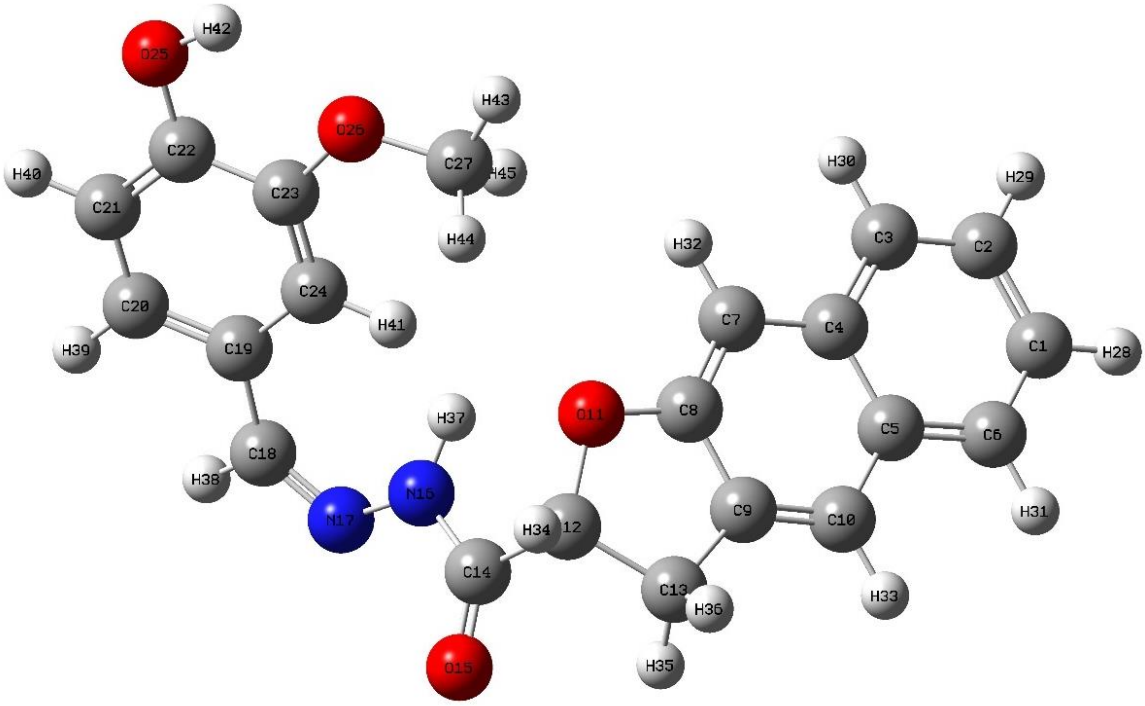

Figure 2. Optimized geometry display using the B3PW91/6-311G(d,p) method and basis set of molecule HMFC

3.3. HOMO and LUMO Analysis

Every molecule has two orbitals: LUMO and HOMO, according to molecular orbital theory. HOMO and LUMO orbitals are also known as leading orbitals because of their significance in chemical reactions [21]. The molecule's HOMO and LUMO energy levels differ from one another, signifying its chemical stability. The easier the reactant-reactant contact and reaction, the lower the ΔE energy difference, that is, the closer the energy levels of the interacting molecular orbitals are [22, 23]. It has been shown that

the energy values of molecules differ based on their hardness or softness, with soft molecules often having lower energy values than hard ones. The formulas for ionization energy, $I=-E_{HOMO}$, and electron affinity, $A=-E_{LUMO}$, represent the least amount of energy required to take one electron out of a molecule and the total energy that rises when an electron is added to the molecule in the gas phase, respectively [24]. $\eta=(I-A)/2$ gives the hardness value, which is a measurement of the blockage of charge transfer inside the molecule. The hardness of the HMFC molecule was calculated as 2.2754 with the B3PW91 method and 2.3249 with the B3LYP method. $S=1/2\eta$ represents the softness parameter, which is the opposite of hardness. The softness of the HMFC molecule was calculated as 1.1377 with the B3PW91 method and 1.1624 with the B3LYP method. When we examined the molecular hardness and softness values of the HMFC molecule calculated with two different methods, we observed that they were very close to each other and compatible. High-chemical-hardness molecules have little to no intramolecular charge transfer. The Mulliken electronegativity parameter, $\chi=(I+A)/2$, denotes a molecule's atom's capacity to draw electrons, except for the hardness and suppleness characteristics. Furthermore, he calculated the chemical capacity using $\mu=-(I+A)/2$ and the electrophilic index using $w=\mu 2/2\eta$ [25]. The densities of the HOMO and LUMO orbital representations for Molecule HMFC have been displayed in Figures 3 and 4. Table 3 shows that the B3PW91 method yielded HOMO-6.0340 eV/LUMO-1.4832 eV, while the B3LYP method yielded HOMO-5.9793 eV/LUMO -1.3295 eV.

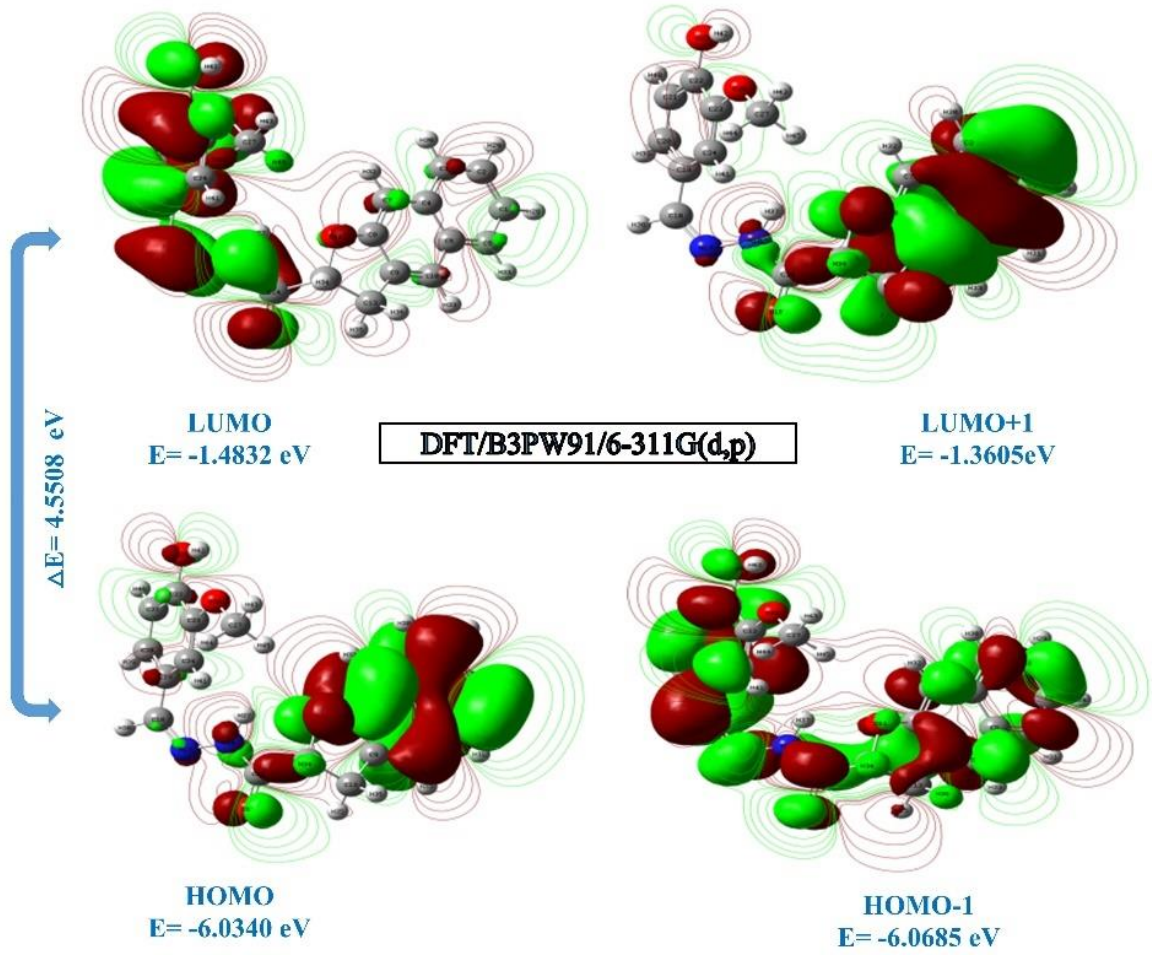

Figure 3. Pictures of frontier molecular orbitals using the B3PW91/6-311G(d,p) method and basis set

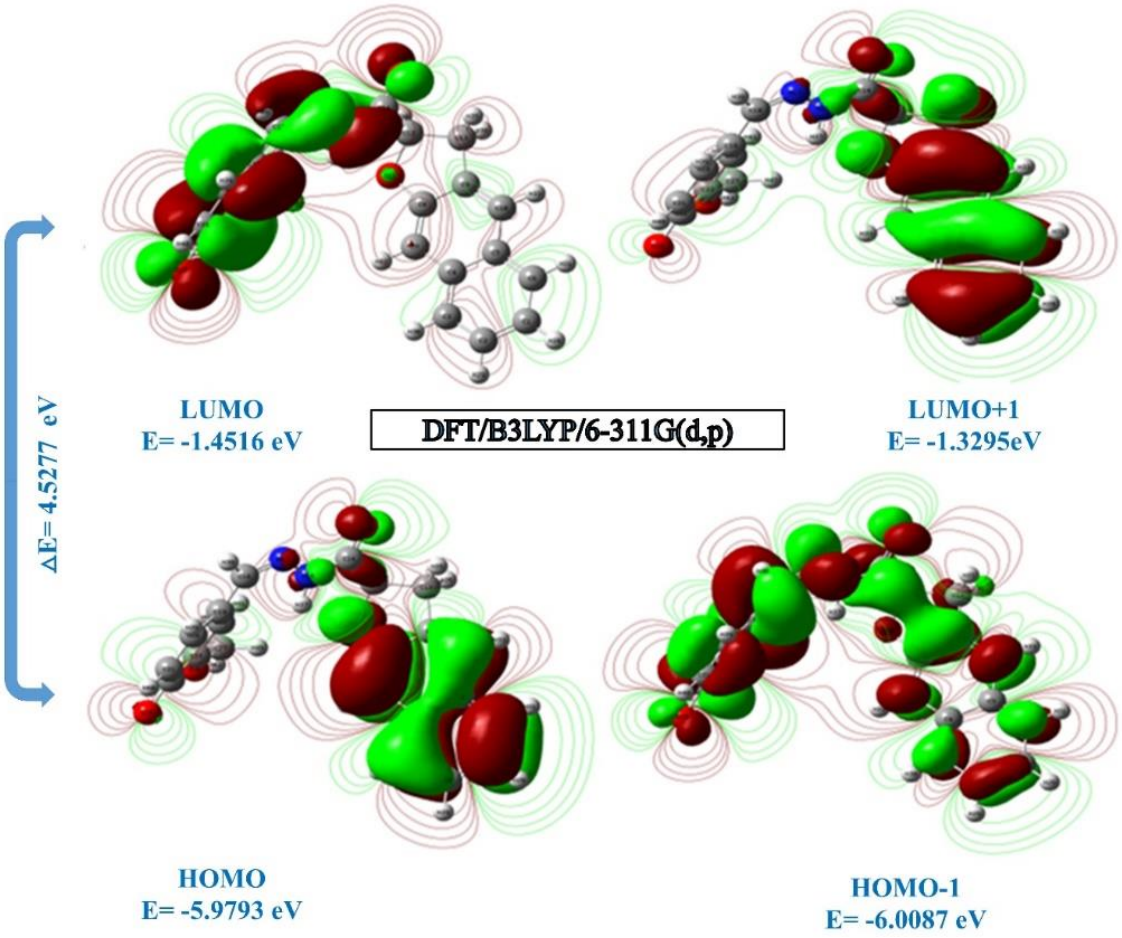

Figure 4. Pictures of frontier molecular orbitals using the B3LYP/6-311G(d,p) method and basis set

Table 3. Calculated quantum chemical parameters*(in eV) for low energy compatibilities by the 6-311G(d,p), B3LYP/B3PW91 basis set and methods of the HMFC molecule

Molecules Energy		**B3PW91/ 6-311G(d,p)**	**B3LYP/ 6-311G(d,p)**
E_{LUMO}		-1.4832	-1.4516
E_{HOMO}		-6.0340	-5.9793
E_{LUMO+1}		-1.3605	-1.3295
E_{HOMO-1}		-6.0685	-6.0087
Energy Gap	$(\Delta E)\lvert E_{HOMO}-E_{LUMO}\rvert$	4.5508	4.5277
Ionization Potential	$(I=-E_{HOMO})$	6.0340	5.9793
Electron Affinity	$(A=-E_{LUMO})$	1.4832	1.3295
Chemical hardness	$(\eta=(I-A)/2)$	2.2754	2.3249
Chemical softness	$(s=1/2\eta)$	1.1377	1.1624
Chemical Potential	$(\mu=-(I+A)/2)$	-3.7586	-3.6544
Electronegativity	$(\chi=(1+A)/2)$	1. 2416	1.16475
Electrophilicity index	$(\omega=\mu^2/2\eta)$	3.1043	2.8720

3.4. Molecular Electrostatic Potential (MEP)

Partial charges, electronegativity, and dipole moment are all connected to the molecular electrostatic potential surface. It is also favored for delineating hydrogen bond interactions and identifying nucleophilic and electrophilic reaction sites [26, 27]. In regions with low electron density, the proton is repelled by positive electrostatic potential, whereas The proton's attraction to the electron density is described by the negative electrostatic potential. The highest electrostatic potential, or nucleophilicity, is represented by the blue zone, while the smallest electrostatic potential, or electrophilicity, is represented by the red region [28]. The polarity of the molecule is connected to the wide gap in the molecular electrostatic potential scale. A molecule is said to be more polar if there are significant variations on the scale from red to blue. Figure 5 demonstrates that whereas oxygen and nitrogen atoms have negative potential zones that might be used for electrophilic assault, hydrogen atoms are more likely to have positive potential zones that could be used for nucleophilic attack.

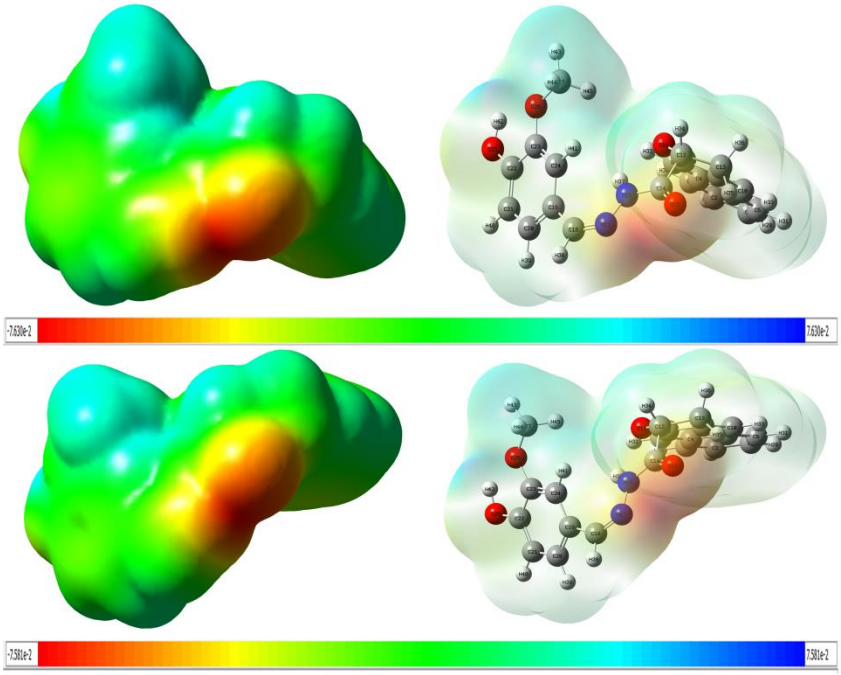

Figure 5. Molecular electrostatic potential surface of the molecule HMFC using the the 6-311G(d,p), B3LYP/B3PW91 basis sets and methods

3.5. Non-Linear Optical Properties (NLO)

NLO materials are widely used in many scientific fields, which has led to their increased attention in recent years. Good NLO qualities may be found in numerous photonic applications, including digital communications, signal processing, optical computing, sensors, and the creation of optical junction materials [29]. A molecule that is isolated has a dipole moment change when an external electrical field is present. In the equation of the total dipole moment, thus, aside from the permanent dipole moment, first- and second-order contributions appear [30]. First-order hyperpolarizability (β), which represents non-linear optical qualities, becomes significant if a stronger electric field is applied, whereas molecule polarizability (α), which represents linear optical properties, is considered if the applied electric field is weak [31]. Using the Gaussian 09 package software, one may determine a molecule's nonlinear optical characteristics by first calculating the energy of the optimized molecule and entering Polar=Enonly in the keyword area. Equations (1-3) are then used to compute the average molecule polarizability value from the output file in cartesian coordinates [32]. The polarization rises due to the simple alteration of

the electron distribution, which raises the β value. Furthermore, the attachment of acceptor-donor groups to the ends of the molecule influences the rise in the β value and the charge asymmetry. In addition to this, when the molecule is extended by adding more conjugated bonds, the β value which is dependent on the polarizability of the electrons in the π bond will also rise [33]. NLO analysis values have been given in Table 4. HMFC compound's first-order hyperpolarization values and molecular polarizability were determined in the 6-311G(d,p), B3LYP/B3PW91 basis sets and methods. After being translated from atomic unit (a.u.) to electrostatic unit (e.s.u.), the predicted molecular polarizability (α) and first-order hyperpolarizability (β) values were found to be $2.50\text{x}10^{-30}$ and $2.52\text{x}10^{-30}$ esu, respectively. When we compared the theoretical results obtained with two different methods, we observed that they were close to each other and compatible. The urea molecule is one of the model molecules used in studies on systems exhibiting NLO properties. The calculated μ and β values for both methods are approximately HMFC and seven times larger, respectively, than those of the typical NLO material "urea." The relatively large dipole moment and hyperpolarizability of HMFC compound may indicate that the substance can serve as a basic element for NLO materials.

$$\mu = \left(\mu_x^2 + \mu_y^2 + \mu_z^2\right)^{\frac{1}{2}} \quad (1)$$

$$\beta_{Total} = (\beta^2 x + \beta^2 y + \beta^2 z)^{1/2} \quad (2)$$

$$= [(\beta xxx + \beta xyy + \beta xzz)^2 + (\beta yyy + \beta yxx + yzz)^2 + (\beta zzz + \beta zxx + \beta zyy)^2]^{\frac{1}{2}} \quad (3)$$

Table 4. The dipole moments (Debye), polarizability (au), components, and total value of molecule HMFC are calculated using the 6-311G(d,p), B3LYP/B3PW91 basis sets and methods

Parameters	B3PW91/ 6-311G(d,p)	B3LYP/ 6-311G(d,p)	Parameters	B3PW91/ 6-311G(d,p)	B3LYP/ 6-311G(d,p)
μ_x	-0.5857	-0.5770	β_{XXX}	14.6593	12.8342
μ_y	0.7810	0.7399	β_{YYY}	4.8202	5.7078
μ_z	-2.1691	-2.1428	β_{ZZZ}	-11.0735	-10.7324
$\mu_{(D)}$	2.3786	2.3392	β_{XYY}	-6.8838	-8.2537
α_{XX}	-144.4681	-146.4085	β_{XXY}	52.8463	53.0179
α_{YY}	-133.8131	-136.1076	β_{XXZ}	50.0598	49.0202
α_{ZZ}	-171.5781	-172.2085	β_{XZZ}	-23.1842	-23.2474
α_{XY}	-7.9039	-7.8356	β_{YZZ}	2.3260	1.6622
α_{XZ}	-0.1837	-0.6591	β_{YYZ}	-26.3724	-25.7985
α_{YZ}	-8.8702	-8.8884	β_{XYZ}	3.3769	3.6133
α(au)	-169.172	-164.8441	**β(esu)**	$2.50\text{x}10^{-30}$	$2.52\text{x}10^{-30}$

3.6. NBO Analysis

The Gaussian 09 software contains a program that may be used to calculate NBO analysis, a commonly used method to look at how molecules interact with one another. This study yields the percentages of electrons present in various bonds for σ and π bonds as well as variations in the proportions of electrons on each atom in the s, p, and d orbitals [34]. Hybridizations that result in bond formation on atoms can also be achieved with this method. Furthermore, the NBO analysis looks at the orbitals' E(2) stabilization energies in addition to the interaction energies between orbitals and transition states. As is well known, π bonds are required to have p atomic orbitals of N, O, and C atoms by definition. It has been noted that the s orbital in the σ bond contributes less to the hybridization at the C atom than the other orbitals together [35]. O atoms saw far less of this alteration than C atoms did. As predicted, these modifications are almost nonexistent for π bonds. Table 5 presents the analytical findings for this data. By overlapping orbitals between bonding and antibonding orbitals, intramolecular hyperconjugative interactions facilitate intermolecular charge transfer, which leads to the molecular system's stability. The electron density in the antibonding orbitals increases as a result of these interactions, weakening the bond character. In the molecule under investigation, these bonds, together with their transition states and energy values, are as follows: π(C1-C2)→π*(C5-C6) 10.44 kcal/mol, π(C3-C4)→π*(C7-C8) 11.78

kcal/mol, π(C5-C6)→π*(C9-C10) 11.33 kcal/mol, and π(C9-C10)→π*(C7-C8) 11.24 kcal/mol. With stability energy data of 8.07, 13.92, 11.88, and 11.29 kcal/mol, respectively, the strongest interactions were found to be π(N17-C18)→ π*(C9), π(C19-C20)→ π*(N17), π (C22)→π*(C23-C24), and π*(23)→π* (C19-C20).

Table 5. Selected NBO results of molecule HMFC calculated using B3PW91/6-311G(d,p) method and basis set

NBO(i)	Type	Occupancies	NBO(j)	Type	Occupancies	E(2)[a] (Kcal/mol)	E (j)-E(i)[b] (a.u.)	F (i, j)[c] (a.u)
C1-C2	π	1.79417	**C5-C6**	π*	1.75478	10.44	0.31	0.051
C1-C6	σ	1.97579	**C5-C10**	σ*	1.96779	5.14	1.01	0.064
C2-C3	σ	1.97515	**C5-C6**	σ*	1.75478	5.22	1.00	0.065
C3-C4	π	1.75770	**C7-C8**	π*	1.84120	11.78	0.30	0.054
C4-C5	σ	1.96826	**C3-C4**	σ*	1.75770	3.16	1.25	0.056
C4-C7	σ	1.96127	**C8-O11**	σ*	1.98575	8.53	0.85	0.076
C5-C6	π	1.75478	**C9-C10**	π*	1.84522	11.33	0.31	0.054
C5-C10	σ	1.96779	**C1-C6**	σ*	1.97579	6.66	1.01	0.073
C7-C8	π	1.84120	**C9-C10**	π*	1.96741	12.04	0.33	0.056
C8-C9	σ	1.96886	**N16-H37**	σ*	1.95636	3.12	1.09	0.052
C9-C10	π	1.84522	**C7-C8**	π*	1.84120	11.24	0.31	0.053
C9-C13	σ	1.96741	**C7-C8**	π*	1.84120	3.33	1.26	0.058
C10-H33	σ	1.97807	**C8-C9**	σ*	1.96886	6.80	0.95	0.072
O11-C12	σ	1.98210	**C7-C8**	σ*	1.98007	3.85	1.42	0.066
C12-C13	σ	1.96624	**C9-C10**	σ*	1.97688	5.01	1.27	0.071
C12-H34	σ	1.96447	**C14-O15**	π*	1.98091	4.87	0.54	0.047
C14-N16	σ	1.98170	**N17-C18**	σ*	1.94446	2.84	1.35	0.055
N16-H37	σ	1.95636	**C24-H41**	π*	1.92377	10.00	1.14	0.095
N17-C18	π	1.94446	**C19-C20**	π*	1.78074	8.07	0.36	0.051
C19-C20	π	1.78074	**N17-C18**	π*	1.94446	13.92	0.29	0.057
C19-C24	σ	1.96628	**C23-O26**	σ*	1.98736	5.16	0.89	0.061
C20-C21	σ	1.97021	**C22-O25**	σ*	1.99212	5.50	0.88	0.062
C21-C22	π	1.79193	**C23-C24**	π*	1.97945	11.88	0.30	0.054
C21-H40	σ	1.97602	**C22-C23**	σ*	1.97582	6.20	0.90	0.067
C23-C24	π	1.82146	**C19-C20**	π*	1.78074	11.29	0.33	0.055
C24-H41	σ	1.92377	**N16-H37**	σ*	1.95636	26.57	0.99	0.145
O25-H42	σ	1.98582	**C21-C22**	σ*	1.79193	2.98	1.35	0.057
C27-H43	σ	1.98981	**C23-O26**	σ*	1.98736	3.66	0.82	0.049

3.7. Molecular Docking Studies

The method of molecular docking analysis is used to determine the affinities of chemical bonds to a receptor by enabling the determination of the proper binding geometries between a ligand and a target protein molecule [36]. Molecular docking analysis was performed with Maestro (version 11.8) [14]. The compound's protein crystal structure was chosen using the Protein Data Bank (http://www.rcsb.org). There are many protein targets on cancer. When we examine the literature, these two proteins have been widely used in cancer diseases [37, 38] We observed that we would obtain a good docking score when proteins were evaluated with reference ligands. Hydrogen atoms were added to the protein, and water molecules were eliminated throughout the preparation procedure using the protein preparation wizard. By clicking on any ligand atom, the Receptor Grid Creation application was launched, and the default grid box was created. Using Standard Precision, the ligand was attached to the protein grid box (SP). Docking scores were displayed as the results in Table 6. When we examined potential anticancer activity of HMFC compound against different proteins PDB ID: 1T46 and PDB ID: 3SXR, it is thought that the study with good docking scores is promising for these diseases and can make a significant contribution to new studies.

Table 6. Docking score of molecule HMFC PDB: 1T46 and PDB: 3SXR

Compound	Docking Score	
	(PDB: 1T46)	(PDB: 3SXR)
Molecule HMFC	-7.356	-6.866

Figure 6 shows 3D and 2D interactions as a result of Molecule-1T46 docking. The shift score with Molecule-1T46 was determined as -7.356 cal/mol in Table 6. In HMFC compound, THR-670 (4.12 Å) is the carbon-hydrogen bond linked to methoxy. CYS-673 (3.73 Å) on the Schiff base carbon is the conventional hydrogen bond. ASP-677 (4.54 Å) is a Pi-Anion bond on the naphthalene ring. In the benzene ring, VAL-603 (5.59 Å) is the Pi-Sigma bond. CYS-809 (4.12), ALA-621 (4.83), and LEU-799 (5.30) are Pi-Alkyl bonds in HMFC compound. GLY-676, GLU-671, and LYS-593 are van der Waals bonds in the binding mechanism of HMFC compound.

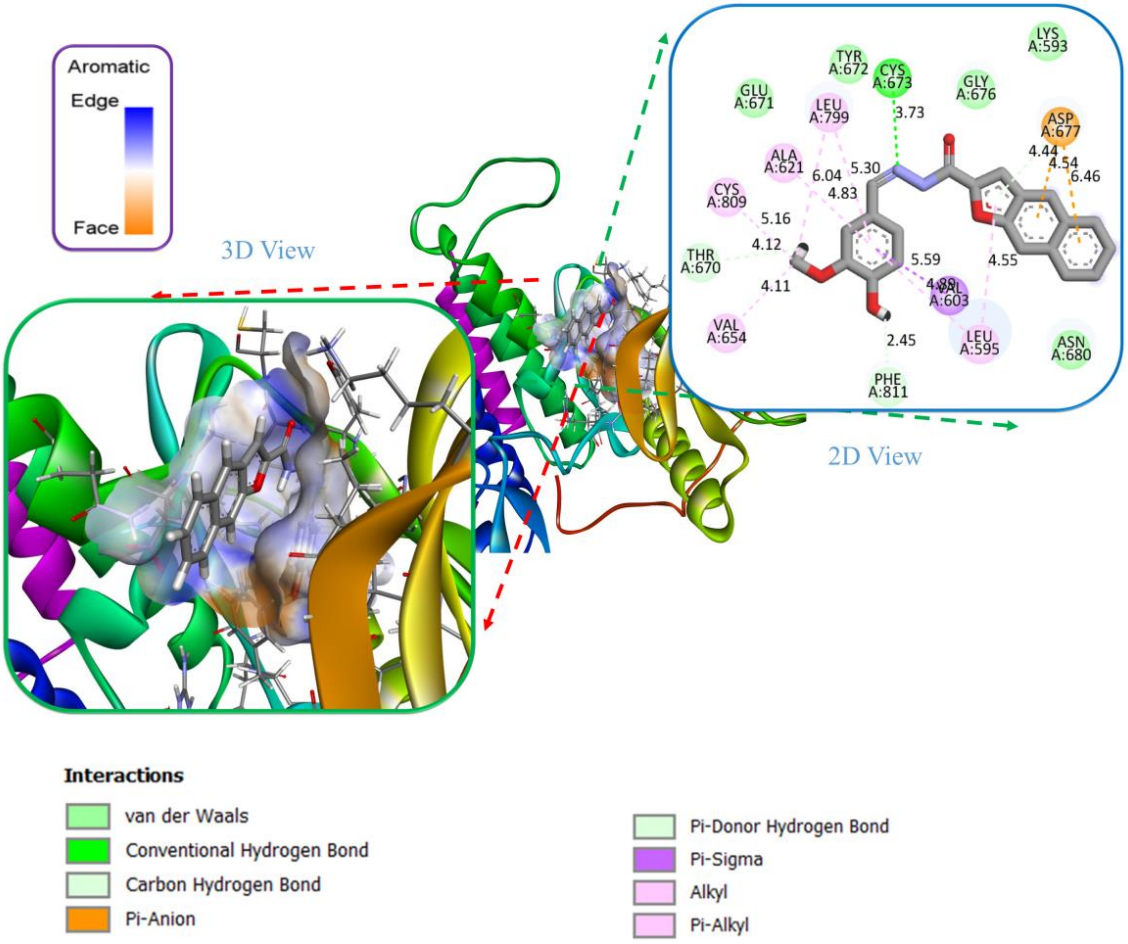

Figure 6. Molecule-1T46 mode of interaction with enzymes; a) 3D view of the donor/acceptor surface of aromatic bonds on the receptor b) 2D view of ligand enzyme interactions

Figure 7 shows 3D and 2D interactions as a result of Molecule-3SXR docking. The shift score with Molecule-3SXR was determined as -6.866 cal/mol in Table 6. VAL-431 (5.01 Å) is the Pi-Sigma bond on the naphthalene ring. In the benzene ring, CYS-496 (4.95 Å) is the Pi-Sulfur bond. In HMFC compound, LYS-445 (4.87), ALA-443 (6.48) and LEU-543 (5.97) are Pi-Alkyl bonds. GLY-429, SER-425 and MET-464 are van der Waals bonds in the binding mechanism of HMFC compound.

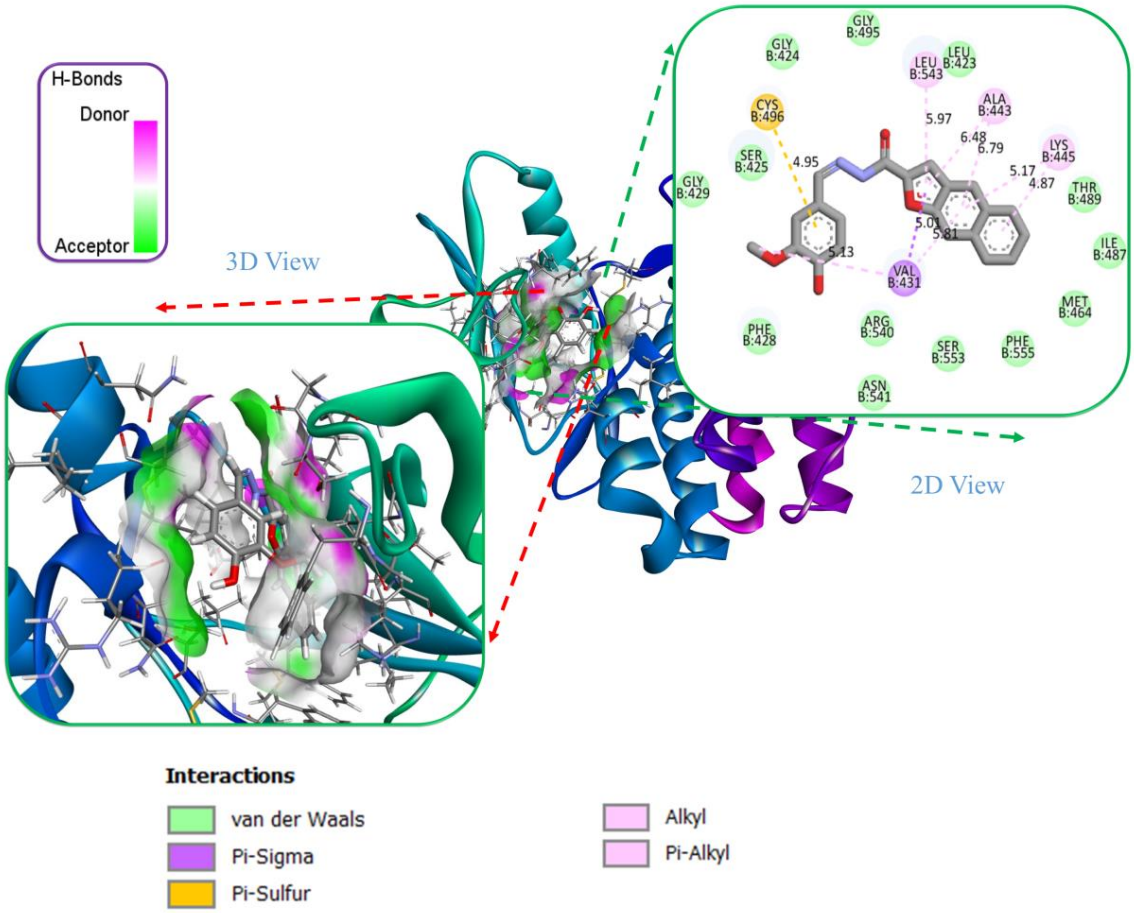

Figure 7. Ligand-3SXR mode of interaction with enzymes; 3D view of the donor/acceptor surface of hydrogen bonds on the receptor and 2D view of ligand enzyme interactions

3.8. ADME Analysis

Drug research and development heavily relies on the prediction of ADME characteristics. Early assessment of ADME characteristics reduces screening and trial time and costs by identifying the best candidates for drug development and rejecting those that are unlikely to succeed. By including kinetic mechanisms, the ultimate purpose of ADME modeling is to anticipate the in vivo propensity behavior of therapeutic candidate chemicals in the human body [39]. ADME analysis was performed to predict the ADME properties of HMFC molecule which is of great importance in drug research and development. Table 7 provides the following information about HMFC compound: molecular weight, percent absorption, topological polar surface region, estimated volume, number of rotatable bonds, and number of hydrogen bond donors and acceptors. When we examine the values in Table 7, according to Lipinski's five important rules; having less than 5 hydrogen bond donors (2), less than 10 hydrogen bond acceptors (5), lipophilicity coefficient LogP being less than 5 (3.46), molar refraction values between 4-130 (103.40) and finally We found that the molecular weight (MW) being lower than 500 (360.36) fits. It demonstrates that Lipinski's criteria has not been broken and that this molecule is appropriate for the drug development process. Using %A=109-(0.345xTPYA) to compute the percent absorption, the compounds had a decent absorption profile of 79.99%. The color regions and physicochemical parameters of molecule HMFC have been shown in Figure 8. When we examine Figure 8, The pink region on polar surface area maps symbolizes the physicochemical area suitable for oral bioavailability. According to the radar diagram, it is aside from the saturation setting, in the pink region. LogP is a measure of the lipophilicity or hydrophobicity of the compound. LogP > 0 indicates that the drug is

lipophilic and LogP < 0 indicates that the drug is hydrophilic. Since the compound has LogP >0 (3.46), it shows that the compound is lipophilic as a drug. According to Lipinski's rule, one of the most important chemical descriptors that correlates well with PK properties is the topological polar surface area (TPSA) and the TPSA of a good drug should be less than 140 Å. The TPSA value of HMFC compound was calculated as 84.06 and we think that it will be evaluated as a good drug candidate.

Table 7. Physicochemical and lipophilicity of molecule HMFC

Code DHPM	Lipophilicity consensus log P	Physico-chemical properties								
		MW[a] g/mol	Heavy Atoms	Aromatic heavy atoms	Rot. bond	H-acceptor bond	H-donor bond	MR[b]	TPSA[c] (A^2)	% ABS[d]
	3.46	360.36	27	19	5	5	2	103.40	84.06	79.99

[a]**MW**, molecular weight; [c]**TPSA**, topological polar surface area; [b]**MR**, molar refractivity; [d]**ABS%:** absorption percent $ABS\% = 109 - [0.345 \times TPSA]$.

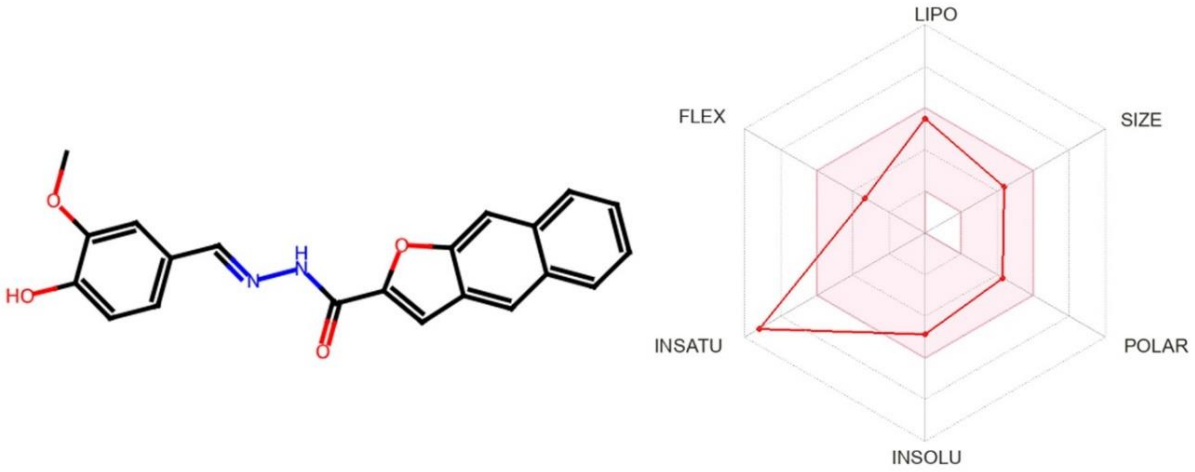

Figure 8. Color regions and physicochemical parameters of molecule HMFC

4. CONCLUSION

The initial step in HMFC investigation was to optimize the geometry to discover the least energy, or stable structure, of the molecule. The optimization process led to the determination of the molecule's bond lengths and bond angles. The molecule's total energies and leading molecular orbital energies were then calculated. These energies were used to calculate the molecular properties (η, or electronegativity, and η, or molecular stiffness), based on HOMO-LUMO energy differences. Examining the variations in NBO hybridization % and Mulliken and NBO atomic charge values, it was discovered that there were relatively few variations. The molecular electrostatic potential energy surface map (MEP) and nonlinear optical characteristics (polarizability, anisotropic polarizability, and high polarizability) were ascertained in order to provide further insight into the molecule under investigation. We were able to determine the regions where the compound might have non-covalent interactions by looking at the MEP map, which showed that the positive potential region was around the hydrogen and methyl atoms, and the negative potential region was around the electronegative atoms. HMFC compound's potential anticancer activity was tested on two different proteins, PDB ID: 1T46 and PDB ID: 3SXR. The optimum docking modes for the proteins PDB: 1T46 and PDB: 3SXR were found to have binding affinities of -7.356 kcal/mol and -6.866 kcal/mol, respectively, in the molecular docking study. Examining the two-dimensional view of the binding interactions to the residues in the molecular docking

analysis, it is evident that the interactions belong to the hydrogen bond, carbon-hydrogen bond, and van der Waals interactions and are active in the region with a high electrophilic nature. Finally, the HMFC investigation included molecular ADME analysis. According to the Adme research, it has an excellent absorption profile of 79.99%, and the field that produces safe and effective medications may find use for the study's findings.

CONFLICT OF INTEREST

There are no conflicts of interest as to publication of this article.

CRediT AUTHOR STATEMENT

Kenan Gören: Supervision, Writing-Review and Editing, **Mehmet Bağlan:** Research, Software, Writing-original draft, **Ümit Yıldıko:** Conceptualization, Formal analysis.

REFERENCES

[1] Raczuk E, Dmochowska B, Samaszko-Fiertek J and Madaj J. Different Schiff bases structure, importance and classification. Molecules. 2022; 27(3): 787.

[2] Ashraf MA, Mahmood K, Wajid A, Maah MJ and Yusoff I. Synthesis, characterization and biological activity of Schiff bases. IPCBEE. 2011; 10(1): 185.

[3] Da Silva CM, da Silva DL, Modolo LV, Alves RB, de Resende MA, Martins C V and de Fátima Â. Schiff bases: A short review of their antimicrobial activities. J. Adv. Res. 2011; 2(1): 1-8.

[4] El-Sonbati A, Mahmoud W, Mohamed GG, Diab M, Morgan SM and Abbas S. Synthesis, characterization of Schiff base metal complexes and their biological investigation. Appl. Organomet. Chem. 2019; 33(9): 5048.

[5] Dalia SA, Afsan F, Hossain MS, Khan MN, Zakaria C, Zahan M-E and Ali M. A short review on chemistry of schiff base metal complexes and their catalytic application. Int. J. Chem. Stud. 2018; 6(3): 2859-2867.

[6] Zhang J, Xu L and Wong W-Y. Energy materials based on metal Schiff base complexes. Coord. Chem. Rev. 2018; 355(180-198.

[7] Juyal VK, Pathak A, Panwar M, Thakuri SC, Prakash O, Agrwal A and Nand V. Schiff base metal complexes as a versatile catalyst: A review. J. Organomet. Chem. 2023; 122825.

[8] Hussain W, Amir A and Rasool N. Computer-aided study of selective flavonoids against chikungunya virus replication using molecular docking and DFT-based approach. Struct. Chem. 2020; 31: 1363-1374.

[9] Bubaš M, and Sancho-Parramon J. DFT-Based Approach Enables Deliberate Tuning of Alloy Nanostructure Plasmonic Properties. J. Phys. Chem. C. 2021; 125(43): 24032-24042.

[10] Gertig C, Leonhard K and Bardow A. Computer-aided molecular and processes design based on quantum chemistry: current status and future prospects. Curr. Opin. Chem. Eng. 2020; (27): 89-97.

[11] Liu Q, Tang K, Zhang J, Feng Y, Xu C, Liu L, Du J and Zhang L, QMaC: a quantum mechanics/machine learning-based computational tool for chemical product design, in Computer Aided Chemical Engineering. 2020, Elsevier. p. 1807-1812.

[12] Papadopoulos-A I, Tsivintzelis I, Linke P and Seferlis P. Computer aided molecular design: fundamentals, methods and applications. Chem., Mol. Sci. and Chem. Eng. 2018;

[13] T. Michael J. Frisch G W, Bernhard Schlegel, Gustavo Scuseria, 2016.

[14] Release S. 3: Maestro Schrödinger. LLC, New York 2019.

[15] Gören K, Bağlan M and Çakmak İ. Dietanol Amin Ditiyokarbamat RAFT Ajanının ^{1}H ve ^{13}C NMR Spektrumlarının Teorik İncelenmesi. J. Integr. Sci. Technol. 2022; 12(3): 1677-1689.

[16] Gören K, Bağlan M and Yıldıko Ü. Melanoma Cancer Evaluation with ADME and Molecular Docking Analysis, DFT Calculations of (E)-methyl 3-(1-(4-methoxybenzyl)-2,3-dioxoindolin-5-yl)-acrylate Molecule. JIST. 2024; 14(3): 1186-1199.

[16] Bağlan M, Gören K and Yıldıko Ü. HOMO–LUMO, NBO, NLO, MEP analysis and molecular docking using DFT calculations in DFPA molecule. Int. J. Chem. Technol. 2023; 7(1): 38-47.

[17] Kinaytürk NK. Elucidation of the Molecular Interaction Mechanism of Bromuconazole by DFT and Molecular Docking Methods. Süleyman Demirel Üniversitesi Fen Bilimleri Enstitüsü Dergisi. 2023; 27(2): 266-272.

[18] Saraç K. Synthesis and Theoretical Chemical Calculations of 4-Chloromethyl-6,8-dimethylcoumarin Compound. Bitlis Eren Üniversitesi Fen Bilimleri Dergisi. 2018; 7(2): 311-319.

[19] Gören K and Yıldıko Ü. Aldose Reductase Evaluation against Diabetic Complications Using ADME and Molecular Docking Studies and DFT Calculations of Spiroindoline Derivative Molecule. Süleyman Demirel Üniversitesi Fen Bilimleri Enstitüsü Dergisi. 2024; 28(2): 281-292.

[20] Bağlan M, Gören K and Yıldıko Ü. DFT Computations and Molecular Docking Studies of 3-(6-(3-aminophenyl) thiazolo [1, 2, 4] triazol-2-yl)-2H-chromen-2-one (ATTC) Molecule. HJSE. 2023; 10(1): 11-19.

[21] Gümüş HP, Tamer Ö, Avcı D and Atalay Y. 4-(Metoksimetil)-1,6-dimetil-2-okso-1,2-dihidropiridin-3-karbonitril molekülünün teorik olarak incelenmesi. Sakarya University Jounal of Science. 2015; 19(3): 303-311.

[22] Choudhary V, Bhatt A, Dash D and Sharma N. DFT calculations on molecular structures, HOMO–LUMO study, reactivity descriptors and spectral analyses of newly synthesized diorganotin (IV) 2-chloridophenylacetohydroxamate complexes. J. Comput. Chem. 2019; 40(27): 2354-2363.

[23] Mumit MA, Pal TK, Alam MA, Islam M, Paul S and Sheikh M C. DFT studies on vibrational and electronic spectra, HOMO–LUMO, MEP, HOMA, NBO and molecular docking analysis of benzyl-3-N-(2,4,5-trimethoxyphenylmethylene) hydrazinecarbodithioate. J. Mol. Struct. 2020; 1220(128715.

[24] Gören K, Bağlan M, Yıldıko Ü and Tahiroğlu V. Molecular Docking and DFT Analysis of Thiazolidinone-Bis Schiff Base for anti-Cancer and anti-Urease Activity. JIST. 2024; 14(2): 822-834.

[25] Bağlan M, Yıldıko Ü and Gören K. Computational Investigation of 5.5,7-trihydroxy-3,7-dimethoxy-4-4-O-biflavone from Flavonoids Using DFT Calculations and Molecular Docking. Adıyaman University Journal of Science. 2022; 12(2): 283-298.

[26] Lakshminarayanan S, Jeyasingh V, Murugesan K, Selvapalam N and Dass G. Molecular electrostatic potential (MEP) surface analysis of chemo sensors: An extra supporting hand for strength, selectivity & non-traditional interactions. J. Photochem. Photobiol. 2021; 6(100022.

[27] Bağlan M, Yıldıko Ü and Gören K. DFT Calculations and Molecular Docking Study in 6-(2"-Pyrrolıdınone-5"-Yl)-(-) Epicatechin Molecule From Flavonoids. Eskişehir Teknik Üniversitesi Bilim ve Teknoloji Dergisi B-Teorik Bilimler. 2023; 11(1): 43-55.

[28] Aziz A, Elantabli FM, Moustafa H, and El-Medani SM. Spectroscopic, DNA binding ability, biological activity, DFT calculations and non-linear optical properties (NLO) of novel Co (II), Cu (II), Zn (II), Cd (II) and Hg (II) complexes with ONS Schiff base. J. Mol. Struct. 2017; 1141(563-576.

[29] Gören K, Çimen E, Tahiroğlu V and Yıldıko Ü. Moleculer Docking and Theoretical Analysis of the (E)-5-((Z)-4-methylbenzylidene)-2-(((E)-4-methylbenzylidene)hydrazineylidene)-3-phenylthiazolidin-4-one Molecule. Bitlis Eren Üniversitesi Fen Bilimleri Dergisi. 2024; 13(3): 659-672.

[30] Shokr EK, Kamel MS, Abdel-Ghany H, Ali M and Abdou A. Synthesis, characterization, and DFT study of linear and non-linear optical properties of some novel thieno-[2, 3-b] thiophene azo dye derivatives. Mater. Chem. 2022; 290(126646.

[31] Khan AU, Khera RA, Anjum N, Shehzad RA, Iqbal S, Ayub K and Iqbal J. DFT study of superhalogen and superalkali doped graphitic carbon nitride and its non-linear optical properties. RSC advances. 2021; 11(14): 7779-7789.

[32] Tanriverdi A, Altun K, Yildiko Ü and Çakmak İ. Structural and spectral properties of 4-(4-(1-(4-Hydroxyphenyl)-1-phenylethyl)phenoxy)phthalonitrile: Analysis by TD-DFT method, ADME analysis and docking studies. Int. J. Chem. Technol. 2021; 5(2): 147-155.

[33] Demircioğlu Z, Kaştaş ÇA and Büyükgüngör O. The spectroscopic (FT-IR, UV–vis), Fukui function, NLO, NBO, NPA and tautomerism effect analysis of (E)-2-[(2-hydroxy-6-methoxybenzylidene) amino] benzonitrile. Mol. Biomol. Spectrosc. 2015; 139(539-548.

[34] Kazachenko AS, Akman F, Abdelmoulahi H, Issaoui N, Malyar YN, Al-Dossary O and Wojcik MJ. Intermolecular hydrogen bonds interactions in water clusters of ammonium sulfamate: FTIR, X-ray diffraction, AIM, DFT, RDG, ELF, NBO analysis. J. Mol. Liq. 2021; 342(117475.

[35] Pisano MB, Kumar A, Medda R, Gatto G, Pal R, Fais A, Era B, Cosentino S, Uriarte E and Santana L. Antibacterial activity and molecular docking studies of a selected series of hydroxy-3-arylcoumarins. Molecules. 2019; 24(15): 2815.

[36] Obuotor TM, Kolawole AO, Apalowo OE and Akamo AJ. Metabolic profiling, ADME pharmacokinetics, molecular docking studies and antibacterial potential of Phyllantus muellerianus leaves. Tradit. Med. 2023; 23(2): 427-442.

[37] Hamed IA, Ashida N and Nagamatsu T. Antitumor studies. Part 4: Design, synthesis, antitumor activity, and molecular docking study of novel 2-substituted 2-deoxoflavin-5-oxides, 2-deoxoalloxazine-5-oxides, and their 5-deaza analogs. BMCL. 2008; 16(2): 922-940.

[38] Liu F et al. Discovery of a Selective Irreversible BMX Inhibitor for Prostate Cancer. Chem. Biol. 2013; 8(7): 1423-1428.

ESKİŞEHİR TEKNİK ÜNİVERSİTESİ BİLİM VE TEKNOLOJİ DERGİSİ
B- TEORİK BİLİMLER

Eskişehir Technical University Journal of Science and Technology B- Theoretical Sciences

Estuscience – Theory, 2025, 13 [1] pp. 24-34, DOI:10.20290/estubtdb.1632300

RESEARCH ARTICLE

ON SOME CLASSES OF WEAKLY SUBDIFFERENTIABLE FUNCTIONS

Samet BILA [1,*], Refail KASIMBEYLI [2]

[1] Department of Mathematics, Faculty of Science, Eskisehir Technical University, Eskisehir, Turkiye.
sametbila@eskisehir.edu.tr - *0000-0002-5228-643X*

[2] Department of Industrial Engineering, Faculty of Engineering, Eskisehir Technical University, Eskisehir, Turkiye.
rkasimbeyli@eskisehir.edu.tr - *000-0002-7339-9409*

Abstract

This work presents a theorem that any Lipschitz function is weakly subdifferentiable with $\boldsymbol{x}^*$ component of the weak subgradient is different from $\mathbf{0}_{\mathbb{R}^n}$. This theorem is based on Kasimbeyli's nonlinear cone separation theorem. Also, we show that any positively homogeneous and continuous function is both upper and lower Lipschitz. Additionally, we show that positively homogeneous and lower semicontinuous functions are weakly subdifferentiable that the pair $(\boldsymbol{x}^*, \boldsymbol{c})$ which is a weak subgradient of a function in this case is different from $(\mathbf{0}_{\mathbb{R}^n}, \mathbf{0})$.

Keywords

Nonconvex Optimization,
The Weak Subdifferential,
Lipschitz functions,
Operations Research

Time Scale of Article

Received :03 Februay 2025
Accepted : 19 Februay 2025
Online date : 28 February 2025

1. INTRODUCTION

It is quite famous in convex analysis that at each boundary point a convex set has a supporting hyperplane. This idea leads to one of the central concepts of convex analysis, which is called subgradient. The study of subgradients in convex optimization has been a cornerstone in developing methods for optimality conditions and duality theorems [4,12,13]. However, if the set is not convex there does not exist any supporting hyperplanes at boundary points. Many researchers have tried to generalize for nonconvex problems on optimality conditions. Among these contributions, Azimov and Gasimov's weak subgradient definition emerges as a significant concept, introducing a novel approach to analyzing nonsmooth functions while retaining computational and theoretical practicality and the idea is very useful for analyzing optimality conditions in nonconvex optimization [1,3,5,6,7,8]. In [1,7] they use support cones instead of supporting hyperplanes. Therefore, this enables us to broaden the subdifferentiable class to the lower Lipschitz function class. This motivates our study on a broader class of weakly subdifferentiable functions.

In [10], it has been introduced a distinct separation property in Banach spaces for two closed cones, along with a nonlinear separation theorem applicable to cones having this relation. It also extends traditional dual cones definitions by introducing augmented dual cones. Also, it is well known that any lower Lipschitz function satisfy the weak subdifferentiability [1,2]. Based on the separation theorem

*Corresponding Author: sametbila@eskisehir.edu.tr

we establish a theorem that any Lipschitz function is weakly subdifferentiable with x^* component of (x^*, c) is different than zero vector of $\mathbb{R}^n$.

It is proven in [9] that positively homogeneous and continuous function is subdifferentiable. In this work, we show that positively homogeneous and lower semicontinuous function is weakly subdifferentiable.

2. PRELIMINARIES

Consider a normed space $(\mathbb{Y}, \|\cdot\|)$.

$$\mathbb{U} = \{\boldsymbol{y} \in \mathbb{Y}: \|\boldsymbol{y}\| = \mathbf{1}\}$$

is referred to as the unit sphere of $(\mathbb{Y}, \|\cdot\|)$ and,

$$\mathbb{B} = \{\boldsymbol{y} \in \mathbb{Y}: \|\boldsymbol{y}\| \leq \mathbf{1}\},$$

is referred to as the *unit ball* of the space $(\mathbb{Y}, \|\cdot\|)$. The nonempty set $\mathbb{C}$ contained in $\mathbb{Y}$ is considered a *cone* if, for any element $\boldsymbol{y}$ in $\mathbb{C}$ and any non-negative scalar $\boldsymbol{\lambda} \geq \mathbf{0}$, then $\boldsymbol{\lambda y}$ also belongs to $\mathbb{C}$.

A cone $\mathbb{C}$ is *pointed* if

$$\mathbb{C} \cap (-\mathbb{C}) = \{\mathbf{0}_{\mathbb{Y}}\}.$$

A cone *generating* by a set $\mathbb{S}$ is denoted by *cone*($\mathbb{S}$):

$$\textit{cone}(\mathbb{S})=\{\boldsymbol{\lambda s}: \boldsymbol{\lambda} \geq \mathbf{0}, \boldsymbol{s} \in \mathbb{S}\}.$$

Let $\mathbb{C} \neq \{\mathbf{0}_{\mathbb{Y}}\}$ be a convex cone. A nonempty convex subset $\mathbb{D}$ of $\mathbb{C}$ a is referred to as a base for $\mathbb{C}$ if each $\boldsymbol{y} \in \mathbb{C}$ if each $\boldsymbol{y} \in \mathbb{C}\backslash\{\mathbf{0}_{\mathbb{Y}}\}$ has a distinct representation in the form $\boldsymbol{y} = \boldsymbol{\lambda d}$ for some $\boldsymbol{\lambda} > \mathbf{0}$ and some $\boldsymbol{d} \in \mathbb{D}$. Throughtout this work, The norm base of the cone $\mathbb{C}$ is represented by $\mathbb{C}_{\mathbb{U}} = \mathbb{C} \cap \mathbb{U}=\{\boldsymbol{y} \in \mathbb{C}: \|\boldsymbol{y}\| = \mathbf{1}\}$.

Definition 2.1: Consider $(\mathbb{Y}, \|\cdot\|)$ as a real normed space where partial ordering is determined by a cone $\mathbb{C}$ which is closed, convex, pointed . The definition of the dual cone $\mathbb{C}^*$ is as follows:

$$\mathbb{C}^* = \{\boldsymbol{z}^* \in \mathbb{Y}^*: \langle \boldsymbol{z}^*, \boldsymbol{z}\rangle \geq \mathbf{0}, \forall \boldsymbol{z} \in \mathbb{C}\}.$$

and quasi interior of $\mathbb{C}^*$ denoted by $\mathbb{C}^{\#}$ is given as follows:

$$\mathbb{C}^{\#} = \{\boldsymbol{z}^* \in \mathbb{Y}^*: \langle \boldsymbol{z}^*, \boldsymbol{z}\rangle > \mathbf{0}, \forall \boldsymbol{z} \in \mathbb{C}\backslash\{\mathbf{0}\}\}.$$

The extended version of these definitions are presented in [10] and called augmented dual cones are given as follows: Let

$$\mathbb{C}^{\boldsymbol{a}*} = \{(\boldsymbol{z}^*, \boldsymbol{a}) \in \mathbb{C}^{\#} \times \mathbb{R}_+: \langle \boldsymbol{z}^*, \boldsymbol{z}\rangle - \boldsymbol{a}\|\boldsymbol{z}\| \geq \mathbf{0}, \forall \boldsymbol{z} \in \mathbb{C}\},$$

$$\mathbb{C}^{\boldsymbol{a}\circ} = \{(\boldsymbol{z}^*, \boldsymbol{a}) \in \mathbb{C}^{\#} \times \mathbb{R}_+: \langle \boldsymbol{z}^*, \boldsymbol{z}\rangle - \boldsymbol{a}\|\boldsymbol{z}\| > \mathbf{0}, \forall \boldsymbol{z} \in \boldsymbol{int}(\mathbb{C})\},$$

and

$$\mathbb{C}^{\boldsymbol{a}\#} = \{(\boldsymbol{z}^*, \boldsymbol{a}) \in \mathbb{C}^{\#} \times \mathbb{R}_+: \langle \boldsymbol{z}^*, \boldsymbol{z}\rangle - \boldsymbol{a}\|\boldsymbol{z}\| > \mathbf{0}, \forall \boldsymbol{z} \in \mathbb{C}\backslash\{\mathbf{0}_{\mathbb{Y}}\}\}.$$

In the definition of $\mathbb{C}^{\boldsymbol{a}\circ}$ assumes that the interior of the ordering cone $\boldsymbol{int}(\mathbb{C})$ is not empty.

Definition 2.2: A pair (x^*, c) which is in $\mathbb{R}^n \times \mathbb{R}_+$is referred to as a weak subgradient of h at x_0 on the set S provided that

$$\langle x^*, x - x_0\rangle - c\|x - x_0\| \leq h(x) - h(x_0) \text{ for all } x \in S \quad (1)$$

The weak subdifferential set contains all weak subgradients of h at x_0 and it is represented as $\partial_S^w h(x)$:

$$\partial_S^w h(x_0) = \{(x^*, c) \in \mathbb{R}^n \times \mathbb{R}_+ : (1) \text{ is satisfied}\}$$

Remark 2.3: If $\partial_S^w h(x_0) \neq \emptyset$, then h is called the weakly subdifferentiable at x_0. If we let $S = \mathbb{R}^n$ then we ignore the subscript S in $\partial_S^w h(x_0)$, and denote it by $\partial^w h(x_0) = \partial_{\mathbb{R}^n}^w h(x_0)$. It is obvious that if function h is subdifferentiable at x_0 then h is also weakly subdifferentiable at x_0. One can check if $x^* \in \partial h(x_0)$ then by definition $(x^*, c) \in \mathbb{R}^n \times \mathbb{R}_+$ for every $c \geq 0$. The weak subgradient of h is geometrically interpreted as:
$(x^*, c) \in \mathbb{R}^n \times \mathbb{R}_+$ is a weak subgradient of h at $x_0 \in X$ if one can found a function

$$f(x) = \langle x^*, x - x_0\rangle - c\|x - x_0\| + h(x_0) \quad (2)$$

which is continuous, concave and, satisfies $h(x) \leq f(x)$, $\forall x \in X$ and $h(x_0) = f(x_0)$. The hypograph of the function f is defined as hypo $(f) = \{(x, a) \in X \times \mathbb{R} \mid f(x) \geq a\}$ and it is a closed cone in $X \times \mathbb{R}$ with its vertex at $(x_0, f(x_0))$. To verify:

$$\begin{aligned} hypo\ (f) - \big(x_0, h(x_0)\big) &= \big\{\big(x - x_0, a - h(x_0)\big) \in X \times \mathbb{R} \mid \langle x^*, x - x_0\rangle - c\|x - x_0\| \geq a - h(x_0)\} \\ &= \{(u, b) \in X \times \mathbb{R} \mid \langle x^*, u\rangle - c\|u\| \geq b\}. \end{aligned}$$

Thus, from (1) and (2) hypo (f) is a supporting cone of the set

$$epi\ (\text{f}) = \{(x, a) \in X \times \mathbb{R} \mid f(x) \leq a\}$$

at the point $(x_0, h(x_0))$ in the way that epi(f) $\subset (X \times \mathbb{R}) \setminus hypo(f)$ and $cl(epi(f)) \cap graph(f) \neq \emptyset$ where $graph\ (f) = \{(x, a) \in X \times \mathbb{R} \mid f(x) = a\}$.

In [1], they derived the weak subdifferential for the specific subclasses of lower Lipschitz functions. Lower Lipschitz function definition is given as follows:

Definition 2.4: A function g from X into $\mathbb{R}$ is referred as "lower locally Lipschitz" at $x_0 \in X$ if there exists a positive constant L and a neighborhood $\mathcal{N}(x_0)$ around x_0 such that

$$-L\|x - x_0\| \leq g(x) - g(x_0), \quad \forall x \in \mathcal{N}(x_0). \quad (3)$$

The function g is said to be lower Lipschitz at x_0 where L is called the Lipschitz constant if for all $x \in X$ the inequality (3) holds true.
An example of the weak subdifferential is presented.

Example 2.4: Let g: $\mathbb{R} \to \mathbb{R}$ be given as

$$g(x) = \begin{cases} (x+1)^2 & if\ x \leq 1, \\ (x-2)^2 + 3 & if\ x > 1. \end{cases}$$

The graph of function g is given below.

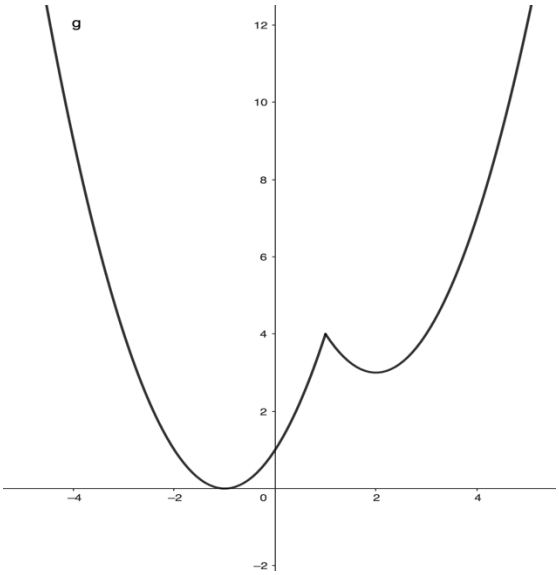

We want to calculate the weak subdifferentiable of g at $x_0 = 1$. Clearly, function g is not subdifferentiable at $x_0 = 1$.

First, the case $x \leq 1$ is considered. The definition 2.2 implies that:

$$\langle t, x - x_0 \rangle - c\|x - x_0\| \leq g(x) - g(x_0) = (x+1)^2 - g(1)$$
$$t(x-1) - c(1-x) \leq (x^2 + 2x + 1) - 4$$
$$(x-1)(t+c) \leq x^2 + 2x - 3$$

Then $\partial^w g(1)$ for the case $x \leq 1$ obtained as:

$$\partial^w g(1) = \{(t,c) \in \mathbb{R} \times \mathbb{R}_+ : v + c > 4\}$$

Then we consider the case $x > 1$. The weak subdifferential definition indicates that:

$$\langle t, x - x_0 \rangle - c\|x - x_0\| \leq g(x) - g(x_0)$$
$$\langle t, x - 1 \rangle - c|x - 1| \leq (x-2)^2 + 3 - g(1)$$
$$(t-c)(x-1) \leq (x^2 - 4x + 4) + 3 - 4$$
$$(x-1)(t-c) \leq x^2 - 4x + 3$$

Then $\partial^w g(1)$ for the case $x > 1$ obtained as:

$$\partial^w g(1) = \{(t,c) \in \mathbb{R} \times \mathbb{R}_+ : t - c \leq -2\}.$$

Then finally we obtained that:

$$\partial^w g(1) = \{(t,c) \in \mathbb{R} \times \mathbb{R}_+ : -c + 4 \leq t \leq c - 2\}.$$

3. A CLASS OF WEAKLY SUBDIFFERENTIABLE FUNCTIONS

The below corollary provides a condition for a function to be weakly subddifferentiable.

Corollary 3.1: [1, Corollary 3.1] Assume that $\boldsymbol{h}$ is bounded from below and proper function from $\boldsymbol{X}$ into $\mathbb{R} \cup \{+\infty\}$ and lower locally Lipschitz at $\bar{\boldsymbol{x}}$. Then $\boldsymbol{h}$ is said to be weakly subdifferentiable at $\bar{\boldsymbol{x}}$.

The following theorem express a criteria for a weakly subddifferentiability of a function.

Theorem 3.2: [2, Theorem 1] Assume that function $\boldsymbol{h}$: $\mathbb{R}^{\boldsymbol{n}}$ is finite at $\boldsymbol{x_0}$ then the following conditions are equivalent:

i) $\boldsymbol{h}$ is lower Lipschitz at $\bar{\boldsymbol{x}}$.
ii) $\boldsymbol{h}$ is weakly subdifferentialbe at $\bar{\boldsymbol{x}}$.
iii) $\boldsymbol{h}$ is lower locally Lipschitz at $\bar{\boldsymbol{x}}$ and there exists numbers $\boldsymbol{p} \geq \boldsymbol{0}$ and $\boldsymbol{q}$ such that

$$\boldsymbol{h}(\boldsymbol{y}) \geq -\boldsymbol{p}\|\boldsymbol{y}\| + \boldsymbol{q}, \forall \boldsymbol{y} \in \mathbb{R}^{\boldsymbol{n}}.$$

Lemma 3.3: [9, Lemma 2.7] Let $\boldsymbol{f}$ be bounded from below on some neighborhood of zero and positively homogeneous function from $\boldsymbol{X}$ into $\mathbb{R}$. Then $\boldsymbol{f}$ is a weakly subdifferentiable at $\boldsymbol{0_X}$.

We define the subsequent norm on $\mathbb{R}^{n+1}$.

Let $v \in \mathbb{R}^n \; and \; a \in \mathbb{R}$ then

$$\|(v, c)\| = \|v\| + |c|$$

defines a norm on $\mathbb{R}^{n+1}$. One can verify the norm properties easily.
The following definition concerns with the separation of the cones in normed spaces.

Definition 3.4: [10, Definition 4.1] Let $(\mathbb{Y}, \|\cdot\|)$ be a normed space and assume that $\mathbb{C}$ and $\mathbb{K}$ be closed cones taken from $(\mathbb{Y}, \|\cdot\|)$ with norm bases $\mathbb{C}_{\mathbb{U}}$ and $\mathbb{K}_{\mathbb{U}}$, respectively. Suppose that ${\mathbb{K}_{\mathbb{U}}}^{\partial} = \mathbb{K}_{\mathbb{U}} \cap bd(\mathbb{K})$, and let $\tilde{\mathbb{K}}^{\partial}$ and $\tilde{\mathbb{C}}$ represent the closures of the sets $co({\mathbb{K}_{\mathbb{U}}}^{\partial} \cup \{0_{\mathbb{Y}}\})$ and $co(\mathbb{C}_{\mathbb{U}})$, respectively. The separation relation holds with respect to norm $\|\cdot\|$ for the cones $\mathbb{C}$ and $\mathbb{K}$ if

$$\tilde{\mathbb{C}} \cap \tilde{\mathbb{K}}^{\partial} = \emptyset. \tag{4}$$

The following lemma is proved in [10] and we rewrite the theorem for the $\mathbb{R}^{n+1}$ case.

Lemma 3.5: Suppose that $\mathbb{C}$ and $\mathbb{K}$ denote two nonempty cones in the space $\mathbb{Y}$. Assume that $\mathbb{C}^{a*} \neq \emptyset$. Then for each $((x^*, a^*), \alpha) \in \mathbb{C}^{a*}$ with $\alpha > 0$, the sublevel sets $S((x^*, a^*), \alpha)$ defined by

$$S((x^*, a^*), \alpha) = \{(x, a) \in \mathbb{Y}: \langle (x^*, a^*), (x, a) \rangle + \alpha\|(x, a)\| \leq 0 \}$$

is a pointed and closed cone that contains $-\mathbb{C}$.

Proof. The proof can be done by following similar steps of the proof of Lemma 3.2 in [9].

We following theorem is presented in [10] and we show that when the cones $\mathbb{C}$ and $\mathbb{K}$ belong to the $\mathbb{R}^{n+1}$ the theorem remains true.

Theorem 3.6: Assume that $\mathbb{C}$ and $\mathbb{K}$ be two closed cones are taken from a reflexive Banach space $(\mathbb{Y}, \|\cdot\|)$. Suppose the cones $-\mathbb{C}$ and $\mathbb{K}$ fulfill the separation relation outlined in definition 3.3,

$$\tilde{\mathbb{C}} \cap \tilde{\mathbb{K}}^{\partial} = \emptyset.$$

It implies that, $\mathbb{C}^{a\#} \neq \emptyset$ and there exists $((x^*, a^*), \alpha) \in \mathbb{C}^{a\#}$ such that the corresponding sublevel set

$S((x^*, a^*), \alpha)$ of the strongly monotonically increasing sublevel function

$$g(x,a) = \langle (x^*, a^*), (x,a) \rangle + \alpha \|(x,a)\|$$

separates the cones $-\mathbb{C}$ and $bd(\mathbb{K})$ in the following manner

$$\langle (x^*, a^*), (\hat{x}, \hat{a}) \rangle + \alpha \|(\hat{x}, \hat{a})\| < 0 \leq \langle (x^*, a^*), (x,a) \rangle + \alpha \|(x,a)\| \tag{5}$$

for all $(\hat{x}, \hat{a}) \in -\mathbb{C} \backslash \{0_{\mathbb{Y}}\}$ and $(x,a) \in bd(\mathbb{K})$. Then $-\mathbb{C}$ is pointed cone. Conversely, if there exists a pair $((x^*, a^*), \alpha) \in \mathbb{C}^{a\#}$ such that the corresponding sublevel set

$S((x^*, a^*), \alpha)$ of the strongly monotonically increasing sublevel function

$$g(x,a) = \langle (x^*, a^*), (x,a) \rangle + \alpha \|(x,a)\|$$

separates the cones $-\mathbb{C}$ and $bd(\mathbb{K})$ in the following manner of (5) and if either $(\mathbb{Y}, \|\cdot\|)$ is a finite dimensional space or $\mathbb{C}$ is closed and convex cone, then the cones $\mathbb{C}$ and $\mathbb{K}$ fulfill the separation relation in (4).

Proof. We omit the proof since it can be done similarly with the proof in [10, Theorem 4.3].

Now we present a separation relation for an arbitrary closed cone $\mathbb{K}$ which belongs to $\mathbb{R}^{n+1}$.

Lemma 3.7: Let $\mathbb{K}$ be a closed cone in $\mathbb{R}^{n+1}$ and assume that $(\hat{y}, \hat{a}) \notin \mathbb{K}$. Then a vector $(y,a) \in \mathbb{R}^{n+1} \backslash \{0_{\mathbb{R}^{n+1}}\}$ and a positive real number $\alpha \geq 0$ exist such that

$$\langle (y^*, a^*), (\hat{y}, \hat{a}) \rangle + \alpha \|(\hat{y}, \hat{a})\| < 0 \leq \langle (y^*, a^*), (y,a) \rangle + \alpha \|(y,a)\| \qquad \text{for all } (y,a) \in \mathbb{K}$$

Proof. In this proof, the idea is based on [11, Lemma 3.1].

Let $\|(\hat{y}, \hat{a})\| = 1$ and $\alpha = 1 - \frac{\varepsilon^2}{2}$. $\mathbb{K}$ is a closed cone and $(\hat{y}, \hat{a}) \notin \mathbb{K}$ thus there exists $\varepsilon \in (0,1)$ such that

$$N_\varepsilon(\hat{y}, \hat{a}) = \{(y,a) \in \mathbb{R}^{n+1} : \|(y - \hat{y}, a - \hat{a})\| \leq \varepsilon\}$$

Assume that

$$\mathbb{C} = cone(N_\varepsilon(\hat{y}, \hat{a}))$$

and

$$\mathbb{C}_{\mathbb{U}} = \{(y,a) \in \mathbb{U} : \|(y - \hat{y}, a - \hat{a})\| \leq \varepsilon\}.$$

$$\begin{aligned}
(y,a) \in \mathbb{C}_{\mathbb{U}} &\Leftrightarrow \|(y - \hat{y}, a - \hat{a})\|^2 \leq \varepsilon^2 \\
&\Leftrightarrow \|(y - \hat{y})\|^2 + (a - \hat{a})^2 \leq \varepsilon^2 \\
&\Leftrightarrow \|\hat{y}\|^2 + 2\langle y, \hat{y} \rangle + \|y\|^2 + a^2 + 2a\hat{a} + \hat{a}^2 \leq \varepsilon^2 \\
&\Leftrightarrow 2 - 2(\langle y, \hat{y} \rangle + a\hat{a}) \leq \varepsilon^2 \\
&\Leftrightarrow 1 - \frac{\varepsilon^2}{2} \leq \langle y - \hat{y}, a - \hat{a} \rangle \text{ for all } (y,a) \in \mathbb{U} \cap \mathbb{K}.
\end{aligned}$$

The rest of the proof follows similarly.

For a given set $\boldsymbol{S} \subset \mathbb{R}^{\boldsymbol{n+1}}$ and a point at $(\bar{\boldsymbol{y}}, \bar{\boldsymbol{a}}) \in \boldsymbol{S}$, we present the separation theorem.

Theorem 3.8: Assume that $\boldsymbol{S} \subset \mathbb{R}^{\boldsymbol{n+1}}$ be cone shaped at $(\bar{\boldsymbol{y}}, \bar{\boldsymbol{a}}) \in \boldsymbol{S}$. In that case, the cone $\mathbb{C} \subset \mathbb{R}^{\boldsymbol{n+1}}$ exists which is pointed and closed that satisfy

$$(\boldsymbol{S} - \{(\bar{\boldsymbol{y}}, \bar{\boldsymbol{a}})\}) \cap \mathbb{C}\backslash\{\boldsymbol{0}_{\mathbb{R}^n}\} = \emptyset$$

and there exists $((\boldsymbol{y}^*, \boldsymbol{a}^*), \boldsymbol{\alpha}) \in (-\mathbb{C})^{\#}$ satisfying

$$\langle (y^*, a^*), (y, a) - (\bar{y}, \bar{a}) \rangle + \alpha \|(y, a) - (\bar{y}, \bar{a})\| \geq 0, \forall (y, a) \in S.$$

Proof: This theorem can be proven easily by following [11, Theorem 3.2].

The subsequent theorem asserts that if a function is positively homogeneous and continuous then it is both lower and upper Lipschitz.

Theorem 3.9: Assume that the function $f: \mathbb{R}^n \to \mathbb{R}$ is a continuous, positively homogeneous. Then f is Lipschitz.

Proof: We know that if f is continuous on $S_1 = \{u \in S: \|u\| = 1\}$ then it attains its minimum and maximum on S_1. Thus there exists real numbers m and M with

$$f(u) \geq m \text{ for all } u \in S_1$$

and

$$f(u) \leq M, \text{ for all } u \in S_1. \tag{6}$$

Take any $x \in S$. Then there exists some $t > 0$ and $x \in S_1$ such that $x = tu$. Therefore,

$$\boldsymbol{f(x) - f(0) = f(x) = f(tu) = tf(u) \geq tm = tm\|u\| = m\|tu\| = m\|x\|} \tag{7}$$

Now, if $\boldsymbol{m > 0}$ then (7) implies that:

$$\boldsymbol{-L\|x\| \leq m\|x\| \leq f(x) - f(0)} \tag{8}$$

where $\boldsymbol{L}$ is an arbitrary positive real number.

If $\boldsymbol{m < 0}$ in (7) then,

$$\boldsymbol{-L\|x\| \leq m\|x\| \leq f(x) - f(0)} \text{ where } \boldsymbol{L > 0} \text{ and } \boldsymbol{-L = m < 0}. \tag{9}$$

Thus (8) and (9) together imply that $\boldsymbol{f}$ is lower Lipschitz. Now since $\boldsymbol{f}$ is bounded above (6) implies that,

$$\boldsymbol{f(x) - f(0) = f(x) = f(tu) = tf(u) \leq tM = tM\|u\| = M\|tu\| = m\|x\|}$$

If $\boldsymbol{M > 0}$, we know that,

$$\boldsymbol{f(x) - f(0) \leq M\|x\| = L\|x\|.} \tag{10}$$

If $\boldsymbol{M < 0}$, then

$$\boldsymbol{f(x) - f(0) \leq M\|x\| \leq L\|x\|} \text{ where } \boldsymbol{L > 0} \text{ and arbitrary.} \tag{11}$$

(9) and (10) imply that $\boldsymbol{f}$ is upper Lipschitz. Thus $\boldsymbol{f}$ is Lipschitz and there exists $\boldsymbol{L > 0}$ such that

$$\boldsymbol{|f(x) - f(0)| \leq L\|x - 0\|.}$$

The proof is completed.

The following theorem shows that positively homogeneous and lower semicontinuous functions are weakly subdifferentiable and it is worth to emphasize that the pair $(\boldsymbol{x^*, c})$ in this case is different from $(\boldsymbol{0_{\mathbb{R}^n}, 0})$.

Theorem 3.10: Let $f: \mathbb{R}^n \to \mathbb{R}$ be lower semicontinuous and positively homogeneous function on the cone S. Then f is weakly subdifferentiable at $x = 0$, that is there exists $(x^*, c) \in (\mathbb{R}^n \times \mathbb{R}_+) \backslash \{(0_{\mathbb{R}^n}, 0)\}$ such that

$$\langle x^*, x\rangle - c\|x\| \leq f(x) - f(0) \text{ for all } x \in S.$$

Proof: Since $\boldsymbol{f}$ is positively homogeneous it implies that $\boldsymbol{f(0) = 0}$. $\boldsymbol{f}$ is bounded below on $\boldsymbol{S_1 = \{x \in S: \|x\| = 1\}}$ since $\boldsymbol{f}$ is lower semicontinuous. Consider an arbitrary element $\boldsymbol{x^* \in \mathbb{R}^n \backslash \{0\}}$. Then it implies that $\boldsymbol{y = \langle x^*, x\rangle}$ is continuous and thus bounded from below on $\boldsymbol{S_1}$. Then there exists a sufficiently large number $\boldsymbol{c > 0}$ such that

$$\boldsymbol{\langle x^*, u\rangle - c\|u\| \leq f(u) - f(0)} \text{ for all } \boldsymbol{x \in S_1}. \tag{12}$$

Consider an arbitrary element $\boldsymbol{x \in S}$. Since $\boldsymbol{S}$ is a cone, then there exists $\boldsymbol{t > 0}$ and $\boldsymbol{u \in S_1}$ such that $\boldsymbol{x = tu}$. For this $\boldsymbol{u}$, multiply both sides of (12) by $\boldsymbol{t > 0}$. Then it yields to

$$\boldsymbol{\langle x^*, x\rangle - c\|x\| \leq f(x) - f(0)} \ ,\forall \boldsymbol{x \in S}.$$

The proof is completed.

Remark 3.11: Theorem 3.8 and Corollary 3.9 show that any lower Lipschitz function is weakly subdifferentiable. However, it is proved for $\boldsymbol{y^*}$ component of the weak subgradient $(\boldsymbol{x^*, \alpha})$ when $\boldsymbol{x^* = 0_{\mathbb{R}^n}}$. The following theorem demonstrate that every Lipschitz function is weakly subdifferentiable with $\boldsymbol{x^*}$ component of the weak subgradient is different from $\boldsymbol{0_{\mathbb{R}^n}}$.

The following theorem shows that a class of weakly subdifferentiable functions.

Theorem 3.12: Assume that $f: \mathbb{R}^n \to \mathbb{R}$ is a Lipschitz continuous where L is a Lipschitz constant. Then f is weakly subdifferentiable at $x_0 \in int\big(dom(f)\big)$, that is $\partial^w f(x_0) \neq \emptyset$ and there exists $(x^*, \alpha) \in \partial^w f(x_0)$ with $x^* \neq 0_{\mathbb{R}^n}$ and $\alpha > 0$.

Proof: The proof is built upon nonlinear cone separation theorem [10]. Assume that $x_0 \in int\big(dom(f)\big)$. Since $(x_0, f(x_0))$ belongs to the boundary of $epi(f) \subset \mathbb{R}^n \times \mathbb{R}$, we can separate it

from $int\big(dom(f)\big)$ by a closed pointed cone. By Theorem 3.8 there exists $((x^*, a^*), \alpha) \in (-\mathbb{C})^{\#}$such that

$$\langle (x^*, a^*), (x, a) - (x_0, a_0)\rangle + \alpha\|(x, a) - (x_0, a_0)\| \geq 0 \text{ for all } (x, a) \in epi(f).$$

$$\langle (x^*, a^*), (x - x_0, a - a_0)\rangle + \alpha\|(x - x_0, a - a_0)\| \geq 0 \text{ for all } (x, a) \in epi(f).$$

By using the norm defined on $\mathbb{R}^{n+1}$ we have,

$$\langle x^*, x - x_0\rangle + a^*(a - a_0) + \alpha\|(x - x_0\| + \alpha|a - a_0| \geq 0 \text{ for all } (x, a) \in epi(f).$$

If we substitute $f(x_0) = a_0$ it yields to,

$$\langle x^*, x - x_0\rangle + a^*(a - f(x_0)) + \alpha\|x - x_0\| + \alpha|a - f(x_0)| \geq 0 \text{ for all } (x, a) \in epi(f).$$

Or equivalently,

$$\langle x^*, x - x_0\rangle + a^*(f(x) - f(x_0)) + \alpha\|(x - x_0\| + \alpha|f(x) - f(x_0)| \geq 0 \text{ for all } x \in dom(f).$$

By the assumption that f is a Lipschitz function, it implies that:

$$\alpha|f(x) - f(x_0)| \leq \alpha L\|x - x_0\| .$$

Then we have,

$$\langle x^*, x - x_0\rangle + a^*\big(f(x) - f(x_0)\big) + \alpha\|x - x_0\| + \alpha L\|x - x_0\| \geq$$
$$\langle x^*, x - x_0\rangle + a^*\big(f(x) - f(x_0)\big) + \alpha\|x - x_0\| + \alpha|f(x) - f(x_0)| \text{ for all } x \in dom(f).$$

Hence, we obtain

$$\langle x^*, x - x_0\rangle + a^*\big(f(x) - f(x_0)\big) + (\alpha + \alpha L)\|x - x_0\| \geq 0 \text{ for all } x \in dom(f).$$

Thus,

$$\langle x^*, x - x_0\rangle + (\alpha + \alpha L)\|x - x_0\| \geq -a^*\big(f(x) - f(x_0)\big) \text{ for all } x \in dom(f).$$

Then finally,

$$\left\langle -\frac{x^*}{a^*}, x - x_0\right\rangle - \left(\frac{\alpha + \alpha L}{a^*}\right)\|x - x_0\| \leq f(x) - f(x_0) \text{ for all } x \in dom(f).$$

Thus, $\left(-\frac{x^*}{a^*}, \frac{\alpha+\alpha L}{a^*}\right) \in \partial^w f(x_0)$. The proof is completed.

4. CONCLUSION

In this work, we showed that a class of functions which are weakly subdifferentiable and with an important distinction that x^* component of the weak subgradient of the pair (x^*, α) in this case is different from $0_{\mathbb{R}^n}$. As shown in Theorem 3.12, we proved that any Lipschitz function is weakly subdifferentiable with a distinct weak gradient component. Our results extend the class of weakly subdifferentiable functions by introducing a new criterion based on nonlinear cone seperation.

CONFLICT OF INTEREST

The authors stated that there are no conflicts of interest regarding the publication of this article.

CRediT AUTHOR STATEMENT

Samet Bila: Formal analysis, Writing- original draft, Investigation, Conceptualization. **Refail Kasımbeyli:** Conceptualization, Visualization, Supervision.

REFERENCES

[1] Azimov AY, Gasimov RN. On weak conjugacy, weak subdifferentials and duality with zero gap in nonconvex optimization, International Journal of Applied Mathematics, 1, 1999, pp. 171–192.

[2] Azimov AY, Gasimov RN. Stability and duality of nonconvex problemsvia augmented lagrangian, Cybernatics and System Analysis, 3(3), 2002, pp. 412–421.

[3] Bila S, Kasimbeyli R. On the some sum rule for the weak subdifferential and some properties of augmented normal cones, Journal of Nonlinear and Convex Analysis, 24(10), 2023, pp. 2239–2257.

[4] Borwein JM, Lewis AS. Convex Analysis and Nonlinear Optimization, CMS Books in Mathematics, Springer Science+Business Media, Inc., New York, 2006.

[5] Dinc Yalcin G, Kasimbeyli R. Weak subgradient method for solving non-smooth nonconvex optimization problems, Optimization, 70(7), 2021, pp. 1513-1553.

[6] Gasimov RN. Duality in nonconvex optimization, Ph.D. Dissertation, Department of Operations Research and Mathematical Modeling, Baku State University, Baku, 1992.

[7] Gasimov RN. Augmented Lagrangian duality and nondifferentiable optimization methods in nonconvex programming, J. Global Optimization, 24, 2002, pp. 187–203.

[8] Kasimbeyli R, Mammadov M. Optimality conditions in nonconvex opti-mization via weak subdifferentials, Nonlinear Analysis: Theory, Methods and Applications, 74, 2011, pp. 2534–2547.

[9] Kasimbeyli R, Mammadov M. On weak subdifferentials, directional derivatives, and radial epiderivatives for nonconvex functions, SIAM J. on Optimization, 20, 2009, pp. 841–855

[10] Kasimbeyli R. A nonlinear cone separation theorem and scalarization in nonconvex vector optimization, SIAM J. on Optimization, 20, 2010, pp. 1591–1619.

[11] Kasimbeyli R, Karimi M. Separation theorems for nonconvex sets and application in optimization, Operations Research Letters, 47, 2019, pp. 569–573.

[12] Rockafellar RT. Convex analysis, Princeton University Press, Princeton, 1970.

[13] Rockafellar RT, Wets R. J-B. Variational analysis, Springer-Verlag Berlin Heidelberg, 2009.

ESKİŞEHİR TEKNİK ÜNİVERSİTESİ BİLİM VE TEKNOLOJİ DERGİSİ
B- TEORİK BİLİMLER

Eskişehir Technical University Journal of Science and Technology B- Theoretical Sciences

Estuscience – Theory, 2025, 13 [1] pp. 35-42, DOI:10.20290/estubtdb.1565576

RESEARCH ARTICLE

EFFECT OF OPTIMIZATION SEQUENCE ON THE STRUCTURAL AND ELECTRONIC PROPERTIES OF IMPURITY ADDED C_{20} FULLERENE: A DFT ASSESMENT

Özge BAĞLAYAN [1], Cemal PARLAK [2], Özgür ALVER [3, *]

[1] Department of Physics, Science Faculty, Eskişehir Technical University, Eskişehir, Türkiye
obaglayan@eskisehir.edu.tr - 0000-0002-0753-0325

[2] Department of Physics, Science Faculty, Ege University, Izmir, 35040, Türkiye
cparlak20@gmail.com- 0000-0002-6115-6098

[3] Department of Physics, Science Faculty, Eskişehir Technical University, Eskişehir, Türkiye
ozguralver@eskisehir.edu.tr- 0000-0003-0647-4242

Abstract

Due to its advantages over experimental works, density functional theory as a computational approach provides many insights before going over the expensive and timely costs of experimental studies. However, the time required to perform a computational study depends on the number of atoms or size of the investigated molecular system and the capacity of the computational sources. In the framework of this study, we have investigated different optimization procedures to see the effect on optimization energy, electronic parameters and some important structural parameters by using modified fullerene-C_{20}. The question that was tried to be answered here is, independent of the computational source, "do we really have to build a given molecular system from the very beginning of its components or can the final structure be directly optimized?". The preliminary results suggested very small differences such as (1-2) cm^{-1} for OH vibrations, 0.003 Å for inter atomic distances at the interaction sites and 0.003-0.018 eV energy alterations for frontier molecular orbitals. The results suggest a way to room more space and time for further studies based on impurity added C_{20}-fullerenes.

Keywords

C_{20},
DFT,
Optimization sequence,
Electronic parameters

Time Scale of Article

Received :11 October 2024
Accepted : 18 December 2024
Online date : 28 February 2025

1. INTRODUCTION

In recent years to evaluate the possible sensor and drug delivery assessments of fullerene-based systems, increasing numbers of theoretical calculations based on the density functional theory (DFT) have been given to the literature [1-4]. DFT assessments of drug interactions with various structural systems seem particularly an ongoing work with increasing number of publications, because of its useful insights and advantages compared to experimental applications [5,6]. Due to their unique physical, chemical and electronic properties, fullerene nano cages have been increasingly popular within the scientific environments particularly for the investigation of sensor and drug delivery applications [7-10]. Therefore, a special attention seems required for the grounded scientific works.

In the essence of many computational studies, the aim is to find the global energy minima or the most stable structure of the examined molecular systems. At this point, there are several factors that might

*Corresponding Author: ozguralver@eskisehir.edu.tr

affect the obtained energy values. If the initial input structure is far from reality, the structure might not converge to a true minimum energy case. It is also expected that the results of vibrational frequency calculations must all yield positive frequency values [11, 12]. The selection of basis sets and functionals depending on their properties, requires different calculation times. Using larger basis sets, require larger computational sources and strong computer systems which might not be available for many scientists around the world due to scarcity of aimed conditions.

In this work, besides already known conditions to obtain true energy minima, we also investigated the effect of the optimization sequence on the energetic parameters using C_{20} fullerene as the main structure. Due to its strong polar nature, water molecule was chosen as the interacting molecule with C_{20} and modified C_{20} systems. The interaction energies were calculated for water interacted surface and endohedrally boron and lithium modified fullerene-C_{20} systems by taking into account different optimization protocols. The effect of the initial geometric structure and the optimization protocol on the resultant geometric structure with its various chemical, physical and electronic characteristics have been discussed in brief.

2. COMPUTATIONAL STUDIES

For all the calculations B3LYP/6-31G(d) level of theory was used. No geometric boundaries were applied, and no point group was considered during the optimization process. At the end of each optimization process, vibrational frequency calculations were also carried out to make sure that the resultant structure is free of any imaginary or negative frequencies. Many medical studies have been carried out in water media because of high natural abundance of water molecules in many organic and inorganic media. Henceforth, the effect of solvent was considered using the polarizable continuum model [13].

Multiple doping and endohedral impurity addition of fullerene systems appear as promising enhancement methods for sensor and drug delivery purposes [14-16]. The main goal of this study is to suggest an optimization procedure yielding the most stable structures for multiple and endohedral impurity added fullerene systems. In Fig. 1, the optimization protocol was summarized. In this figure, the question is what happens if the system is optimized step-by-step or directly to reach the final structure. The related possible differences were discussed in the results and discussion section. According to Fig. 1, six different optimization protocols were suggested labelled as I, II, III, A, B and C. I, II and III are related to the surface modification of C_{20} with boron (B) atom. A, B and C are related to both endohedral with lithium (Li) and surface modification with B of C_{20} fullerene cage.

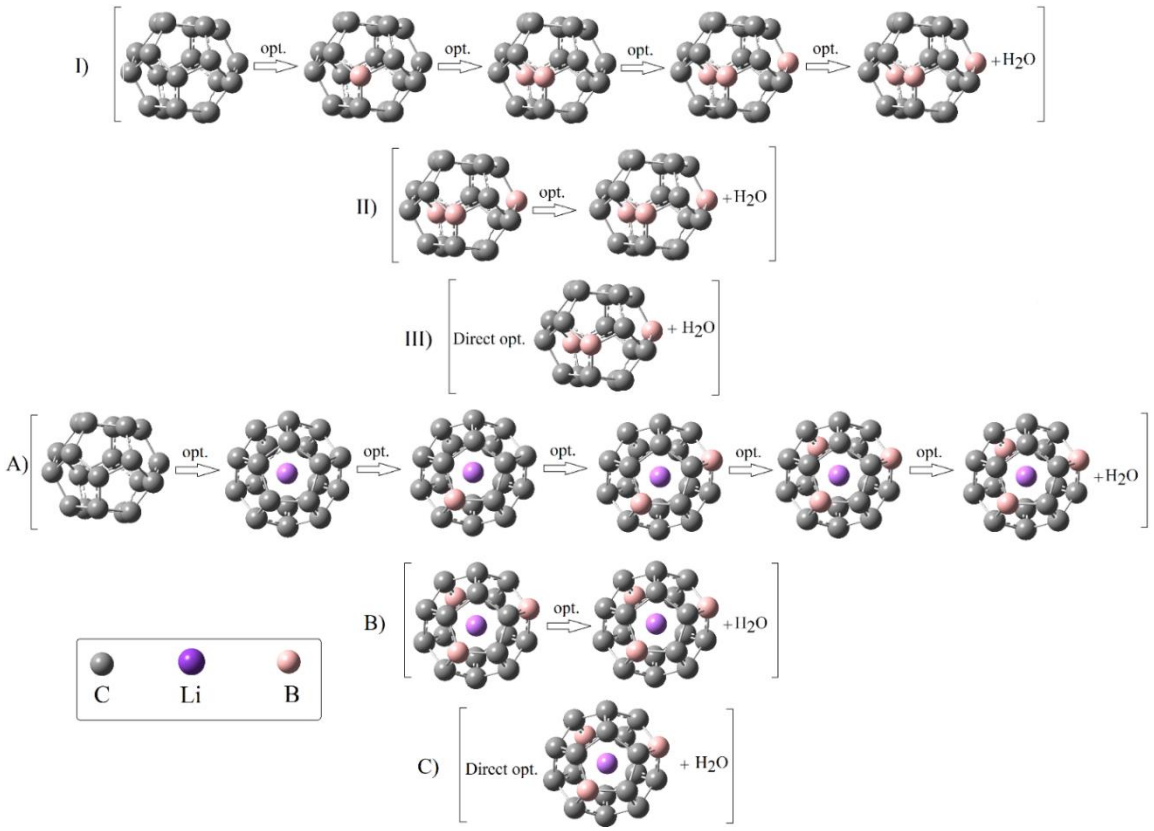

Figure 1. Optimization protocols with initial geometric structures and color codes.

Particularly, at the final stage of the optimization protocol, it is very important to provide similar initial input geometric structures which requires identical structural parameters before the optimization. In this way, it is truly possible to see the effect of ordered and direct optimization procedures. Otherwise, the deviations of optimized energy values which is expected to be small might result from different initial geometries as well. The initial geometric structures for the H_2O interacted system are given in Fig. 2.

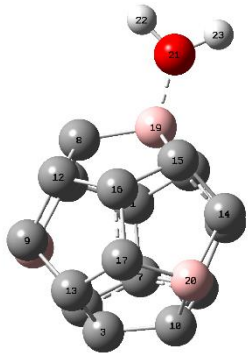

Distance (19;21)=1.5Å

Angle (3;19;21)=180°, Angle (8;19;21&15;19;21)=113°

Dihedral angle (8;19;21;22)=0°, Dihedral angle (8;19;21;23)=180°

Figure 2. Initial geometry of H_2O interacted system.

E_g energies refer to the magnitudes of differences between the highest occupied molecular (HOMO) and the lowest unoccupied molecular orbitals (LUMO). Binding energies (E_b) were calculated as given below:

$$E_b = [E_{C_{17}B_3 \ldots H_2O} - (E_{H_2O} + E_{C_{17}B_3})]$$

$$E_b = [E_{Li@C_{17}B_3 \ldots H_2O} - (E_{H_2O} + E_{Li@C_{17}B_3})]$$

In the equations given above, all the structures refer to the energies of the optimized systems. Li@$C_{17}B_3$ indicates the endohedral lithium (Li) doped $C_{17}B_3$ fullerene. It is worth noting that Li atom was inserted at the centroid of the fullerene cage before the optimization process. Gaussian and GaussView programs were used for DFT calculations, molecular design of the structures and visualization [17,18].

3. RESULTS AND DISCUSSIONS

In this part of the study, comparisons were made for different optimization protocols. The obtained structural, electronic, and vibrational properties of the examined systems were compared against each other, and the results were analyzed in brief.

3.1. Analysis of Surface Modified C_{20}

In Table 1, the optimized energies (in a.u.) of the examined structures were given. Interestingly, in sequence-II which refers to the direct optimization of the $C_{17}B_3$ system, a slightly more stable structure was obtained from the energy consideration. However, this difference is around 0.0026 kcal/mol and it is quite small to make a visible and a healthy comparison. However, with the help of this fact it can be still suggested that rather than step-by-step insertion of boron atom on the surface of C_{20} (sequence-I), the direct replacement of three carbon atoms with three boron atoms (sequence-II) can be preferred for the optimization process which means saving a large amount of time for similar C_{20} based studies.

Table 1. Optimized energies (a.u.) for the examined structures for sequences I, II and III.

Sequence-I	**C_{20}**	**$C_{19}B$**	**$C_{18}B_2$**	**$C_{17}B_3$**	**$C_{17}B_3 \ldots H_2O$**
Optimized energy	-761.44532737	-748.24879814	-735.04276533	-721.79826583	-798.26233830
Sequence-II	**$C_{17}B_3$**	**$C_{17}B_3 \ldots H_2O$**			
Optimized energy	-721.79827001	-798.26235056			
Sequence-III	**$C_{17}B_3 \ldots H_2O$**				
Optimized energy	-798.26235065				

As for H_2O interacted fullerene system similar results were observed. The energetically most favorable structure was observed with sequence-III which refers to the directly optimized structure. The optimized energy difference between sequence III and sequence II was found as 0.000056 kcal/mol. Further, the optimized energy difference between sequence II and sequence I was calculated as 0.007693 kcal/mol. Henceforth, the surface modified C_{20} fullerenes with boron atoms can be directly optimized by building the structures. Step-by-step optimization seems not necessarily required. The antisymmetric & symmetric stretching (3717.26, 3718.21 and 3718.22 & 3636.46, 3637.95 and 3638.00 cm^{-1}) and bending (1691.26, 1689.45 and 1689.52 cm^{-1}) vibrations of H_2O molecule showed a very small difference around 1 cm^{-1} when compared to results of all optimization sequence. Therefore, it is hard to differentiate the obtained results regarding to their optimization procedure from the point of view of vibrational band assignment. Mulliken charge analyses particularly for O, B atom at the interaction site and the rest two B atoms on the surface of fullerene cage produced nearly the same results for all three optimization sequences with the respective values (in a.u.) -0.639, 0.338, 0.188 and 0.186 & 0.187. Therefore, it can be concluded that partial charge behavior is almost independent of the optimization protocol followed in this study. The B…O interatomic distance at the interaction site was calculated as 1.578 Å for all the optimization sequences. The average carbon-to-carbon bond length over the isolated

C_{20} was calculated between 1.400-1.540 Å. The average B—C bond distances of boron atom with three adjacent carbon atoms at the interaction site was calculated as 1.617 Å for the optimization sequences I and III. As for the optimization sequence II, the related bond length was calculated as 1.620 Å. It was seen that replacement of carbon atom with boron atom leads increasing bond length where the impurity atoms inserted. Furthermore, as can be seen from the findings, the effect of the optimization sequence is quite small for the mentioned interatomic distances or bond lengths.

The total CPU time (hour/minute/second) required for the optimization of structures given in sequences I, II and III are 9/5/7.1, 3/50/53.8 and 2/6/35.1, respectively. This result shows that there is around a 7-hour difference which can be saved between sequence I and sequence III. For more complicated interacting molecules rather than H_2O, this difference is supposed to be higher. E_b energies for optimization sequences I, II and III were calculated as -29.9799, -29.9849 and -29.9850 kcal/mol, respectively. The largest difference in here is 0.0051 kcal/mol. It is seen that there is a very small difference between the E_b energies for the ordered optimization sequences and the direct optimization of the examined structure. HOMO-LUMO, E_g energy for optimization sequence I was calculated as 2.855 eV. As for sequences II and III, it was calculated as 2.858 eV.

3.2. Analysis of Endohedral and Surface Modified C_{20}

The optimized energies of the examined systems are given in Table 2. The most stable energy configuration for the final structure which is the H_2O interacted system was obtained in sequence-C which is related to the directly optimized system. For the endohedral Li added system it seems not necessary to follow a partial optimization procedure as it happens for sequence-A. However, the final structure obtained in sequence-A appears slightly more stable than in sequence-B. Therefore, both endohedral and surface impurity inserted systems, in here they are Li and B atoms, it seems enough to build and optimize the interacted system rather than to follow a step-by-step optimization procedure.

Table 2. Optimized energies (a.u.) for the examined structures for sequences A, B and C.

Sequence-A	**Li@C_{20}**	**Li@$C_{19}B$**	**Li@$C_{18}B_2$**	**Li@$C_{17}B_3$**	**Li@$C_{17}B_3$...H_2O**
Optimized energy	-768.93631771	-755.74376962	-742.54642271	-729.33894887	-805.79668140
Sequence-B	**Li@$C_{17}B_3$**	**Li@$C_{17}B_3$...H_2O**			
Optimized energy	-729.33889044	-805.79667125			
Sequence-C	**Li@$C_{17}B_3$...H_2O**				
Optimized energy	-805.79686511				

The antisymmetric & symmetric stretching and bending vibrations of the H_2O molecule showed only a difference around 1-2 cm^{-1} when compared to the results of all optimization sequences. Therefore, no matter if one flows as step-by-step optimization protocol or directly optimize the given system undertaken in this study. The total CPU time (hour/minute/second) required for the optimization of structures given in sequences A, B and C are 10/26/42.8, 2/44/18.8 and 1/33/35.4, correspondingly. This result also indicates that there is around 9-hour difference between sequence A and sequence C. E_b energies for optimization sequences A, B and C were found as -26.0016, -26.0319 and -26.1535 kcal/mol, respectively. It is seen that the difference between the E_b energies for the ordered optimization sequences and for the direct optimization of the examined structure is negligible. HOMO-LUMO, E_g energy for optimization sequences A, B and C were calculated as 2.503, 2.502 and 2.520 eV. Mulliken charge analyses for O, endohedrally inserted Li, B at the interaction site and the rest two B atoms on the surface of fullerene yielded -0.646, -0.946, 0.437 & 0.439 & 0.441, 0.327 and 0.328 & 0.327. As can be seen from the obtained results, optimization protocol or the sequence has nearly no effect on the partial charge distribution for selected atoms. It was further observed that partial charges of surface dopant atoms for Li@$C_{17}B_3$ system became more positive when compared to surface modified $C_{17}B_3$ system which indicates that upon insertion of Li atom some number of electrons move away from the dopant

atoms. The B…O interatomic distances at the interaction site were calculated as 1.585, 1.586 and 1.583 Å, for optimization sequences A, B and C. The average B—C bond distance of boron atom with three neighbor carbon atoms at the interaction site was calculated as 1.628 Å for all the optimization sequences. In addition to that the average carbon to carbon bond length over the isolated and endohedrally Li inserted C_{20} was calculated between 1.410-1.530 Å. It was also seen that endohedrally inserted Li atom has negligible effect on carbon-to-carbon bond lengths.

3.3. Analysis of Recovery Times

Another important parameter to investigate the reversibility of the interaction process is known as the recovery time (τ) which can be calculated using the following relation [19]:

$$\boldsymbol{\tau = \upsilon_0^{-1} \exp\left(\frac{-E_b}{K_B T}\right)}$$

In this equation υ_0, K_B and T are known as attempt frequency, Boltzmann constant and temperature in the corresponding order. In the scope of this work, υ_0 was chosen as 10^{12} Hz. For the examined structures undertaken in this work, the values of τ were calculated around $9.4x10^9$s for sequence I and $9.5x10^9$s for sequences II and III. Further, the related τ values for sequence A, B, and C were calculated around $1.1x10^7$, $1.2x10^7$ and $1.5x10^7$s, respectively. It was observed that the only differences were occurred in the decimal parts and around 0.1 and 0.4 s, for both systems.

4. CONCLUSIONS

For all the examined systems, endohedral or surface impurity addition over the C_{20} fullerene, direct replacement of the required number of carbon atoms on the surface of C_{20} and direct addition and optimization of endohedral impurity atom inserted system resulted in a slightly more stable structure. Recovery time measurements yielded negligible differences between the examined systems. Therefore, to save time and to reach the minimum energy case, instead of step-by-step optimization direct optimization can be preferred for C_{20} based impurity added systems.

ACKNOWLEDGEMENTS

Authors acknowledge Fencluster system of Ege University for the calculations.

CONFLICT OF INTEREST

The authors stated that there are no conflicts of interest regarding the publication of this article.

CRediT AUTHOR STATEMENT

Özge Bağlayan: Investigation, Methodology, Writing – Review & Editing. **Cemal Parlak:** Supervision, Software, Visualization, Resources. **Özgür Alver:** Conceptualization, Validation, Writing – original draft.

REFERENCES

[1] Tabtimsai C, Watkhaolam S, Palasri S, Rakrai W, Kaewtong C, Wanno B. Ibuprofen adsorption and detection of pristine, Fe–, Ni–, and Pt–doped boron nitride nanotubes: A DFT investigation. J Mol Graph Model 2024; 126: 108654.

[2] Odey MO, Okon GA, Al-Sehemi AG, Adindu EA, Kavil YN, Agwamba EC, Bakheet AM, Pembere AMS, Louis H. Single-atoms (B, P, S, Si) doping of Pt-coordinated graphitic carbon nitride (Pt@g-C3N4) nanostructured as sensors for Buprofezin (BPF) insecticide: Outlook from computational study. J Organomet Chem 2023; 1002: 122923.

[3] Salem-Bekhit MM, Al Zahrani S, Alhabib NA, Maaliw III, RR, Da'i M, Mirzaei M. Metal-doped fullerenes as promising drug carriers of hydroxycarbamide anticancer: Insights from density functional theory. Chem Phys Impact 2023; 7: 100347.

[4] Roy RS, Banerjee S, Ghosh S, Ghosh A, Das AK. A comparative study of electronic structure, adsorption properties, and optical responses of furan and tetrahydrofuran adsorbed pristine, Al and Ga doped B12X12 (X=N and P) nanocages. J Mol Struct 2024; 1296: 136854.

[5] Zainula R, Khaleel AQ, Ahmed HH, Menon SV, Hamid JA, Al Khatib AO, Aljeboree AM, Elawad A. Exploring the interaction between graphyne and Purinethol: A DFT study of drug loading capacity. Comput Theor Chem 2024; 1238: 114731.

[6] Daboe M, Parlak C, Alver Ö. Density Functional Theory Investigation On Drug-Drug Interactions: Escitalopram And Salicylic Acid, Eskişehir Technical Univ J of Sci and Tech B–Theo. Sci. 2023; 11(1); 36-42.

[7] Shettia NP, Mishra A, Basu S, Aminabhavi TM. Versatile fullerenes as sensor materials. Mat Today Chem 2021; 20: 100454.

[8] Ogunwale GJ, Louis H, Gber TE, Adeyinka AS. Modeling of pristine, Ir- and Au-decorated C60 fullerenes as sensors for detection of hydroxyurea and nitrosourea drugs. J Environ Chem Eng 2022; 10: 108802.

[9] Saadh MJ, Alsaedi II, Abbood MA, Yadav A, ALsailawi HA, Mudhafar M, Jihad Hemid Al-Athari A, Elmasry Y, Alawadi AH. Therapeutic potential of CX (X = 48, 60, and 70) fullerenes as drug delivery carriers for ifosfamide anti-cancer drug. Diam Relat Mater 2023; 140: 110494.

[10] Kalika EB, Bondarev NV, Katin KP, Kochaev AI, Grekova AA, Kaya S, Bauetdinov YA, Maslov MM. Adsorption of 40 low molecular weight drugs on pristine and fluorinated C60 fullerenes: Ab initio, statistical and neural networks analysis. J Mol Liq 2023; 377: 121559.

[11] Milon Roy D, Ahmed F. A DFT study to investigate the physical, electrical, optical properties and thermodynamic functions of boron nanoclusters (MxB2n0; x=1,2, n=3,4,5). Heliyon 2023; 9(7): 17886.

[12] Gupta D, Ranjan R, Shukla M. Molecular interaction of curcumin with silver nanocluster: A DFT study. Vib Spectrosc 2023; 129: 103604.

[13] Tomasi J, Mennucci B, Cammi R. Quantum mechanical continuum solvation models. Chem Rev 2005; 105: 2999–3094.

[14] Kosar N, Tahir H, Ayub K, Mahmood T. DFT studies of single and multiple alkali metals doped C24 fullerene for electronics and nonlinear optical applications. J Mol Graph Model 2024; 105: 107867.

[15] Esrafili MD, Sadeghi S. A DFT investigation into the possibility of using noble gas encapsulated fullerenes for Li storage. Chem Phys Lett 2022; 787: 139236.

[16] Mittal M, Kumar A. Carbon nanotube (CNT) gas sensors for emissions from fossil fuel burning. Sens Actuators B Chem 2014; 203: 349–362.

[17] Frisch MJ, Trucks GW, Schlegel HB. et al. Gaussian 09, Revision A.1, Gaussian Inc., Wallingford, CT, 2009.

[18] Dennington RD, Keith TA, Millam JM. GaussView 5.0.8, Gaussian Inc., 2008.

[19] Hadipour NL, Peyghan AA, Soleymanabadi H. Theoretical study on the Al-doped ZnO nanoclusters for CO chemical sensors. J Phys Chem C 2015; 119: 6398–6404.

ESKİŞEHİR TEKNİK ÜNİVERSİTESİ BİLİM VE TEKNOLOJİ DERGİSİ
B- TEORİK BİLİMLER

Eskişehir Technical University Journal of Science and Technology B- Theoretical Sciences

Estuscience – Theory, 2025, 13 [1] pp. 43-66, DOI:10.20290/estubtdb.1523286

RESEARCH ARTICLE

EVALUATION AND ANALYSIS OF RISK FACTORS IN RAILWAY ACCIDENTS IN TÜRKİYE

Burçin PAÇACI [1,*], Hulusi AYDEMİR [2], Metin ESER [3], Serpil EROL[4], M. Kürşat ÇUBUK [5]

[1] Civil Engineering, Engineering Faculty, Gazi University, Ankara, Türkiye
burcinpcc@gmail.com - 0000-0001-6053-0458

[2] Republic of Turkey General Directorate of State Railways, Railway Modernization Department, Ankara, Türkiye
hulusiaydemir1@gmail.com - 000-0002-7989-4136

[3] Republic of Turkey Ministry of Transport and Infrastructure, General Directorate of Infrastructure Investments, Bursa, Türkiye
metineser@hotmail.com - 0000-0002-7956-6079

[4] Endustry Engineering, Engineering Faculty, Gazi University, Ankara, Türkiye
serpiler@gazi.edu.tr - 0000-0002-6885-3849

[5] Civil Engineering, Engineering Faculty, Gazi University, Ankara, Türkiye
ckursat@gazi.edu.tr - 0000-0001-8155-7123

Abstract

The main purpose of transportation is to transport passengers and cargo in the shortest possible time, safely and economically. In order to achieve this goal, the safety factor constitutes one of the most basic elements of transportation. In recent years, many countries have made various legal regulations to increase the safety and efficiency of the railway sector and have produced targets and policies to reduce railway accidents and loss of life. In this study, the current situation of the number of accidents, deaths, and types of accidents occurring in Turkish railways was shown, and a statistical comparison was made with the European Union (EU). When we evaluate it from Türkiye's perspective, it seems that it has some deficiencies in this regard compared to the European Union countries. The main purpose of the study is to examine railway accidents in Türkiye. In this context, the factors that may cause an accident are classified into 58 parameters. AHP (Analytic Hierarchy Process) from MCDM (Multi Criteria Decision Method) and L-Decision Matrix were used, and risk analysis was carried out by scoring likelihood and severity. Risk analysis was evaluated for the first time in Türkiye by employees of investor companies, investor organizations, and consultancy firms that built railways. In conclusion, the riskiest activity of the sector stakeholders that constitute the infrastructure was determined as uncontrolled entrances of pedestrians to level crossings as a high risk with the L-Decision Matrix method and the B4 risk index score. By using the AHP method, it is obtained uncontrolled pedestrian access to level crossings has a risk importance weight of p = 0.28 (0-1), and uncontrolled access to the road due to closures has a risk importance weight of p = 0.21. (0-1). Suggestions were made to prevent accidents.

Keywords

Railway,
Railway Accident,
Risk,
L-Decision Matrix,
AHP

Time Scale of Article

Received :27 July 2024
Accepted : 26 Februay 2025
Online date: 28 February 2025

*Corresponding Author: burcinpcc@gmail.com

1. INTRODUCTION

Railways, which played a decisive role in the development of societies, are critical in ensuring balanced transportation policies by being in a very favorable position to all modes of transportation due to Türkiye's geopolitical and geostrategic position in the future perspective. In this respect, according to the 2053 investment projections, it is estimated that the investments to be made in railways will constitute one-third of all transportation modes [1].

The way to provide safe, balanced, and economical railway transportation is through security. Since there are no limits to security measures, engineering studies are carried out to ensure acceptable costs and maximum security together at the optimum points, which are essential here. However, the risk of accidents will always exist because there is mobility on the railways, and transportation by rail cannot be completely isolated from external environments. For this reason, many measures have been taken in the country's policies. According to the 2022 Safety Report of the International Railway Association, it is observed that between 2016 and 2021, the number of accidents, the number of serious accidents per million train-km, the number of deaths, the number of deaths per million train-km tend to decelerate [2]. However, with all the technical knowledge, rules, and technological advances in the world, the safety elements that need to be improved in railway safety continue to exist.

In railways, an accident is defined as an unwanted, unexpected, sudden, and unintentional event or chain of events with harmful consequences such as property damage, death, or injury. A significant accident is an accident involving at least one moving railway vehicle in which at least one person is killed or seriously injured, causing significant damage to the vehicle or even structures or the environment, or extensive disruption to traffic, and costing €150,000 or more [3]. Because of the importance of the subject, lots of studies regarding railway accidents were carried out. In a study examining Slovak railways by collecting various accident reports, models were developed, and the accident risk of the railway system was evaluated [4]. In a study conducted in France, railway accident risks were analyzed and predicted using machine learning technique [5]. In a study conducted in Taiwan using accident counting data models, risk factors at level crossings were investigated [6].

Many studies on railway accidents and railway safety were conducted in Türkiye. Akbayır statistically examined various accident data in different years after 2003, showing that the number of accidents and deaths decreased. It has been concluded that by increasing the number of active level crossings, the crossing collision fatality rate will be reduced; active level crossings should be built in the right places; and signaling systems are not used correctly [7]. Kıyıldı examined the statistical data on level crossing accidents between 2000 and 2019 and suggested that the number of level crossings should be reduced or converted to under/overpasses, and the crossings should be modernized and equipped with barriers [8]. Ilıcalı, on the other hand, examined railway fencing in the world, stated that the accidents along the line were due to unauthorized crossings and that this was mainly due to need, and made various determinations and evaluations such as preventing pedestrians from entering the railway lines and building underpasses and overpasses in areas in need of passage [9]. Ghanem and Xuemei compared Türkiye's railway safety with EU countries using Charnes, Cooper, and Rhodes (CCR) and Banker–Charnes–Cooper (BCC) analyses, which are basic data envelopment analyses; line length/km, number of locomotives and wagons, number of passenger transport vehicles and number of goods transport wagons were used as input. According to the analysis results, using the number of accidents, the number of deaths and the number of injured as outputs, they concluded that Türkiye was more successful than EU countries in reducing the number of accidents and deaths [10].

Among related studies conducted in Türkiye, there is a study conducted using the Fuzzy SWARA (Step-Wise Weight Assessment Ratio Analysis) method. In this study, eight parameters were determined, and railway infrastructure periodic maintenance was ranked first, railway superstructure maintenance

second, and rolling stock maintenance third. Level crossings, railway fencings, and tunnel fire safety were ranked last, respectively. Thus, the importance of the parameters chosen in railway safety in guiding the outcome of the assessment and the experience of individuals can influence the outcome [11]. Özarpa, Avcı and Kınacı carried out signalization system risk analysis using AHP analysis with five experts and found that signalization systems, with 26.65%, and switching systems, with 23.47%, were the priority risk topics [12].

The primary purpose of this study is to ensure safe transportation by preventing the risk factors determined by experts on the railway. In this direction, firstly, the number of railway accidents occurring in Türkiye and European Union countries and the types of accidents were examined separately and comparatively. In the second part of the study, the risks that may cause accidents to occur on the railways were determined by literature review and expert opinions. The identified risks have been evaluated in accordance with the experiences and opinions of the investor organizations and consultant teams operating on the railway. There are studies in the literature where AHP and L-Decision Matrix are used together in risk analysis [13, 14]. These methods were also used in this study. In the study, 58 factors determined as the cause of railway accidents were examined in five different groups. The ability of AHP to solve complex problems and the ease and practicality of L-Decision Matrix are the reasons why these two methods were used in this study. As a result of these methods used, the risks with the highest rate that can cause an accident on the railways have been identified. In addition, in this study, suggestions have also been made about the measures that should be taken to address risks in order to reduce accidents on railways. Our study is essential in that it includes an overall assessment of railway safety in Türkiye over 58 different factors, with 20 expert opinions, and for the first time directly from the perspective of infrastructure stakeholders. These factors will be used as "*Criteria*" in AHP application of our study. It is also important to strengthen the compatibility of the concerns of infrastructure stakeholders with statistics.

When the sample sizes in similar studies are examined, it is thought that the number of determined criteria for railway safety evaluated and the number of participants is sufficient for this study. Criteria that pose the risk have been prepared comprehensively. However, in addition to the criteria examined in the study, different criteria that may cause railway accidents can also be examined. In certain areas, different risk analysis methods may use different numbers criteria. The study period is limited to the years 2002-2021. Data after the Covid 19 pandemic have not been examined.

2. RAILWAY ACCIDENT IN TÜRKİYE AND THE COMPARISON WITH EU COUNTRIES

In this part of our study, which is prepared to contribute to the provision of safe railway transportation in Türkiye, the number of accidents occurring in Türkiye and European Union countries and the types of these accidents are examined. A statistical introduction about railway accidents in Türkiye and various information are given. Train-km was used as the scale. Train-km is the unit of measurement representing the distance a train travels one kilometer. Within the scope of data, TCDD (General Directorate of Turkish State Railways) Statistical annuals [15-19] and TUIK (Turkish Statistical Institute) transport statistics [20], European Commission Statistical Pocketbook [21] and Eurostat Railway statistics on railway accidents were compiled and examined [22-24]. The number and types of accidents in Türkiye were compared with those in EU countries. The number of railway accidents per million train-km mobility in Türkiye between 2002 and 2021 is given in Figure 1. The number of deaths per million train-km mobility in Türkiye between 2002 and 2021 is given in Figure 2. Figures 1 and 2 are obtained by dividing the number of accidents and fatalities in those years by the train mobility values in the same years.

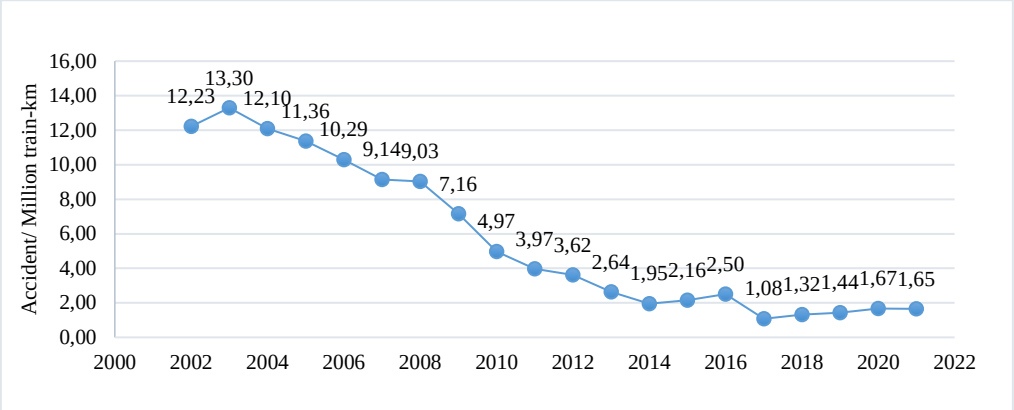

Figure 1. Number of accidents per million train-km between 2002-2021 in Türkiye [15-20]

The values shown in Figure 1 are obtained by dividing the number of accidents that occurred in those years by the million train-km value in the same year. While there were 12.23 accidents per million train-km in 2002, this rate decreased by 86% to 1.65 in 2021.

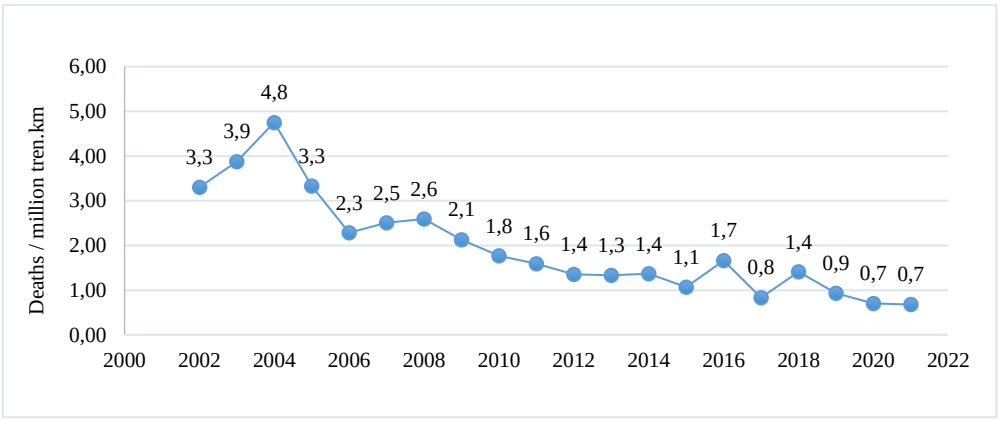

Figure 2. Number of deaths per million train.km between 2002 and 2021 in Türkiye [15-20]

According to Figure 2, the highest death rate occurred in 2004, with 4.8 deaths per million train-km, and it is seen that it showed a general decreasing trend over the years, decreasing from 3.3 in 2002 to 0.7 deaths in 2021.

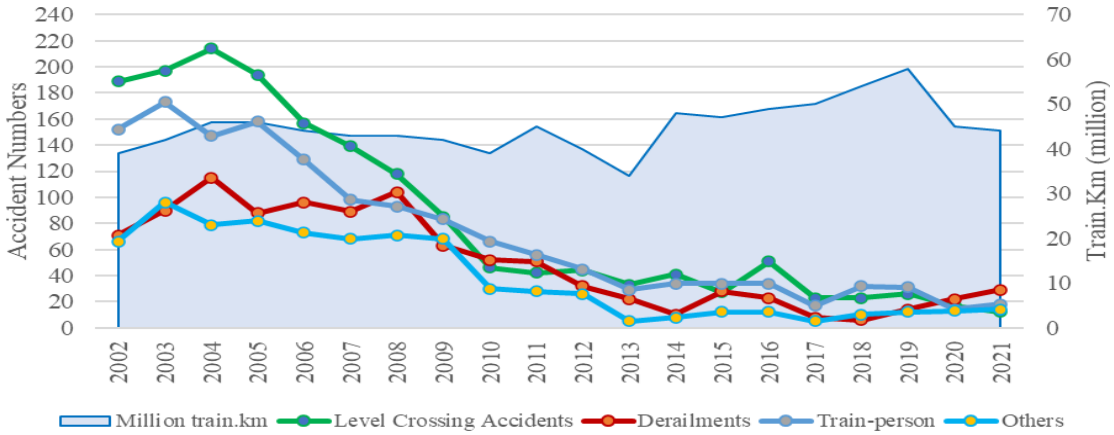

Figure 3. Types of railway accidents in Türkiye between 2002 and 2021 [15-20]

Types of railway accidents in Türkiye between 2002 and 2021 are given in Figure 3. According to Figure 3, from 2002 to 2021, it was observed that level crossing accidents decreased by 93% from 189 to 12; human accidents caused by moving trains decreased by 88% from 152 to 18; derailment cases decreased by 60% from 71 to 29; and collisions decreased by 57% from 21 to 9. At the beginning of the 2000s, level crossing accidents and personal collisions were among the highest types of accidents, while by the 2020s, it was observed that derailment and train personal collisions were higher, respectively.

The number of accidents per million train-km in Türkiye and EU countries and their comparison are shown in Figure 4. Figure 5 shows the number of deaths per million train-km between 2010 and 2020. Figures 4 and 5 are obtained by dividing the 11-year total number of accidents and fatalities by the total number of train movements.

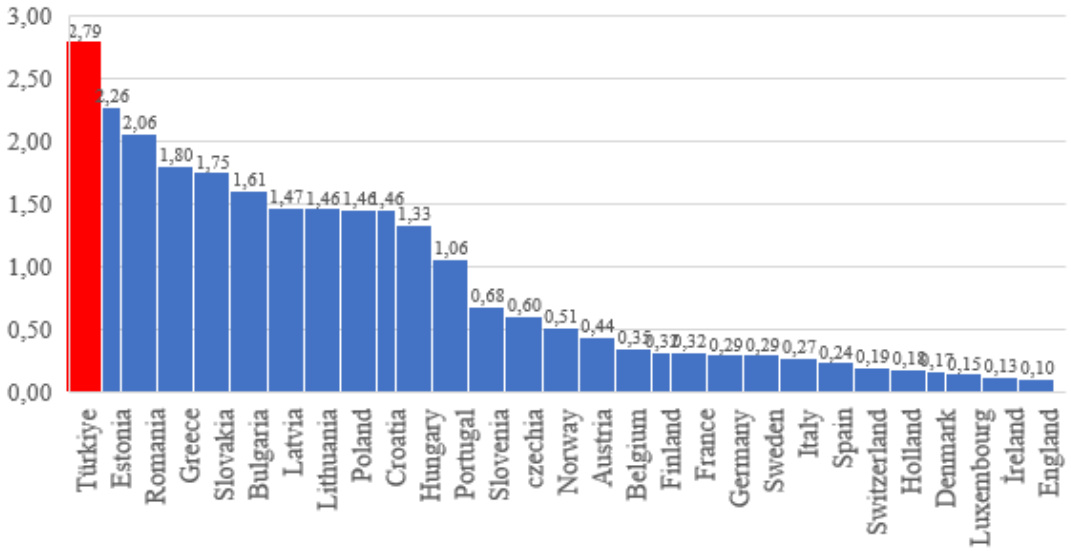

Figure 4. Number of accidents per million train-km in Türkiye and EU countries (2010-2020) [20-21]

When the total data for the last 11 years is examined in Figure 4, it is seen that the highest number per million train-km is in Türkiye. The highest number of accidents per million train-km is seen in Türkiye with 2.79, followed by Estonia with 2.26, and Romania with 2.06. Additionally, the lowest number of railway accidents per million train-km occurs in England with 0.1 and Ireland with 0.13. In other words, in the same years, the number of railway accidents occurring in Türkiye is approximately 27 times more than in England, 22 times more than in Ireland, 16 times more than in Denmark, and 1.5 times more than in Greece.

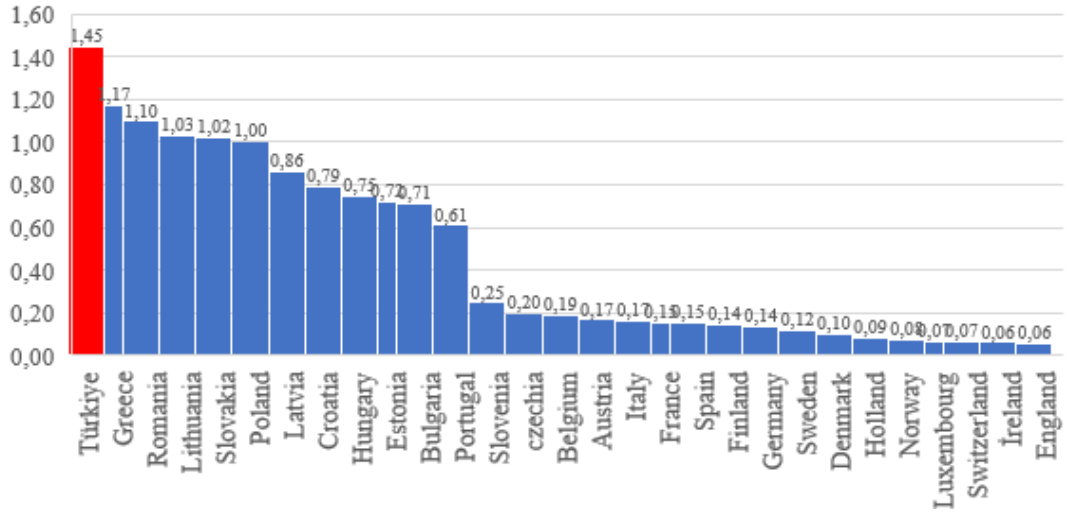

Figure 5. Number of deaths per million train-km in Türkiye and EU countries (2010-2020) [20, 21]

When Figure 5 is examined, the highest number of deaths is seen in Türkiye, with 1.45. Türkiye is followed by Greece with 1.17, Romania with 1.10 and Lithuania with 1.03. The lowest number of deaths per million train-km is England and Ireland with 0.06, and Switzerland with 0.07. In other words, when the number of deaths per million train-km between 2010 and 2020 is examined, the rate in Türkiye is approximately 26 times that of England, 24 times that of Ireland, 22 times that of Switzerland, and 1.23 times compared to Greece. There appears to be a higher number of deaths. Table 1 includes the number of railway accidents in European Union-27 countries and Türkiye between 2010 and 2020. European Railway Agency data was used [22].

Table 1. EU-27 and Türkiye railway accidents by type between 2010 and 2020 [22]

		2010	2011	2012	2013	2014	2015	2016	2017	2018	2019	2020	Total
European Union	Collision	79	70	87	80	121	123	99	102	109	103	110	1,083
	Derailment	89	85	94	100	93	72	62	88	74	73	69	899
	Level Crossing	585	506	563	498	495	465	424	456	442	432	350	5,216
	Human accidents caused by moving trains	1,354	1,395	1,158	1,121	1,186	989	1,042	1,034	939	794	685	11,697
	Others	122	88	90	96	127	114	115	97	102	113	117	1,181
Türkiye	Collision	8	8	4	2	2	4	6	2	6	4	9	55
	Derailment	52	51	32	22	10	28	23	8	6	14	22	268
	Level Crossing	46	42	44	33	41	27	51	23	23	26	17	373
	Human accidents caused by moving trains	84	73	58	31	37	36	36	19	33	33	14	454
	Others	4	3	9	1	3	6	4	1	3	6	4	44

Percent accident rates of railway accidents in Türkiye and the European Union countries between 2010 and 2020 are shown in Figure 6.

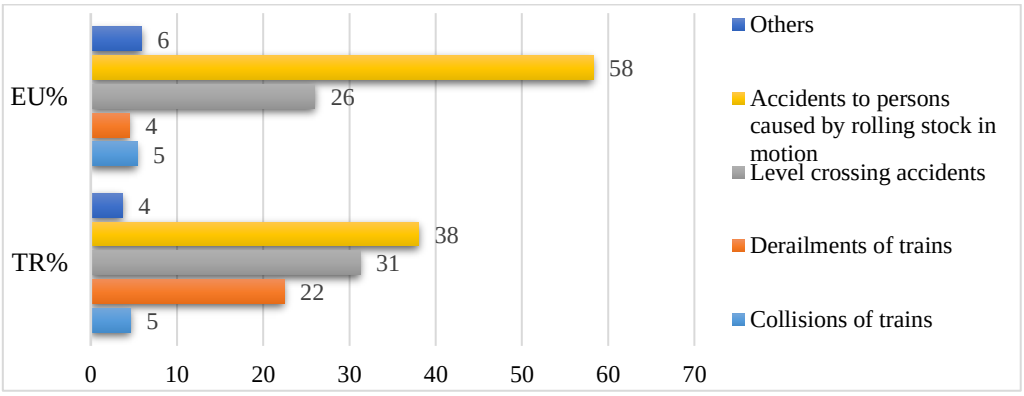

Figure 6. Railway accidents in the European Union (EU) and Türkiye (TR) by type (2010-2020) [22]

When Figure 6 is examined, it is observed that while train-person collisions are seen at a very high rate throughout the European Union and Türkiye, there is a much higher rate of derailment accidents in Türkiye compared to European countries. According to D-Rail reports supported by the European Commission, the causes of derailment in Europe between 2005 and 2010 were revealed as axle breaks, track expansion, wheel defects, asymmetric loading, line twists, rail defects, and spring and suspension defects, respectively [25]. Statistical data regarding the causes of delays in Türkiye are not sufficient, and it is thought that criteria such as inadequacy of our signaling and line infrastructure, transportation at speeds higher than the limits allowed by the infrastructure, road twists and gauge defects, and component failures related to vehicles are effective.

3. MATERIAL AND METHOD

In the study, the risks that cause accidents on the railway were prepared by taking into account the literature and the opinions of experts and analyzed according to the opinions of 20 experts. All of these evaluations are included in the study conducted by Eser [26]. The expert's scorings are attached in the appendix. These experts consist of four head of department-level investor organization (public) employees, nine consultant company employees, and seven contractor company site chiefs and controllers who have completed at least one work in the railway sector. The experts are two mechanical engineers, five electrical-electronics and/or communication engineers, and 13 civil engineers according to their professions. Thirteen participants were interviewed face to face, and seven people were contacted online. The results of this evaluation aim to determine the risks with the highest rate and to take precautions for safe railway transportation in this direction.

This study used L-Decision Matrix and AHP techniques to rank the risks, respectively. However, these methods are listed in alphabetical order in the study. There are differences in the application of AHP and L-Decision Matrix. The AHP method, which can solve complex and difficult-to-understand problems [27] and can rank, was used to weigh and rank the identified risks. One of the biggest advantages of AHP is that it helps decision makers to separate a complex issue in a simpler way [28]. For this reason, the AHP method was deemed appropriate for ranking the fifty-eight criteria which are the factors determined for railway safety in this study. The application of AHP was realized by taking the geometric average of twenty experts' opinions. According to both method procedures, the risks were ranked and compared at the end of the study. The L-Decision Matrix (5x5) method is an easy-to-apply method where risks are identified and scored, and cause and effect relationships are included in the evaluation. In the L-Decision Matrix, the evaluation is based on the arithmetic average. Risks are ranked by the arithmetic average of the opinions of each of the twenty experts.

Currently, various studies are being carried out to analyze the risks of AHP and L-Decision Matrix. Kılıç used the Fuzzy AHP method in his study to study the risks related to marine accidents in the Istanbul Strait [29]. Arslan and Turan analyzed the factors causing marine accidents by SWOT (Strengths, Weaknesses, Opportunities, Threats) analysis and found the weights of these factors using the AHP method [30]. Bayazit used the AHP method for safety assessment at railway-level crossings in his study [31]. Bureika and his colleagues used the AHP technique to examine factors that may threaten railway safety by aiming to prevent accidents on railway lines in Lithuania in their study [32]. Liu and his colleagues used AHP, MAWR (Maximum Absolute Weighted Residual), MEM (Maximum Entropy Method) techniques for risk assessment in the safety analysis of railway signaling systems in their study [33]. Similarly, the 5x5 L-Matrix method is one of the methods used to analyze possible risks. For example, Uray used a matrix to determine the possible effects of risks in railway maintenance [34], and Damat and Utlu used a matrix to expand the scope of work in metro stations in Istanbul [35]. In their studies, Bayraktar and his colleagues aimed to determine the possible effects of earthquake-related non-structural risks in schools using the 5x5 L-Matrix method [36]. Information about the methods and their application are described below.

3.1. AHP Method

AHP developed by Saaty, is one of the most popular techniques for complex decision-making problems. There are lots of advantages of AHP. Some of these are its flexibility, intuitive expression to decision makers, and ability to check inconsistencies. To be simple, the method of AHP is the most important advantage. Also, the biggest advantage of AHP is that it can easily form groups to handle inconsistencies in judgments, which is the case when compared to other multicriteria methods of AHP [37]. The AHP method is expressed as a technique based on a pairwise comparison of criteria to determine their superiority over each other. It is a widely used method. The application stages of AHP are listed below.

Step 1: In the first step of the AHP method, the problem is defined.

Step 2: Hierarchy is created, and the purpose of the hierarchy is revealed. Criteria, and alternatives are included.

Step 3: Pairwise comparisons matrix is created. Each criterion is compared in pairs according to the importance scale shown in Table 2 [38].

Table 2. Importance Levels (Scale) [38]

Importance Level	Explanation
1	Equal importance
3	Moderate importance
5	Strong importance.
7	Very strong importance.
9	Extreme importance.
2, 4, 6, 8	Intermediate values

Step 4: Pairwise comparison matrices are normalized. The weights of criteria based on generated pairwise comparison matrices are calculated. For this calculation, the column sum of the pairwise comparison matrix is taken and divided by the column sum corresponding to each element of the pairwise comparison matrix, and a normalized pairwise comparison matrix is obtained. Formulization is shown below (1).

$$B_i = \begin{bmatrix} b_{11} \\ b_{21} \\ . \\ . \\ . \\ b_{n1} \end{bmatrix} \qquad b_{ij} = \frac{a_{ij}}{\sum_{i=1}^{n} a_{ij}} \tag{1}$$

Here, aij; represents the i-th row and j-th column element of the comparison matrix, and bij represents the i-th row and j-th column of the normalized matrix.

Step 5: Then, the values of each row are summed and divided by the matrix size to determine the importance values (Wi) for each criterion. Equation is shown below (2).

$$C = \begin{bmatrix} b_{11} & b_{12} & \dots & b_{1n} \\ b_{21} & b_{22} & \dots & b_{2n} \\ . & & & . \\ . & & & . \\ . & & & . \\ b_{n1} & b_{n2} & \dots & b_{nn} \end{bmatrix} \qquad w_i = \frac{\sum_{j=1}^{n} c_{ij}}{n} \tag{2}$$

Step 6: Since the comparisons are subjective, the consistency rate must be calculated. If the calculated rate is below 10%, it is considered sufficient. Whether the evaluation is consistent or not is determined by the consistency rate. The lower the consistency rate, the more consistent the evaluation. If the consistency ratio is higher than 0.1, that evaluation is not consistent. Accordingly, It is returned to the pairwise comparison matrix, and the process is performed again. After all these processes, the decision matrix is created [39]. In order to calculate the CR value, the largest eigenvector (λmax) value of the pairwise comparison matrix must first be calculated. Formulization is shown below in 3., 4., and 5. equations.

where i= 1, 2,..., n and j= 1, 2,..., n,

$$[a_{ij}]_{nxm} * [w_i]_{nx1} = [d_i]_{nx1} \tag{3}$$

$$\lambda max = \frac{\sum_{i=1}^{n} \frac{di}{wi}}{n} \tag{4}$$

In calculating the consistency ratio, the Randomness Index (RI), depending on the number of criteria (n) included in the comparison, is used. The RI values determined according to the n values are shown in Table 3. The calculation of the CR value according to the obtained inputs is shown in equation 5.

$$CR = \frac{\lambda - n}{(n-1).RI} \tag{5}$$

Table 3. Randomness index (RI)

n	**1**	**2**	**3**	**4**	**5**	**6**	**7**	**8**	**9**	**10**	**11**	**12**	**13**	**14**	**15**
RI	0	0	0,58	0,9	1,12	1,24	1,32	1,41	1,45	1,49	1,51	1,48	1,56	1,57	1,59

In the AHP process, the criteria weights are determined as a result of surveys conducted with experts on the subject, that is, based on a group decision. Accordingly, three approaches can be used. These are the consensus of experts on a certain criterion, voting on options when experts cannot express a common opinion, and geometric mean approaches. In the geometric mean approach, the joint decision of n experts is reduced to a single value using the geometric mean method. In the geometric mean approach, “k”, “i” and “j” stand for “expert”, “criterion”,”criterion”, respectively. “kij” is the value of the comparison of

the i. and the j. criteria according to k. expert. The geometric mean method is one of the most used approaches, as shown in equation 6 [39].

$$a_{kij} = [a_{1ij} * a_{2ij} * a_{3ij} * ..... * a_{nij}]^{1/n} \quad (6)$$

3.2. L-Decision Matrix Method

Known as the American Military standard "MIL_STD_882-D", 5x5 Matrix diagram (L-Type Matrix), one of the widely used risk assessment matrix approaches and was developed to meet the system security program requirement, is used especially in evaluating the cause-effect connection [40]. The method is one of the most frequently used methods because it is easy, and even one person can do it. The 5x5 Risk Matrix consists of two main dimensions: likelihood and severity. Likelihood refers to the probability or chance of a hazard occurring, while severity relates to the potential impact or consequences of that hazard. Each dimension is divided into five levels, creating a matrix with 25 cells. To put it briefly, the L-Type Matrix (L-Decision Matrix) method is a subjective evaluation method. Therefore, the reliability of subjective results depends on the experience of the specialized people who make the application. Formulization of risk is shown below (7).

$$\text{Risk} = \text{Likelihood x Severity} \quad (7)$$

The L-decision matrix risk score evaluation matrix will be considered as follows, and the areas indicated in red refer to the sections that are unacceptable areas, and it is necessary to intervene and stop work, and definitely not to start work until it reaches an acceptable risk level. Yellow areas refer to areas that need to be intervened as soon as possible using risk mitigation measures, while green areas refer to areas that can be intervened in the longer term or do not need additional controls to reduce the risk. The analysis results of the risks were evaluated according to the risk likelihood score (Table 4), severity score (Table 5), risk matrix (Table 6) and risk acceptance levels (Table 7) prepared within the scope of the study.

Table 4. Likelihood score [40]

(It refers to the probability of an accident or event.)

Grade	Probability of Occurrence	Definition	Period
A	Very High	The incident may occur at any moment.	Daily
B	High	The event may occur frequently.	2 days - 1 month
C	Medium	The incident may occur Decently from time to time.	1 month - 1 year
D	Low	The event may occur rarely.	1 year- 10 years
E	Very Low	The event can occur very, very rarely.	More than 10 years

The likelihood table prepared to determine the risk score is classified as grade related to the criterion, probability of occurrence, definition, and period. Ranges are as shown in the table.

Table 5. Severity score [40]

(The severity of an accident or incident in the situation where it occurred)

Grade	The Severity of the Incident	Depiction of possible harm or loss
5	Disaster	Multiple deaths / severe environmental damage / severe property damage
4	Severe	One death/significant environmental damage/significant property damage
3	Medium	Multiple severe injuries/not worth recording environmental damage/property damage that is not worth recording
2	Slight	Single serious injury / minor environmental damage / minor property damage
1	Insignificant	Minor injury/possible minor environmental and property damage

Severity table is prepared to determine the risk score. It is classified according to the severity of the incident, description of possible harm or loss, and its grade. The ranges are shown in Table 5.

Table 6. Railway risk matrix (5x5 L Type Matrix)

			Severity				
			Disaster	Severe	Medium	Slight	Insignificant
			5	4	3	2	1
Probability	Very High (Once a week/day)	A	A5	A4	A3	A2	A1
	High (Once a month)	B	B5	B4	B3	B2	B1
	Middle (Several times a year)	C	C5	C4	C3	C2	C1
	Very little (Once a year)	D	D5	D4	D3	D2	D1
	Impossible/rare	E	E5	E4	E3	E2	E1

The risk matrix was created by the authorsusing the literature, depending on the likelihood and severity values.

Table 7. Risk acceptability levels for railways of Türkiye

Risk Index	Risk Category	Action
A4, A5, B5	Unacceptable Risks	The identified works and transactions should be stopped immediately, and activities should be prevented if risk reduction processes are applied and the current risk cannot be reduced to the desired level.
A3, B4, C5	High-Grade Risks	Until the identified risks are reduced, work and operations should be stopped, and the risk should be reduced with additional control processes. The continuation of the work should be re-evaluated according to the data obtained as a result of the risk reduction methods.
A2, B2, B3, C3, C4, D4, D5, E5	Moderate Risks	It is necessary to implement risk reduction activities, and the business can be continued by taking responsibility.
A1, B1, C1, C2, D1, D2, D3, E1, E2, E3, E4	Low-Grade Risks	Existing controls should be maintained and audited, and additional security processes may not be required.

The table of risk acceptability levels is shown under three headings: risk index, risk category, and action.

In the study, when calculating the risk score in the 5x5 L-Decision Matrix analysis, likelihood values (A, B, C, D, E) were converted into numerical form (1, 2, 3, 4, 5). For each criterion, the overall average was taken, and the results were rounded to the nearest numerical value and converted back to their letter equivalents. Severity values were taken as the general average, and the results were also rounded to the nearest numerical value. For example “Implementation of the work in full compliance with the projects” which coded a1 and twenty people evaluated it, the average likelihood score was 2.65 and the average severity score was 3.65. The average likelihood score is 2.65, which corresponds to level C according to Table 3, the average severity score is 3.65, which corresponds to 4 according to Table 4. It means risk score is C4 level according to Table 5 railway risk matrix (5x5 L Type Matrix). The risk average weight multiplied by the numbers 2.65 and 3.65 is 9.67. The evaluation of the criteria that cause railway accidents according to the L-Decision Matrix of 20 experts and the risk obtained according to this evaluation are given in APENDIX-1.

In the study, the criteria that may cause railway accidents were examined in five separate groups and the AHP method was applied separately for each group. In addition, AHP was applied separately for risk, severity and likelihood for these five groups. In the application of the AHP method, the evaluations made by experts according to Saaty’s importance scale. In the evaluations, the L-Decision Matrix is based on the values of “1,2,3,4,5”, and the AHP technique is based on “1,2,3,...., 9” values. In this study,

the AHP technique was applied with reference to the values given in the L-Decision Matrix. For example, the value "1" in the L-Decision Matrix is taken as "1" for AHP, and the value "5" in the L-Decision Matrix is taken as "9" for AHP. Other values are also proportioned between this scale. A pairwise comparison matrix is applied with the evaluations obtained. Then, AHP was applied after taking the geometric mean of the obtained values for each criterion. Lettering and numbering were made taking into account the obtained criterion weights. An example of the application stages of the AHP method in this study is given in APENDIX-2.

4. RISK ANALYSIS AND EVALUATION FOR TÜRKİYE

In this study, which was prepared to ensure safe transportation in the railway transportation system in Türkiye, statistical data was obtained from the relevant institutions, the criteria that caused accidents on the railway were determined according to the literature and expert opinion, and these risks were evaluated by experts in the field. According to this evaluation, the criteria were ranked by applying the L-Decision Matrix and AHP methods. The study flow chart is shown in Figure 7.

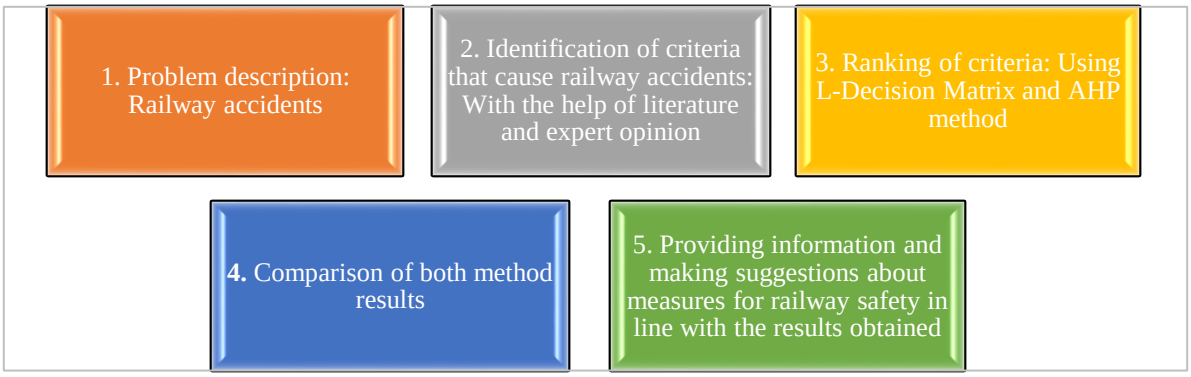

Figure 7. Railway risk analysis flow chart

The criteria that may cause railway accidents were determined by taking into consideration TCDD's accident investigation and investigation manuals [41], TCDD's and Minister of Transport of Türkiye's published and unpublished corporate documents, training manuals such as Education Catalog Manuals 2024 [42], Transport Safety Investigation Center of Türkiye's accident investigation reports between 2015 and 2022 [43] and participant suggestions, and literature review. The determined 58 criteria are examined under five headings. Figure 8 shows the determined criteria in the study.

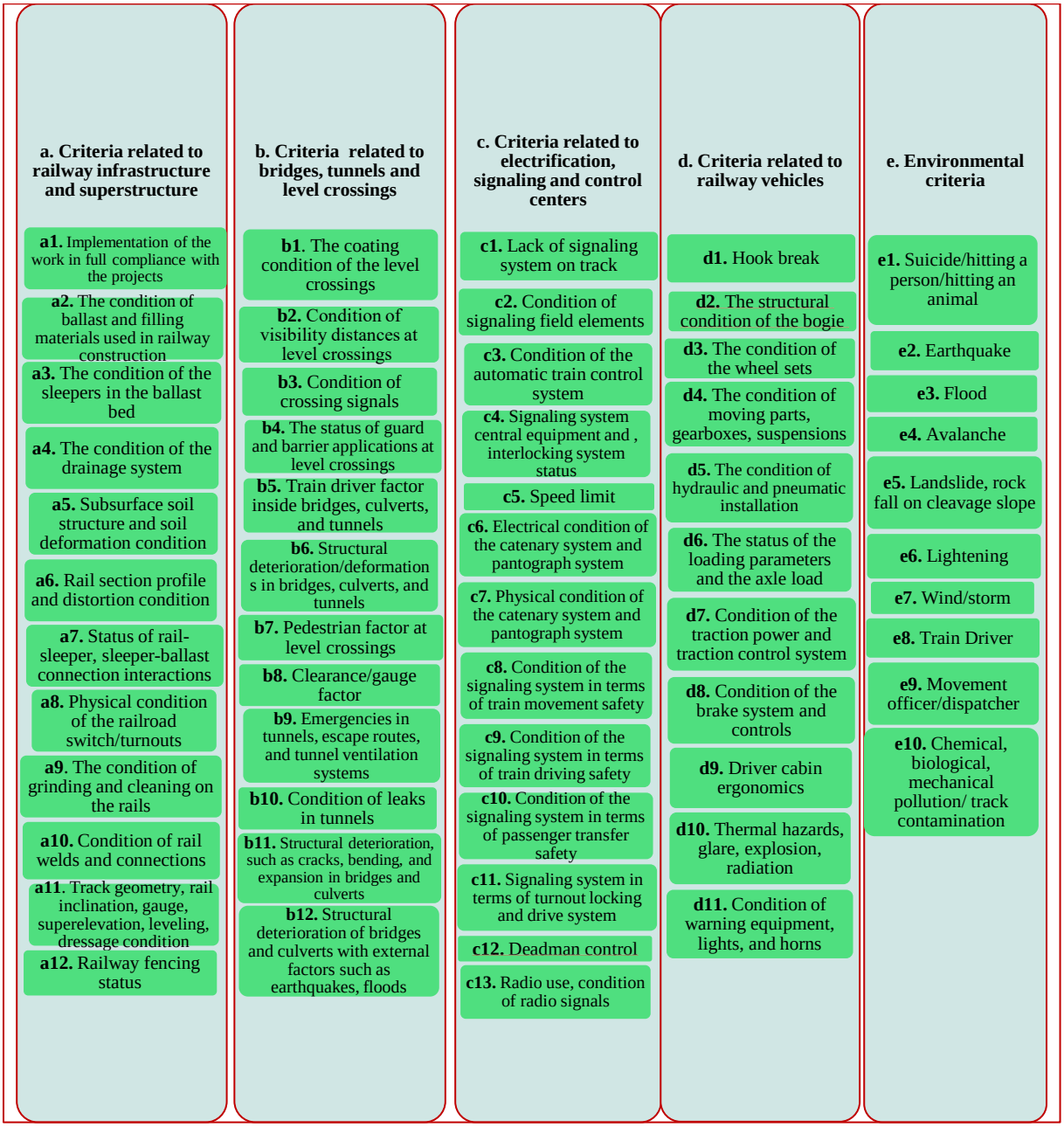

Figure 8. Determined Factors (Criteria) Related to Railway Accidents

In the study, the five groups in which the 58 criteria causing railway accidents are classified are "Criteria related to railway infrastructure and superstructure", "Criteria related to bridges, tunnels and level crossings", "Criteria related to electrification, signaling and control centers", "Criteria related to railway vehicles" and "Environmental criteria". In the study, each criterion was evaluated separately by the experts and the relationship between the criteria was not taken into consideration according to the L-Decision Matrix. The weight of the groups relative to each other in railway accidents was not analyzed and each group was considered to have equal weight.

Similarly, in AHP, Although the relationship of each criterion in each group is evaluated, the relative status of the groups as the main criterion is not taken into account. For example, the relative impact of the "Criteria related to railway infrastructure and superstructure" and "Criteria related to bridges, tunnels

and level crossings" groups on railway accidents was not examined in the study. However, the relationship of each criterion with other criteria within its group was analyzed separately.

5. FINDINGS AND RECOMMENDATIONS

The risk results obtained according to the methods used in the study are listed below. Tables 8 and 9 show the likelihood, severity, and risk results of the AHP and L-Decision Matrix method used in the study, respectively. Table 10 shows the results obtained in the study according to risk index and categories.

Table 8. Likelihood, severity, and risk results of L-Decision Matrix according to importance weight of criteria

AHP Method													
Criteria	**a1**	**a2**	**a3**	**a4**	**a5**	**a6**	**a7**	**a8**	**a9**	**a10**	**a11**	**a12**	**-**
Likelihood Importance Weight	0,0693	0,0693	0,0693	0,0693	0,0693	0,0693	0,0693	0,1325	0,0370	0,0693	0,0693	**0,2068**	-
Likelihood Class	D	D	D	D	D	D	D	C	E	D	C	B	-
Severity Importance Weight	0,0744	**0,1455**	**0,1455**	0,0744	0,0744	0,0744	0,0744	0,0744	0,0392	0,0744	0,0744	0,0744	-
Severity Score	3	4	4	3	3	3	3	3	2	3	3	3	-
Risk Importance Weight (p)	0,0797	**0,1357**	0,0797	0,0451	0,0451	0,0451	0,0451	0,0797	0,0206	0,0797	**0,1357**	0,0797	-
Risk Index	D3	D4	D4	D3	D3	D3	D3	C3	E2	D3	C3	B3	-
Criteria	**b1**	**b2**	**b3**	**b4**	**b5**	**b6**	**b7**	**b8**	**b9**	**b10**	**b11**	**b12**	**-**
Likelihood Importance Weight	0,1346	0,0779	0,0779	0,1346	0,0779	0,0423	**0,2082**	0,0423	0,0423	0,0779	0,0423	0,0423	-
Likelihood Class	C	D	D	C	D	E	B	E	E	D	E	E	-
Severity Importance Weight	0,0650	**0,1224**	0,0650	**0,1224**	0,0650	**0,1224**	**0,1224**	0,0379	0,0650	0,0254	0,0650	**0,1224**	-
Severity Score	3	4	3	4	3	4	4	2	3	1	3	4	-
Risk Importance Weight (p)	0,0639	0,1034	0,1034	0,1553	0,0639	0,0639	**0,2835**	0,0240	0,0382	0,0240	0,0382	0,0382	-
Risk Index	C3	D4	D3	C4	D3	E4	B4	E2	E3	D1	E3	E4	-
Criteria	**c1**	**c2**	**c3**	**c4**	**c5**	**c6**	**c7**	**c8**	**c9**	**c10**	**c11**	**c12**	**c13**
Likelihood Importance Weight	**0,0952**	**0,0952**	**0,0952**	**0,0952**	**0,0952**	0,0476	0,0476	0,0476	0,0952	0,0476	**0,0952**	0,0476	**0,0952**
Likelihood Class	C	C	C	C	C	D	D	D	D	D	C	D	C
Severity Importance Weight	0,0410	0,0731	0,0731	0,0731	**0,1295**	0,0410	0,0410	**0,1295**	**0,1295**	0,0410	**0,1295**	0,0731	0,0257
Severity Score	3	4	4	4	5	3	3	5	5	3	5	4	2
Risk Importance Weight (p)	0,0440	0,1305	0,0777	0,1305	**0,1986**	0,0440	0,0267	0,0777	0,0777	0,0267	0,0777	0,0440	0,0440
Risk Index	C3	C4	C4	C4	C5	D3	D3	D5	D5	D3	C5	D4	C2
Criteria	**d1**	**d2**	**d3**	**d4**	**d5**	**d6**	**d7**	**d8**	**d9**	**d10**	**d11**	**-**	**-**
Likelihood Importance Weight	0,0833	0,0833	0,0833	0,0833	0,0833	0,0833	**0,1667**	0,0833	0,0833	0,0833	0,0833	-	-
Likelihood Class	D	D	D	D	D	D	C	D	D	D	D	-	-
Severity Importance Weight	0,0985	**0,1731**	**0,1731**	0,0985	0,0519	0,0985	0,0519	0,0985	0,0519	0,0519	0,0519	-	-
Severity Score	3	4	4	3	2	3	2	3	2	2	2	-	-
Risk Importance Weight (p)	0,1021	**0,1760**	**0,1760**	0,1021	0,0570	0,1021	0,0570	0,1021	0,0343	0,0343	0,0570	-	-
Risk Index	D3	D4	D4	D3	D2	D3	C2	D3	D2	D2	D2	-	-
Criteria	**e1**	**e2**	**e3**	**e4**	**e5**	**e6**	**e7**	**e8**	**e9**	**e10**	**-**	**-**	**-**
Likelihood Importance Weight	**0,1538**	0,0769	0,0769	0,0769	0,0769	0,0769	0,0769	**0,1538**	**0,1538**	0,0769	-	-	-
Likelihood Class	C	D	D	D	D	D	D	C	C	D	-	-	-
Severity Importance Weight	**0,1828**	0,1022	0,1022	0,1022	0,1022	0,0589	0,0381	**0,1828**	0,1022	0,0265	-	-	-
Severity Score	5	4	4	4	4	3	2	5	4	1	-	-	-
Risk Importance Weight (p)	**0,2120**	0,0865	0,1355	0,0535	0,0535	0,0535	0,0342	**0,2120**	0,1355	0,0239	-	-	-
Risk Index	C5	D4	C4	D4	D4	D3	D2	C5	C4	D1	-	-	-

Table 9. Likelihood, severity, and risk results of L-Decision Matrix according to average weight of criteria

L-Decision Matrix Method													
Criteria	**a1**	**a2**	**a3**	**a4**	**a5**	**a6**	**a7**	**a8**	**a9**	**a10**	**a11**	**a12**	**-**
Likelihood Average Weight	2,65	2,50	2,47	2,37	2,26	2,25	2,35	2,60	1,95	2,45	2,55	**3,45**	-
Likelihood Class	C	C	D	D	D	D	D	C	D	D	C	C	-
Severity Average Weight	3,65	3,80	**3,89**	3,37	3,37	3,25	3,4	3,55	2,80	3,55	3,75	3,55	-
Severity Score	4	4	4	3	3	3	3	4	3	4	4	4	-
Risk Average Weight (p)	9,67	9,50	9,63	7,98	7,62	7,31	7,99	9,23	5,46	8,70	9,56	**12,25**	-
Risk Index	C4	C4	D4	D3	D3	D3	D3	C4	D3	D4	C4	C4	-
Criteria	**b1**	**b2**	**b3**	**b4**	**b5**	**b6**	**b7**	**b8**	**b9**	**b10**	**b11**	**b12**	**-**
Likelihood Average Weight	2,74	2,68	2,80	3,00	2,47	1,95	**3,68**	1,70	1,80	2,15	1,68	1,74	-
Likelihood Class	C	C	C	C	D	D	B	D	D	D	D	D	-
Severity Average Weight	3,37	3,84	3,70	3,79	3,42	**4,11**	**4,11**	2,80	3,85	2,70	3,68	3,95	-
Severity Score	3	4	4	4	3	4	4	3	4	3	4	4	-
Risk Average Weight (p)	9,22	10,31	10,36	11,37	8,46	7,99	**15,12**	4,76	6,93	5,81	6,2	6,86	-
Risk Index	C3	C4	C4	C4	D3	D4	B4	D3	D3	D3	D3	D3	-
Criteria	**c1**	**c2**	**c3**	**c4**	**c5**	**c6**	**c7**	**c8**	**c9**	**c10**	**c11**	**c12**	**c13**
Likelihood Average Weight	2,32	2,42	2,26	**2,47**	**2,47**	2,11	1,95	2,05	2,16	1,95	2,11	1,82	2,39
Likelihood Class	D	D	D	D	D	D	D	D	D	D	D	D	D
Severity Average Weight	3,74	4,11	4,21	4,26	**4,74**	3,84	3,26	4,26	4,37	3,63	4,37	4,24	3,28
Severity Score	4	4	4	4	5	4	3	4	4	4	4	4	3
Risk Average Weight (p)	8,65	9,94	9,53	10,55	**11,72**	8,09	6,35	8,75	9,43	7,07	9,2	7,72	7,83
Risk Index	D4	D4	D4	D4	D5	D4	D3	D4	D4	D4	D4	D4	D3
Criteria	**d1**	**d2**	**d3**	**d4**	**d5**	**d6**	**d7**	**d8**	**d9**	**d10**	**d11**	**-**	**-**
Likelihood Average Weight	2,06	1,95	1,89	1,89	1,94	1,84	**2,21**	2,05	1,79	1,95	2,11	-	-
Likelihood Class	D	D	D	D	D	D	D	D	D	D	D	-	-
Severity Average Weight	3,65	4,00	3,83	3,78	3,28	3,68	2,84	3,47	2,84	3,11	3,32	-	-
Severity Score	4	**4**	4	4	3	4	3	3	3	3	3	-	-
Risk Average Weight (p)	7,51	**7,79**	7,24	7,14	6,37	6,79	6,28	7,13	5,09	6,05	6,98	-	-
Risk Index	D4	D4	D4	D4	D3	D4	D3	D3	D3	D3	D3	-	-
Criteria	**e1**	**e2**	**e3**	**e4**	**e5**	**e6**	**e7**	**e8**	**e9**	**e10**	**-**	**-**	**-**
Likelihood Average Weight	2,16	2,00	2,00	1,68	1,89	1,89	1,89	**2,21**	2,11	1,76	-	-	-
Likelihood Class	D	D	D	D	D	D	D	D	D	D	-	-	-
Severity Average Weight	**4,32**	3,89	3,95	3,89	3,89	3,58	3,05	4,26	3,83	2,41	-	-	-
Severity Score	4	4	4	4	4	4	3	4	4	2	-	-	-
Risk Average Weight (p)	9,31	7,79	7,89	6,56	7,38	6,78	5,78	**9,42**	8,09	4,26	-	-	-
Risk Index	D4	D4	D4	D4	D4	D4	D3	D4	D4	D2	-	-	-

In Table 9, “Likelihood Average Weight” is the sum of the likelihood scores given by the participants divided by the number of participants; “The Average of Severity Weight” is the sum of the severity scores given by the participants divided by the number of participants; “Significant Weight of Risk” is the multiplication result of these two figures for L-Decision Matrix.

In Tables 8 and 9, the results for both methods are given separately. The results obtained for both methods are given in Table 10.

Table 10. Risk analysis result

Risk Index	Risk Category	Criteria Codes (L-Decision Matrix Method)	Criteria Codes (AHP Method)
A4, A5, B5	Unacceptable Risks		
A3, B4, C5	High-Grade Risks	b7	b7, c5, c11, e1 and e8
A2, B2, B3, C3, C4, D4, D5, E5	Moderate Risks	a1, a2, a3, a8, a10, a11, a12, b1, b2, b3, b4, b6, b9, b11, b12, c1, c2, c3, c4, c5, c6, c8, c9, c10, c11, c12, d1, d2, d3, d4, d6, e1, e2, e3, e4, e5, e6, e8 and e9.	a2, a3, a8, a11, a12, b1, b2, c1, c2, c3, c4, c8, c9, c12, d2, d3, e2, e3, e4, e5 and c4
B4, A1, B1, C1, C2, D1, D2, D3, E1, E2, E3, E4	Low-Grade Risks	a4, a5, a6, a7, a9, b5, b8, b10, c7, c13, d5, d7, d8, d9, d10, d11, d12, e7 and e10.	a1, a4, a5, a6,a7,a9, a10, b3, b5, b6, b8, b9, b10, b11, b12, c6, c7, c10, c13, d1, d4, d5, d6, d7, d8, d9, d10, d11, e6, e7 and e10

As a result of the L-Decision Matrix (5x5) study, the highest risk scores were determined as "Uncontrolled entrances to level crossings by pedestrians" with code b7. The results were also compared with the AHP method, and in addition to the b7 risk obtained in the L-Decision Matrix at the highest risk scores according to the AHP method, c5, c11, e1 and e8 risks were also included in the high-grade risks category.

The high-grade risks category obtained in the AHP and L Decision Matrix are given in Table 11 below, together with the possible results related to the identified risk definitions and mitigation activities. Also, risk definitions and mitigation activities belong to "Railway fencing status" with code a12, "Condition of signaling field elements" with code c2, "Condition of the automatic train control system" with code c3, "Signaling system central equipment and, interlocking system status" with code c4, "Condition of the signaling system in terms of train movement safety" with code c8 and "Condition of the signaling system in terms of train driving safety" with code c9 are given in Table 11, because it is considered important according to experts.

Table 11. Risks related to railways and recommended risk reduction activities

Criterion Code	Criteria	Possible Consequences	Risk Reduction/Prevention Activities
a12	Condition of railway fencings	Injury, Death, Property Damage	Although railway fencings are not applicable along the track, fence/wall enclosures should be taken along the station and residential areas. Even illegal and uncontrolled entrances should be prevented. The condition of the railway fence applications should be checked regularly. The drivers' field of vision should be clear. Elevated lines can be built; ecological bridges can be built; law enforcement agencies should tighten patrols.
b7	Pedestrian behaviour at level crossings	Injury, Death, Property Damage, Derailment, Collision	One of the precursors that cause the most accidents at level crossings is uncontrolled entrances on the line. The public should be informed about the issue, and social awareness should be developed. Traffic signs and crossing signals are placed. Active protection measures should be taken for pedestrians, physical speed breakers (manual opening doors, maze entrances, active protected doors) should be applied, separate sections should be created for pedestrians at level crossings, barriers must completely block the passage of pedestrians, they must not be short.
c2	Inability to determine the location and understand the line's occupation due to the lack or failure of signaling system field elements, rail circuits, signal booths and signals, relays, balises, and axle meters in the line infrastructure (Condition of signaling field elements)	Injury, Death, Property Damage, Derailment, Collision	They must be in sufficient numbers; they must be regularly and periodically maintained
c3	Failure or malfunction of the appropriate train protection system (automatic train stopping-ATS/automatic train protection- ATP) to be operated by the train on the track (Condition of the automatic train control system)	Injury, Death, Property Damage, Derailment, Collision	There should be periodic checks and maintenance follow-up at regular intervals. At the first exit station, train movement should not be allowed if necessary, depending on the type of fault.
c4	Not opening and closing the switches automatically and completely, not being able to organize a safe route due to system malfunctions, organizing the wrong route, not ensuring continuity of radio communication, and not paying attention to incoming notifications (Signaling system central equipment and interlocking system status).	Injury, Death, Property damage, Derailment, Collision	Tracking systems should be installed in monitoring centers. Staff should be given the necessary training, and periodic checks of the system should be made.
c5	High speed	Injury, Death, Property damage, Derailment, Collision	Machinists must be ensured to comply with the speed limits along the routes and must be monitored from monitoring centers.
c8	Inability to command and control the route created for safe driving and inability to control the speed with automatic systems (Condition of the signaling system in terms of train movement safety).	Injury, Death, Property damage, Derailment, Collision	Primary or advanced signaling systems such as IXL, CBTC, DRS, ATS, and ETCS should be installed.
c9	High speed by train driver	Injury, Death, Property damage, Derailment, Collision	Machinists must be ensured to comply with livre speeds along the routes. Automatic train automation systems should be installed for driving safety.
c11	Locking and drive system malfunctions in turnouts, system errors, sending wrong signals, and incorrect route determination (Signaling system in terms of turnout locking and drive system)	Injury, Death, Property damage, Derailment, Collision	Periodic maintenance should be performed. Personnel training should be provided periodically.
e1	Suicide/hitting a person/hitting an animal	Injury, Death, Property damage, Derailment, Collision	Speed limits appropriate to the visibility of drivers should be set; the track should be isolated from the environment; public awareness should be raised. Obstacle recognition sensors can be used.

e8	Train driver	Injury, Death, Property damage, Derailment, Collision	Train drivers should receive regular training, practice in training simulators, psycho-technical tests should be organized to asses their psychological and physical competence, adequate rest periods should be provided.

6.CONCLUSION

Turkish railways will be a more modern, efficient, and competitive sector in the future if the right policies and investments are implemented. For healthy and sustainable railway transportation, security will always remain the most critical issue. In this study carried out to ensure railway safety, the L-Decision Matrix and AHP method, were used to examine the status of the risks determined after the evaluation made by benefiting from the knowledge, experience, and opinions of experts.

The number of railway accidents and deaths in Türkiye between 2002 and 2021 tend to decrease. Between the mentioned years, the number of accidents per million train-km of mobility decreased by 86% from 12.23 accidents to 1.65 accidents. The number of deaths decreased by 79%, from 3.3 deaths to 0.7 deaths. Comparing the data for the period between 2010 and 2020, when the safety culture in Türkiye started to increase with the development and modernization of legislation and modernization efforts and was more successful compared to the previous years, the highest values per million train-km movement in Türkiye were 2.79 accidents and 1.45 fatalities.

While level crossing accidents and personal collisions seemed to be higher than other types in the early 2000s, derailment accidents have been higher than other types in recent years. When the types of accidents between EU countries and Türkiye are compared between 2010 and 2020, it is noteworthy that the rate of derailment accidents in Türkiye is approximately 4.5 times higher than the EU average.

When the risk analyses were compared according to the risk average weight score, it was observed that the “Uncontrolled entrances of pedestrians to level crossings” with the factor code b7, L-Decision Matrix p = 15.12 (0 - 25) and AHP method p = 0.28 (0 - 1) b7 is in the high-grade risk category. In addition, in the AHP analysis, factors with codes c5, c11, e1 and e8 were also found to be in the high-grade risk category. AHP analysis was found to give more precise results. Pedestrian-train interactions have emerged as the parameters that cause the most accidents, and the statistics seem to confirm these results.

Precautions regarding the hazards detected in the high-grade risk category are explained in Table 11. It is essential to take a multi-pronged approach to accident prevention at level crossings. Working in collaboration with infrastructure improvements, education, legislation, and technological solutions can improve safety and prevent accidents at level crossings. In order to prevent accidents at level crossings, the primary thing to do is to separate the roadway and railway intersections as much as possible with the help of upper and lower crossings. At intersections that cannot be separated from each other, level crossings should be made as controlled as possible. Crossing routes, especially for pedestrians, should be separated from the railways. At level crossings where roads intersect, crossings should be made relatively difficult to ensure pedestrians are aware of trains. For example, physical speed breakers (manual opening doors, maze entrances, active protected doors) should be applied; separate sections should be created for pedestrians at level crossings; barriers must completely block the passage of pedestrians, and they must not be short.

Signaling system and high speeds are also high grade risk according to AHP on table 10. Train drivers must be ensured to comply with the speed limits along the routes and must be monitored from monitoring centers. Personnel training should be provided periodically. Periodic maintenance should be performed. On the other hand it is seen that signaling systems in Türkiye are made in parts and by different companies with different software and hardware. This situation causes incompatibilities in software, hardware, and integration. Therefore, when establishing signaling systems, the integration and operation

difficulties of different systems should be taken into account, and studies should be carried out to reduce this system diversity, for example, by implementing domestic signaling systems.

Yet another high grade risks came from train drivers' themselves and suicide/hitting a person/hitting an animal. Train drivers should receive regular training, practice in training simulators, psycho-technical tests should be organized to asses their psychological and physical competence, adequate rest periods should be provided. In order to prevent suicide/hitting people/hitting animals, train drivers should receive regular training, practice in training simulators, psychotechnical tests should be organized to evaluate their psychological and physical competencies, adequate rest periods should be provided, speed limits appropriate to the visibility of the drivers should be determined, the track should be isolated from the environment, public awareness should be raised, obstacle recognition sensors should be used.

As a continuation of this study, similar risk analysis studies should be carried out at periodic intervals; developments should be monitored; initiatives to minimize possible risks by taking advantage of rapid measures and new technological developments should be followed up to date. Further studies should be conducted in specifically identified areas.

CONFLICT OF INTEREST

The authors stated that there are no conflicts of interest regarding the publication of this article.

CREDIT AUTHOR STATEMENT

Burçin Paçacı: Formal analysis, Writing - original draft, Visualization, Writing – Review & Editing. **Hulusi Aydemir:** Conceptualization, Formal analysis, Writing – Original Draft. **Metin Eser:**Conceptualization, Formal analysis, Resources, Writing – Original Draft, Writing – Review & Editing, Visualization. **Serpil Erol:** Methodology, Formal analysis. **M. Kürşat Çubuk:** Conceptualization, Formal analysis, Writing – Original Draft.

REFERENCES

[1] Strategy development directorate, 2053 logistics master plan. Turkish Ministry of Transport and Infrastructure. Available: https://www.uab.gov.tr/uploads/pages/bakanlik-yayinlari/uab-u2053-borsur-a4-180822-ecs.pdf Accessed: 30.09.2022.

[2] UIC Safety Report 2022. International Union of Railways (UIC). Available: https://safetydb.uic.org/IMG/pdf/uic_safety_report_2022.pdf Accessed: 01.11.2022.

[3] Directive (EU) 2016/798 on railway safety, Official Journal of the European Union. Available: https://eur-lex.europa.eu/legal-content/EN/TXT/?uri=CELEX%3A32016L0798 Accessed: 01.11.2022.

[4] Leitner B. A general model for railway systems risk assessment with the use of railway accident scenarios analysis. Procedia engineering 2017; 187: 150-159.

[5] Hadj-Mabrouk H. Analysis and prediction of railway accident risks using machine learning. AIMS Electronics and Electrical Engineering 2020; 4(1): 19-46.

[6] Hu S-R and Wu K.-H. Accident risk analysis and model applications of railway level crossings. In 2008 11th International IEEE Conference on Intelligent Transportation Systems. 2008; IEEE.

[7] Akbayır Ö. Comparison of Railway Fatality Rate Between Turkey and The World. In: Third ISERSE16, 13-15 November 2016, Karabük, Turkey.

[8] Kıyıldı RK. Developments in open line rail transportation in our country with statistics. NOHU J. Eng. Sci., 2022; 11(4), 990-998.

[9] lıcalı M. Demiryollarında ihata uygulaması ve dünyadan örneklerin değerlendirilmesi raporu. Istanbul Commerce University. 2016.

[10] Ghanem O, Xuemei L. An evaluation and efficiency analysis of railways safety: A case study of EU and Turkey. International Journal of Sustainable Economies Management (IJSEM), IGI Global, 2016, 8(1):1-16.

[11] Bakioğlu G. Evaluation of railway transport safety measures using picture Fuzzy SWARA approach. Railway Engineering 2024; (20), 107-122.

[12] Özarpa C, Avcı İ, and Kınacı BF. Critical level analysis of subsystems in smart Rail Systems. Railway Engineering 2021; 14: 143-153

[13] Narlı M, Göçmen E and Derse O. Risk assessment using a novel hybrid method: A case study at the biochemistry department. Hacettepe Journal of Health Administration 2021; 24(3): 571-588.

[14] Doğan O and Keskin MÖ. Evaluation of risks using L-Type Matrix method and AHP method: A sample application. Journal of Engineering Sciences and Design 2023; 11(4): 1282-1293.

[15] Annuel statistics 2001-2005. State Railways of the Republic of Turkey (2005). Available: https://static.tcdd.gov.tr/webfiles/userfiles/files/tcddistatistik2005(1).pdf Accessed: 31.09.2022.

[16] Annuel statistics 2005-2009. State Railways of the Republic of Turkey 2009. Available: https://static.tcdd.gov.tr/webfiles/userfiles/files/20052009ist.pdf Accessed: 31.09.2022.

[17] Annuel statistics 2009-2013. State Railways of the Republic of Turkey 2013. Available: https://static.tcdd.gov.tr/webfiles/userfiles/files/20092013yillik.pdf Accessed: 31.09.2022.

[18] Annuel statistics 2013-2017. State Railways of the Republic of Turkey 2017. Available: https://static.tcdd.gov.tr/webfiles/userfiles/files/20132017yillik.pdf Accessed: 31.09.2022.

[19] Annuel statistics 2017-2021. State Railways of the Republic of Turkey 2021. Available: https://static.tcdd.gov.tr/webfiles/userfiles/files/istrapor/ist20172021.pdf Accessed: 31.09.2022.

[20] Transportation and communications statistical tables. TUIK. Available: https://data.tuik.gov.tr/Kategori/GetKategori?p=ulastirma-ve-haberlesme-112 Accessed: 09.09.2022.

[21] European Commission – Statistical Pocketbook, European Commission. Available: https://transport.ec.europa.eu/facts-funding/studies-data/eu-transport-figures-statistical-pocketbook/statistical-pocketbook-2022_en Accessed: 2022.

[22] Rail accidents by type of accident. Eurostat. Available: https://ec.europa.eu/eurostat/databrowser/view/tran_sf_railac/default/table?lang=en Accessed:30.09.2022.

[23] Railway Transport (t-rail), Eurostat (t.y.). Available: https://ec.europa.eu/eurostat/data/database Accessed:30.09.2022.

[24] Rail accidents victims by type of accident and category of persons involved. Eurostat. Available: https://ec.europa.eu/eurostat/databrowser/-explore/all/transp?lang=mt&display=card&sort=category&extractionId=MIGR_ASYAPPCTZM Accessed: 01.10.2022.

[25] Analysis and mitigation of derailment, assessment and commercial impact. D-rail 2013. Available: https://d-rail-project.eu/IMG/pdf/DR-D32-F3-Analysis_mitigation_derailment-assessment_commercial_impact.pdf

[26] Eser M. Statistical comparison and risk assesment of railway accidents in Turkey. MSc, Gazi University, Ankara, Turkey, 2023.

[27] Çetinbaş M. Excel applications on multi-criteria decision making methods. Pamukkale University Journal of Business Research 2018; 4(1): 12-29.

[28] Liberatore MJ and Nydick RL, An analytic hierarchy approach for evaluating product formulations. Computer aided formulation: A manual for implementation 1990; 179-94.

[29] Kılıç İ. Bulanık-analitik hiyerarşi sürecini kullanarak İstanbul Boğazı'nda deniz kazaları risk analizi. Msc, Istanbul Technical University, İstanbul, Turkey, 2015.

[30] Arslan Ö, Turan O. Analytical investigation of marine casualties at the Strait of Istanbul with SWOT–AHP method. Maritime Policy & Management 2009; 36(2):131-145.

[31] Bayazıt G. Safety assessment at railway level crossings: Developing a sample model for Turkey. MSc, Istanbul Technical University, İstanbul, Turkey, 2019.

[32] Bureıka G, Bekıntıs G, Lıudvınavıčıus L, Vaıčıūnas G. Applying analytic hierarchy process to assess traffic safety riskof railway infrastructure. Eksploatacja Niezawodnosc, Maintenance and Reliability 2013; 15 (4): 376–383.

[33] Liu C, Yang S, Cui Y, Yang Y. An improved risk assessment method based on a comprehensive weighting algorithm in railway signaling safety analysis. Safety Science 2020; 128:104768.

[34] Uray K. Determination of Possible Effects of Risks Using Matrix Method in Railway Maintenance Works. Journal of Disaster and Risk 2021; 4(2): 121-134.

[35] Damat A and Utlu Z, Occupational Health And Safety Applicatıons In Istanbul Metro Stations. Railway Engineering 2018; (8): 52-69.

[36] Bayraktar H, Sahtiyancı E, Kuru A. Determination of The Possible Effects of Non-Structural Risks Originating From Earthquake in Schools By Using Risk Assessment Matrix Method. Journal of Disaster and Risk 2019; 2(2): 128-152.

[37] Saaty TL, Tran LT. On the invalidity of fuzzifying numerical judgments in the analytic hierarchy process. Mathematical and Computer Modelling 2007; (46): 962-975.

[38] Paçacı B, Erol S and Çubuk MK. AHP Application for logistics center location selection according to criteria. Bitlis Eren University Journal of Science 2022; 11(4): 943-952.

[39] Arıbaş M and Özcan U. Evaluation of Academic Research Projects Using AHP and TOPSIS Methods. Journal of Polytechnic 2016; 19 (2) : 163-173.

[40] Özkılıç Ö. Occupational health and safety, management systems and risk assessment methodologies. Ministry of Labor and Social Security Labor Inspection Board Istanbul Group Presidency. Available: http://egitim.druz.com.tr/upload/docs/26042012105841_vAq1THf-6-105841_risk-analizi-ozlem-ozkilic-kitabi.pdf Accessed: 08.01.2022.

[41] TCDD, The State Railways of the Republic of Türkiye Accident investigation and investigation manuals. https://www.tcdd.gov.tr/kurumsal/yonergeler Accessed: 09.11.2023.

[42] TCDD, The State Railways of the Republic of Türkiye. Available: https://akademi.tcdd.gov.tr/Egitim Accessed: 09.05.2024.

[43] Official Railway Accident Investigation Reports, Transport Safety Investigation Center of Türkiye. Available: https://ulasimemniyeti.uab.gov.tr/demiryolu Accessed: 09.05.2022.

APENDIX-1

		1. person		2. person		3. person		4. person		5. person		6. person		7. person		8. person		9. person		10. person		11. person		12. person		13. person		14. person		15. person		16. person		17. person		18. person		19. person		20. person		Possibility/likelihood ABCDE	Severity 12345	Risk importance score	RISK	
		Possibility/likelihood	Severity	Possibility/likelihood	Severity	Possibility/likelihood	Severity	Possibility/likelihood	Severity	Possibility/likelihood	Severity	Possibility/likelihood	Severity	Possibility/likelihood	Severity	Possibility/likelihood	Severity	Possibility/likelihood	Severity	Possibility/likelihood	Severity	Possibility/likelihood	Severity	Possibility/likelihood	Severity	Possibility/likelihood	Severity	Possibility/likelihood	Severity	Possibility/likelihood	Severity	Possibility/likelihood	Severity	Possibility/likelihood	Severity	Possibility/likelihood	Severity	Possibility/likelihood	Severity	Possibility/likelihood	Severity				
A1	Implementation of the work in full compliance with the projects	5	5	1	1	3	2	3	3	3	3	3	3	2	5	3	5	3	3	2	2	4	3	5	5	2	3	2	3	2	4	3	4	2	5	2	5	2	4	1	5	2,65	3,65	9,67	C	4	C 4
A2	The condition of ballast and filling materials used in railway construction	3	5	2	4	3	3	3	4	2	4	2	4	3	4	4	5	3	3	3	4	2	3	2	2	2	3	2	3	2	4	3	2	2	5	2	5	2	5	3	4	2,50	3,80	9,50	C	4	C 4
A3	The condition of the sleepers in the ballast bed	3	5	2	4	3	3	2	5	4	4	2	2	3	4	3	5	3	5	2	2	1	2	2	2	3	4	3	4	1	4			2	5	2	5	2	5	4	4	2,47	3,89	9,63	D	4	D 4
A4	The condition of the drainage system	3	5	2	4	3	2	4	2	3	4	3	3	2	4	2	3	2	2	3	2	2	3	2	2	2	4	2	4	1	4			2	5	2	5	2	3	3	3	2,37	3,37	7,98	D	3	D 3
A5	Subsurface soil structure and soil deformation condition	3	5	1	4	3	2	1	5	4	3	2	3	2	3	2	3	2	3	2	2	2	3	2	2	2	3	2	3	1	4			3	5	3	5	3	3	3	3	2,26	3,37	7,62	D	3	D 3
A6	Rail section profile and distortion condition	2	3	2	2	3	2	1	4	3	4	2	4	2	3	2	3	2	3	2	2	3	3	2	2	3	3	3	3	2	3	2	2	2	5	2	5	2	5	3	4	2,25	3,25	7,31	D	3	D 3
A7	Status of rail-sleeper, sleeper-ballast connection interactions	3	4	1	3	3	3	2	4	3	4	2	4	2	3	2	3	2	3	3	3	2	2	2	2	3	3	3	3	2	3	3	2	2	5	2	5	2	5	4	4	2,35	3,40	7,99	D	3	D 3
A8	Physical condition of the railroad switch/turnouts	3	3	2	3	3	4	3	3	3	3	2	2	2	5	3	5	3	4	3	3	3	3	2	2	2	3	2	3	2	4	3	2	2	5	2	5	2	5	4	4	2,60	3,55	9,23	C	4	C 4
A9	Condition of grinding and cleaning of rails	1	4	1	2	3	3	2	2	2	2	3	3	2	3	2	2	2	2	1	1	2	2	2	2	2	3	2	3	1	2	1	1	2	5	2	5	2	5	4	4	1,95	2,80	5,46	D	3	D 3
A10	Condition of rail welds and connections	2	4	3	3	3	3	2	4	3	3	3	3	2	4	3	4	2	2	3	2	2	3	3	3	2	4	2	4	1	4	3	2	2	5	2	5	2	5	4	4	2,45	3,55	8,70	D	4	D 4
A11	Track geometry, rail inclination, gauge, superelevation, leveling, dressage, condition	2	5	2	3	2	2	2	3	3	4	2	4	3	4	3	5	3	5	2	4	4	4	2	2	3	3	3	3	2	3	2	2	3	5	3	5	2	5	3	4	2,55	3,75	9,56	C	4	C 4
A12	Enclosure status	2	3	5	4	1	1	5	4	2	4	2	3	4	3	3	5	4	5	2	3	4	4	3	2	4	4	4	4	3	4	2	2	5	5	4	5	5	3	5	3	3,45	3,55	12,25	C	4	C 4
B1	Coating condition of level crossings	3	4	1	1	1	2	3	4	2	2	3	3	3	3	3	3	4	5	2	3	2	3	2	4	3	3	3	3	2	4			4	5	4	5	4	4	3	3	2,74	3,37	9,22	C	3	C 3
B2	Condition of Visibility Distances at level crossings	2	4	2	4	1	3	1	5	2	2	3	2	3	3	3	3	3	3	2	5	4	4	2	4	3	4	3	4	2	4			4	5	4	5	4	5	3	4	2,68	3,84	10,31	C	4	C 4
B3	The status of traffic sign applications at level crossings	2	4	1	4	1	4	1	5	2	2	4	3	3	3	3	3	2	3	2	4	3	3	3	4	4	4	4	4	1	4	3	2	4	5	4	5	4	4	5	4	2,80	3,70	10,36	C	4	C 4
B4	Status of guards and barriers at level crossings	2	4	1	4	1	4	3	4	2	2	3	3	3	3	3	3			2	4	4	5	3	4	4	4	4	4	2	4	3	2	4	5	4	5	4	4	5	4	3,00	3,79	11,37	C	4	C 4
B5	Train driver factor inside bridges, culverts, tunnels	2	4	1	2	1	2	2	3	3	3	4	2	3	3	3	3	3	3	2	3	2	3	2	3	3	4	3	4	2	4			2	5	2	5	2	5	5	4	2,47	3,42	8,46	D	3	D 3
B6	Structural deterioration/deformations in bridges, culverts and tunnels	2	2	1	4	1	1	1	5	3	3	1	5	1	5	3	5	3	3	1	5	1	5	2	4	3	4	3	4	2	3			2	5	2	5	2	5	3	5	1,95	4,11	7,99	D	4	D 4
B7	Pedestrian factor at level crossings	3	5	2	4	1	5	5	4	3	4	4	3	5	3	3	2	2	2	3	5	4	5	3	4	5	5	5	4	2	4			5	5	5	5	5	5	5	4	3,68	4,11	15,12	B	4	B 4
B8	Clearence/gauge factor	1	5	1	1	1	2	1	5	2	2	2	3	2	3	3	2	2	2	1	1	1	2	2	2	2	4	1	3	2	3	1	1	2	4	2	4	2	4	3	3	1,70	2,80	4,76	D	3	D 3
B9	Emergency situations in tunnels, escape routes and tunnel ventilation systems	1	5	1	1	1	4	1	5	2	2	1	5	2	4	2	5	2	2	1	5	3	3	2	2	2	3	2	3	1	3	2	5	2	5	2	5	2	5	4	5	1,80	3,85	6,93	D	4	D 4
B10	Condition of leaks in tunnels	2	5	1	1	1	1	2	3	1	1	2	4	2	2	2	2	2	2	3	1	2	2	2	2	3	3	5	3	2	3	2	2	2	4	2	5	2	4	3	4	2,15	2,70	5,81	D	3	D 3
B11	Structural deterioration such as cracks, bending, expansion in bridges and culverts	2	5	1	1	1	3	1	5	2	2	2	3	2	5	2	3	2	2	1	5	1	4	1	3	2	3	2	3	1	3			2	5	2	5	2	5	3	5	1,68	3,68	6,20	D	4	D 4
B12	Structural deterioration of bridges and culverts due to external factors such as earthquakes and floods	2	5	1	4	1	4	1	5	2	2	2	4	2	5	2	2	3	3	1	5	1	4	1	4	2	2	2	2	1	4			2	5	2	5	2	5	3	5	1,74	3,95	6,86	D	4	D 4
C1	Lack of signalization system on the lines	2	5	1	1	1	3	4	2	5	1	2	3	4	3	5	2	2				4	5	2	4	2	3	2	3	2	4	3	3	2	5	2	5	2	5	5	5	2,32	3,74	8,65	D	4	D 4
C2	Condition of signaling field elements	2	5	2	4	1	5	4	3	2	5	2	2	3	5	3	5	2	4			3	4	2	4	2	3	2	3	2	4	3	3	2	5	2	5	2	5	5	4	2,42	4,11	9,94	D	4	D 4
C3	Condition of the automatic train control system	2	5	2	3	1	5	2	3	2	5	1	2	3	5	3	5	4	5			3	4	2	3	2	4	2	4	2	4	2	4	2	5	2	5	2	5	4	4	2,26	4,21	9,53	D	4	D 4
C4	Signalization system, interlocking system status	2	5	2	4	1	5	3	3	2	5	1	3	3	5	3	5	4	5			3	4	2	4	3	3	3	3	2	5	2	2	2	5	2	5	2	5	5	5	2,47	4,26	10,55	D	4	D 4
C5	Speed limit	2	5	2	4	1	5	2	5	2	5	1	4	4	5	2	5	3	5			3	4	2	4	3	5	3	5	2	5	1	4	3	5	3	5	5	5	5	5	2,47	4,74	11,72	D	5	D 5
C6	Electrical condition of the catenary system and pantograph system	2	5	1	1	1	5	1	4	2	3	2	3	2	4	2	5	2	4			2	3	1	4	4	5	4	5	2	2	1	2	2	5	2	5	2	5	5	3	2,11	3,84	8,09	D	4	D 4
C7	Physical condition of the catenary system and pantograph system	2	3	1	4	1	5	1	5	2	2	2	4	2	3	2	2	2	4			1	4	1	4	3	4	3	4	2	3	1	2	2	2	2	2	2	5	3	3	1,95	3,26	6,35	D	3	D 3
C8	Condition of the signaling system in terms of train movement safety	2	5	2	4	1	4	3	4	2	5	1	3	2	5	3	5	2	4			3	3	1	4	2	4	2	4	2	5	1	4	2	5	2	5	2	5	4	3	2,05	4,26	8,75	D	4	D 4
C9	Condition of the signaling system in terms of train driving safety	2	5	2	4	1	4	2	5	2	5	2	3	4	4	2	5	2	4			3	4	2	4	1	4	1	4	2	5	2	3	2	5	2	5	2	5	5	5	2,16	4,37	9,43	D	4	D 4
C10	Condition of the signaling system in terms of passenger transfer safety	2	4	1	1	1	5	4	2	2	5	1	4	2	4	2	4	2	3			2	3	1	4	1	3	1	3	2	4	2	2	2	5	2	5	2	5	5	3	1,95	3,63	7,07	D	4	D 4
C11	Signaling system in terms of turnout locking and drive system	2	5	2	4	1	5	1	5	2	5	1	4	2	5	2	5	2	2			2	3	2	4	3	4	2	5	2	4	2	5	2	5	2	5	5	4	2,11	4,37	9,20	D	4	D 4
C12	Deadman control	2	5	1	1	1	4	1	5	1	5			2	5	2	4					1	3	1	5	2	3	2	3	2	5	2	4	2	5	2	5	5	5	1,82	4,24	7,72	D	4	D 4
C13	Radio use, condition of radios	2	3	1	1	1	3	4		2	3	2	4	2	5	2	3					3	3	3	2	3	3	2	3	2	4	3	2	2	5	2	5	5	5	2,39	3,28	7,83	D	3	D 3
D1	Hook break	2	5	1	1	1	1	1	4	2	3			2	4	2	3					4	5	1	3	3	3	3	3	2	4	2	4	2	5	2	5	2	5	3	4	2,06	3,65	7,51	D	4	D 4
D2	Structural condition of the bogie	2	5	1	1	1	4	2	5	1	5	2	4	2	4	2	3	2	4			3	4	1	4	3	3	3	3	2	5	2	3	2	5	2	5	2	5	4	4	1,95	4,00	7,79	D	4	D 4
D3	Condition of the wheelsets	2	5	2	4	2	1	2	4	1	5	2	3	2	4	2	3	2	3			2	4	1	3	2	4	2	4	2	3			2	5	2	5	2	5	4	4	1,89	3,83	7,24	D	4	D 4
D4	Condition of moving parts, gearboxes, suspensions	2	5	1	1	2	3	2	5	1	3	2	4	2	4	3	5	2	4			2	4	1	3	2	3	2	3	2	3			2	5	2	5	2	5	2	3	1,89	3,78	7,14	D	4	D 4
D5	Condition of hydraulic and pneumatic	2	5	1	1	2	1	1	3	2	4	2	3	2	2	2	4					1	3	2	2	2	4	2	4	2	3			2	5	2	5	2	5	5	3	1,94	3,28	6,37	D	3	D 3
D6	Condition of loading parameters and axle load	2	5	2	4	1	3	2	4	1	3	2	3	2	4	2	3	2	5			2	4	1	2	2	3	2	3	3	4	1	3	2	5	2	3	2	5	2	4	1,84	3,68	6,79	D	4	D 4
D7	Condition of the traction and traction control system	2	2	1	1	1	2	2	1	4	3	3	2	2	5	2	3					3	3	2	2	3	4	3	4	2	3	2	1	2	3	2	5	2	3	5	3	2,21	2,84	6,28	D	3	D 3
D8	Condition of the brake system and controls	2	3	1	1	1	1	1	5	1	3	2	4	2	4	2	5	2	3			2	4	2	2	3	4	3	4	3	3	3	2	2	5	2	4	2	5	3	4	2,05	3,47	7,13	D	3	D 3
D9	Driver cabin ergonomics	2	5	1	1	1	1	2	3	1	2	1	5	2	2	2	2	2	4			2	3	2	2	1	2	1	2	1	2	3	3	2	2	2	4	2	5	2	4	1,79	2,84	5,09	D	3	D 3
D10	Thermal hazards: flash, explosion, radiation	2	5	1	1	1	1	3	4	1	5	1	5	2	2	2	2	2	3			2	3	2	2	2	3	2	3	2	3	2	3	1	2	2	4	2	5	2	4	5	2	1,95	3,11	6,05	D	3	D 3
D11	Condition of warning equipment, lights and horns	2	5	1	1	1	3	4	1	5	3	2	2	2	2	3	2	2	2			1	2	2	3	4	2	4	2	4	3	3	1	2	5	2	5	2	5	4	4	2,11	3,32	6,98	D	3	D 3
E1	Suicide/hitting a person/hitting an animal	2	4	2	4	1	5	1	4	2	5	2	5	2	3	2	3	2	5			3	5	2	4	3	4	3	4	2	4	2	4	2	5	2	5	2	5	4	4	2,16	4,32	9,31	D	4	D 4
E2	Earthquake	3	5	2	4	1	1	1	5	1	5	2	4	2	5	3	5	2	4			1	5	1	4	2	3	2	3	2	3	2	3	2	4	2	3	2	3	5	5	2,00	3,89	7,79	D	4	D 4
E3	Flood	3	5	2	4	1	3	1	5	1	5	2	4	2	4	2	4	2	4			2	4	2	4	2	3	2	3	2	3	2	3	2	4	2	4	2	4	4	5	2,00	3,95	7,89	D	4	D 4
E4	Avalanche	3	5	2	4	1	1	1	5	1	5	2	2	2	4	2	4	2	4			1	5	2	4	2	3	2	3	2	3	2	4	1	5	1	5	1	2	2	5	1,68	3,89	6,56	D	4	D 4
E5	Landslide, rock fall on cleavage slope	3	5	2	4	1	1	1	5	1	5	2	2	2	4	2	4	2	4			2	4	2	4	2	3	2	3	2	5	2	4	1	5	1	5	1	2	5	5	1,89	3,89	7,38	D	4	D 4
E6	Lightening	3	5	1	1	1	4	1	5	1	5	2	2	2	3	2	3	1	3			1	4	2	4	2	4	2	3	2	2	2	5	2	5	2	5	2	5	4	4	1,89	3,58	6,78	D	4	D 4
E7	Wind/storm	1	5	1	1	1	1	4	2	1	5	2	2	2	3	2	4	2	4			1	4	1	1	2	4	2	4	2	3	1	1	2	4	2	3	2	4	5	3	1,89	3,05	5,78	D	3	D 3
E8	Train driver	2	5	2	4	1	4	3	4	2	4	1	5	2	5	3	5	2	4			3	4	2	5	2	3	2	3	2	5	2	3	2	5	2	5	2	3	5	5	2,21	4,26	9,42	D	4	D 4
E9	Movement officer/dispatcher	2	5	2	4	1	3	2	5	2	4	2	2	2	4	2	3	2	3			3	4			2	3	2	3	2	5	2	4	2	5	2	5	2	2	4	5	2,11	3,83	8,09	D	4	D 4
E10	Chemical, biological mechanical pollution/ track contamination	2	3	1	1	1	2	1	1	1	1	2	2	4	2	2	2					1	3			1	2	1	2	3	3	1	2	2	4	2	4	2	4	3	3	1,76	2,41	4,26	D	2	D 2

1- The scores of the participants are shown in the table.
2- Participants were not given any response restrictions and were asked to make evaluations based on their own areas of expertise, if possible.
3- Only example of the L-Matrix method is given here.
4- For the L matrix, the probability and severity scores are averaged among themselves and rounded to the nearest number or letter value. Risk importance weight is expressed as the numerical value multiplication of the averages.

APENDIX-2

Application of the criteria in group "D" according to the AHP technique: "Risk" example

	d1	d2	d3	d4	d5	c6	d7	d8	d9	d10	d11
d1	1,0000	0,5000	0,5000	1,0000	2,0000	1,0000	2,0000	1,0000	3,0000	3,0000	2,0000
d2	2,0000	1,0000	1,0000	1,0000	1,0000	1,0000	1,0000	1,0000	1,0000	1,0000	1,0000
d3	2,0000	1,0000	1,0000	1,0000	1,0000	1,0000	1,0000	1,0000	1,0000	1,0000	1,0000
d4	1,0000	1,0000	1,0000	1,0000	1,0000	1,0000	1,0000	1,0000	1,0000	1,0000	1,0000
d5	0,5000	1,0000	1,0000	1,0000	1,0000	0,5000	1,0000	0,5000	1,0000	1,0000	1,0000
d6	1,0000	1,0000	1,0000	1,0000	2,0000	1,0000	1,0000	1,0000	1,0000	1,0000	1,0000
d7	0,5000	1,0000	1,0000	1,0000	1,0000	1,0000	1,0000	0,5000	1,0000	1,0000	1,0000
d8	1,0000	1,0000	1,0000	1,0000	2,0000	1,0000	2,0000	1,0000	1,0000	1,0000	1,0000
d9	0,3333	1,0000	1,0000	1,0000	1,0000	1,0000	1,0000	1,0000	1,0000	1,0000	0,5000
d10	0,3333	1,0000	1,0000	1,0000	1,0000	1,0000	1,0000	1,0000	1,0000	1,0000	0,5000
d11	0,5000	1,0000	1,0000	1,0000	1,0000	1,0000	1,0000	1,0000	2,0000	2,0000	1,0000
Totally	10,1667	10,5000	10,5000	11,0000	14,0000	10,5000	13,0000	10,0000	14,0000	14,0000	11,0000

	d1	d2	d3	d4	d5	c6	d7	d8	d9	d10	d11	Criteria Weight (wi) (Equation 2)
d1	0,0984	0,0909	0,0909	0,0984	0,1111	0,0984	0,1111	0,0984	0,1071	0,1071	0,1111	0,1021
d2	0,1967	0,1818	0,1818	0,1967	0,1667	0,1967	0,1667	0,1967	0,1429	0,1429	0,1667	0,1760
d3	0,1967	0,1818	0,1818	0,1967	0,1667	0,1967	0,1667	0,1967	0,1429	0,1429	0,1667	0,1760
d4	0,0984	0,0909	0,0909	0,0984	0,1111	0,0984	0,1111	0,0984	0,1071	0,1071	0,1111	0,1021
d5	0,0492	0,0606	0,0606	0,0492	0,0556	0,0492	0,0556	0,0492	0,0714	0,0714	0,0556	0,0570
d6	0,0984	0,0909	0,0909	0,0984	0,1111	0,0984	0,1111	0,0984	0,1071	0,1071	0,1111	0,1021
d7	0,0492	0,0606	0,0606	0,0492	0,0556	0,0492	0,0556	0,0492	0,0714	0,0714	0,0556	0,0570
d8	0,0984	0,0909	0,0909	0,0984	0,1111	0,0984	0,1111	0,0984	0,1071	0,1071	0,1111	0,1021
d9	0,0328	0,0455	0,0455	0,0328	0,0278	0,0328	0,0278	0,0328	0,0357	0,0357	0,0278	0,0343
d10	0,0328	0,0455	0,0455	0,0328	0,0278	0,0328	0,0278	0,0328	0,0357	0,0357	0,0278	0,0343
d11	0,0492	0,0606	0,0606	0,0492	0,0556	0,0492	0,0556	0,0492	0,0714	0,0714	0,0556	0,0570

	d1	d2	d3	d4	d5	c6	d7	d8	d9	d10	d11	Totally (di) (Equation 3)
d1	0,1021	0,0880	0,0880	0,1021	0,1141	0,1021	0,1141	0,1021	0,1028	0,1028	0,1141	1,1321
d2	0,2042	0,1760	0,1760	0,2042	0,1711	0,2042	0,1711	0,2042	0,1370	0,1370	0,1711	1,9561
d3	0,2042	0,1760	0,1760	0,2042	0,1711	0,2042	0,1711	0,2042	0,1370	0,1370	0,1711	1,9561
d4	0,1021	0,0880	0,0880	0,1021	0,1141	0,1021	0,1141	0,1021	0,1028	0,1028	0,1141	1,1321
d5	0,0510	0,0587	0,0587	0,0510	0,0570	0,0510	0,0570	0,0510	0,0685	0,0685	0,0570	0,6297
d6	0,1021	0,0880	0,0880	0,1021	0,1141	0,1021	0,1141	0,1021	0,1028	0,1028	0,1141	1,1321
d7	0,0510	0,0587	0,0587	0,0510	0,0570	0,0510	0,0570	0,0510	0,0685	0,0685	0,0570	0,6297
d8	0,1021	0,0880	0,0880	0,1021	0,1141	0,1021	0,1141	0,1021	0,1028	0,1028	0,1141	1,1321
d9	0,0340	0,0440	0,0440	0,0340	0,0285	0,0340	0,0285	0,0340	0,0343	0,0343	0,0285	0,3782
d10	0,0340	0,0440	0,0440	0,0340	0,0285	0,0340	0,0285	0,0340	0,0343	0,0343	0,0285	0,3782
d11	0,0510	0,0587	0,0587	0,0510	0,0570	0,0510	0,0570	0,0510	0,0685	0,0685	0,0570	0,6297

	di	wi	di/wi	
d1	1,1321	0,1021	11,0906	$\lambda max=\frac{\sum_{i=1}^{n}\frac{di}{wi}}{n}$ (Equation 4)
d2	1,9561	0,1760	11,1129	λ =11,0713, n=11 (n=number of criteria)
d3	1,9561	0,1760	11,1129	
d4	1,1321	0,1021	11,0906	
d5	0,6297	0,0570	11,0386	Consistency Ratio (CR)=(λ-n)/((n-1)*RI) (Equation 5)
d6	1,1321	0,1021	11,0906	RI=1,51 for n=11 (Table 3)
d7	0,6297	0,0570	11,0386	CR=(11,0713-11)/(10*1,51)=0,0071<0,1
d8	1,1321	0,1021	11,0906	
d9	0,3782	0,0343	11,0401	
d10	0,3782	0,0343	11,0401	
d11	0,6297	0,0570	11,0386	

ESKİŞEHİR TEKNİK ÜNİVERSİTESİ BİLİM VE TEKNOLOJİ DERGİSİ
B- TEORİK BİLİMLER

Eskişehir Technical University Journal of Science and Technology B- Theoretical Sciences

Estuscience – Theory, 2025, 13 [1] pp. 67-76, DOI:10.20290/estubtdb.1632350

ON THE WEAK SUBDIFFERENTIAL, AUGMENTED NORMAL CONES AND DUALITY IN NONCONVEX OPTIMIZATION

Samet BILA [1,*], Refail KASIMBEYLI [2]

[1] Department of Mathematics, Faculty of Science, Eskisehir Technical University, Eskisehir, Turkiye
sametbila@eskisehir.edu.tr - 0000-0002-5228-643X

[2] Department of Industrial Engineering, Faculty of Engineering, Eskisehir Technical University, Eskisehir, Turkiye
rkasimbeyli@eskisehir.edu.tr - 000-0002-7339-9409

Abstract

This article studies the properties of the weak subdifferential for nonsmooth and nonconvex analysis studied. This study presents a formulation that is directly involved in convex analysis carried out in the nonconvex case. In this work, we present a theory that applies epigraphs to obtain augmented normal cones.

The perturbation function plays a crucial role in establishing optimality conditions. This study demonstrates that positively homogeneous and lower semicontinuous functions are weakly subdifferentiable. Moreover, under specific conditions related to the objective function, the constraint function, and the feasible set, we show that the perturbation function is positively homogeneous. Thus we obtain a zero duality gap condition by implementing conditions on the objective function, constraint functions, and the set S.

Keywords

Operations Research,
Nonconvex Optimization,
Weak Subdifferential,
Augmented Normal Cone

Time Scale of Article

Received :03 Februay 2025
Accepted : 18 Februay 2025
Online date : 28 February 2025

1. INTRODUCTION

The concept of subgradient marked the real beginning of the convex analysis in the way it is seen now. It is associated with a convex function and provides many useful properties of the derivative from an optimization perspective [3,10]. At boundary points, a convex set has a supporting hyperplane, which gives rise to the notion of the subdifferential, denoted by ∂f. This concept forms the foundation of convex analysis and was introduced by R.T. Rockafellar in his 1963 thesis [11] for convex functions. Later, F.H. Clarke, in his 1973 thesis [4], extended this definition to Lipschitz continuous functions by introducing the Clarke subdifferential $\partial_o f$. Indeed, there is a drawback to this subdifferential notion. The function must be convex to be able to use many nice consequences of this concept.

When dealing with nonconvex functions, $\boldsymbol{h}: \mathbb{R}^{\boldsymbol{n}} \to \mathbb{R}$ was addressed, the original definition of subgradients through the affine support inequality applicable to convex functions had to be replaced with an alternative approach.

Clarke introduced the use of distance functions d_C to get a new concept of normal cones to nonconvex set C. Then he applied this concept to epigraphs to obtain normal cones $(v, -1)$ whose v component could be interpreted as a subgradient. This innovation appeared in Clarke [5] and it sparked years of

*Corresponding Author: sametbila@eskisehir.edu.tr

efforts by many researchers to advance the idea in various areas and apply then to a range of topics, with one of the most notable one is to optimal control.

Another alternative approach to the subgradient concept to nonconvex functions, known as the weak subdifferential $\partial^w f$ was presented by R.N. Gasimov in his 1992 thesis [7]. The weak subdifferential generalizes the subdifferential concept from convex analysis to nonconvex functions. This concept is founded on the idea of using supporting cones for the epigraph of a given function, which serves as a substitute for the supporting hyperplanes typically used in convex analysis. The idea behind the supporting cones is extremely helpful for nonconvex separation theorems and investigating nonconvex optimality problems.

Azimov and Gasimov well established a necessary and sufficient condition in nonconvex optimization based on the zero duality gap property [1,8] by relating the definition of the weak subdifferential and the perturbation function. Some of the weak subdifferential properties are investigated in [2,9].

The zero duality gap condition defined by an augmented Lagrangian dual function is well studied in [10]. It has been applied to zero duality gap conditions for optimality and approaches for finding solutions in nonconvex mathematical programming.

Motivation:

The subgradient can be viewed as a special case of the normal cone when the set is the epigraph of a convex function. In this study, we have presented a theorem that establishes a connection between the augmented normal cone of the epigraph and the weak subdifferential. Our findings demonstrate the existence of this theorem within the framework of nonconvex analysis.

Furthermore, we derive a zero duality gap condition by imposing conditions on the objective function, constraint functions, and the set S.

2. PROPERTIES OF THE WEAK SUBGRADIENT AND AUGMENTED NORMAL CONE

In convex duality theory, the definitions of conjugate functions and subdifferentials are as follows:

Let $\boldsymbol{X}$ be a normed space and $\boldsymbol{X}^*$ be the topological dual of $\boldsymbol{X}$. Suppose that $\overline{\mathbb{R}} = \mathbb{R} \cup \{\pm\infty\}$. We will denote the norm of $\boldsymbol{X}$ by $\|\cdot\|$, the norm of $\boldsymbol{X}^*$ by $\|\cdot\|_*$, and the value of a linear functional $\boldsymbol{x}^* \in \boldsymbol{X}^*$ at a point $\boldsymbol{x} \in \boldsymbol{X}$ by $\boldsymbol{x}^*, \boldsymbol{x}\rangle$. Let $\boldsymbol{h}: \mathbb{R}^{\boldsymbol{n}} \to \overline{\mathbb{R}}$ be a given function.

Definition 1: (a) A function $\boldsymbol{h^w}: \boldsymbol{X} \times \boldsymbol{X}^* \times \mathbb{R}_+ \to \overline{\mathbb{R}}$ defined by

$$\boldsymbol{h^w(x_0, x^*, c)} = \sup_{\mathbf{x}\in\mathbf{X}} \{-\boldsymbol{c}\|\boldsymbol{x} - \boldsymbol{x_0}\| + \boldsymbol{c}\|\boldsymbol{x_0}\| + \langle \boldsymbol{x}, \boldsymbol{x}^*\rangle - \boldsymbol{h}(\boldsymbol{x})\}$$

is called the weak conjugate of $\boldsymbol{h}$.

(b) A function $\boldsymbol{h^{ww}}: \boldsymbol{X} \to \overline{\mathbb{R}}$ defined by

$$\boldsymbol{h^{ww}(x)} = \sup_{(\boldsymbol{x}^*, \boldsymbol{c}) \in \boldsymbol{X}^* \times \mathbb{R}_+} \{-\boldsymbol{c}\|\boldsymbol{x} - \boldsymbol{x_0}\| + \boldsymbol{c}\|\boldsymbol{x_0}\| + \langle \boldsymbol{x}, \boldsymbol{x}^*\rangle - \boldsymbol{h^w}(\boldsymbol{x_0}, \boldsymbol{x}^*, \boldsymbol{c})\}$$

is called the weak biconjugate of $\boldsymbol{h}$.

For $\boldsymbol{c = 0}$, $\boldsymbol{h^w(x_0, x^*, c) = h^*(x^*)}$, where $\boldsymbol{h^*}$ is the ordinary conjugate function in convex analysis.

Azimov and Gasimov introduced the following weak subdifferential notion, which is the generalization of the classic subdifferential from convex analysis [1].

Definition 2: A pair $(x^*, c) \in \mathbb{R}^n \times \mathbb{R}_+$ is referred to as a weak subgradient of h at x_0 on S provided that

$$\langle x^*, x - x_0\rangle - c\|x - x_0\| \leq h(x) - h(x_0) \text{ for all } x \in S \tag{1}$$

The set of all weak subgradients of h at $x_0$is referred to as the weak subdifferential of h at x_0 and is denoted as $\partial_S^w h(x)$:

$$\partial_S^w h(\bar{x})=\{(x^*, c) \in \mathbb{R}^n \times \mathbb{R}_+ : (1) \text{ is satisfied}\}.$$

If $\partial_S^w h(x_0) \neq \emptyset$, then h is called the weakly subdifferentiable at x_0. If we let $S = \mathbb{R}^n$ then we ignore the subscript S in $\partial_S^w f(x_0)$, and denote it by $\partial^w h(x_0) = \partial_{\mathbb{R}^n}^w h(x_0)$. It is obvious that if function h is subdifferentiable at x_0 then h is also weakly subdifferentiable at x_0 . One can check if $x^* \in \partial h(x_0)$ then by definition $(x^*, c) \in \mathbb{R}^n \times \mathbb{R}_+$ for every $c \geq 0$. The weak subgradient of a function h is geometrically interpreted as:
$(x^*, c) \in \mathbb{R}^n \times \mathbb{R}_+$ is a weak subgradient of h at $x \in X$ if one can found a function

$$f(x) = \langle x^*, x - x_0\rangle - c\|x - x_0\| + h(x_0)$$

which is a continuous, concave, and satisfies $h(x) \leq f(x), \forall x \in X$ and $h(x_0) = f(x_0)$. The hypograph of the function f is defined as hypo $(f) = \{(x, a) \in X \times \mathbb{R} \mid f(x) \geq a\}$ and it is a closed cone in $X \times \mathbb{R}$ with its vertex at $(x_0, f(x_0))$. To verify:

$$\begin{aligned}\text{hypo } (f) - \big(x_0, h(x_0)\big) &= \big\{\big(x - x_0, a - h(x_0)\big) \in X \times \mathbb{R} \mid \langle x^*, x - x_0\rangle - c\|x - x_0\| \geq a - h(x_0)\} \\ &= \{(u, b) \in X \times \mathbb{R} \mid \langle x^*, u\rangle - c\|u\| \geq b\}.\end{aligned}$$

Thus, from (2.1) and (2.2) that hypo (f) is a supporting cone of the set

$$epi(h) = \{(x, a) \in X \times \mathbb{R} \mid h(x) \leq a\}$$

at the point $(x_0, h(x_0))$ in the way that epi(h) $\subset (X \times \mathbb{R}) \setminus hypo(f)$ and $cl(epi(h)) \cap graph(f) \neq \emptyset$ where $graph\ (f) = \{(x, a) \in X \times \mathbb{R} \mid f(x) = a\}$.
Azimov and Gasimov obtained the weak subdifferential for subclasses of lower Lipschitz functions [1]. Lower Lipschitz function definition is given as follows:

Definition 3: A $g: X \to \mathbb{R}$ is said to be "lower locally Lipschitz" at $x_0 \in X$ if there exists a positive constant L and a neighborhood $\mathcal{N}(x_0)$ around x_0 such that

$$-L\|x - x_0\| \leq g(x) - g(x_0), \quad \forall x \in \mathcal{N}(x_0). \tag{2}$$

g is lower Lipschitz at x_0 with the Lipschitz constant L if the inequality (2) holds for all $x \in X$.
An example of the weak subdifferential is presented.
Example 4: Let $h: \mathbb{R} \to \mathbb{R}$ be given as

$$h(x) = \begin{cases} |x+2| & if\ x \le 0 \\ 4x+2 & if\ 0 < x \le 1 \\ 2|x-2|+4 & if\ x > 1 \end{cases}$$

The graph of function h is given below.

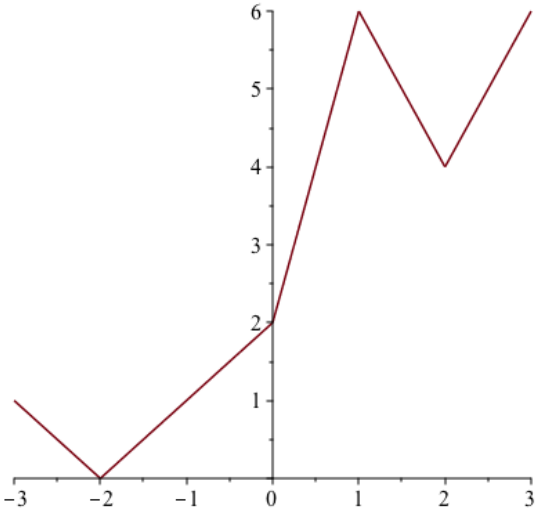

We want to calculate the weak subdifferentiable of h at $x_0 = 1$.

First, we consider the case $x < -2$. It follows from definition (2.1) that:

$$\langle y, x - x_0\rangle - c\|x - x_0\| \le h(x) - h(x_0)$$
$$\langle y, x - 1\rangle + c(x-1) \le -(x+2) - h(1)$$
$$y(x-1) + c(x-1) \le (-x-2) - 6$$
$$(x-1)(y+c) \le -x - 8$$

Then $\partial^w h(1)$ for the case $x < -2$ obtained as:

$$\partial^w h(1) = \{(y,c) \in \mathbb{R} \times \mathbb{R}_+ : y + c > 2\}$$

Then we consider the case $-2 \le x \le 0$. It follows from the definition (2.1),

$$\langle y, x - x_0\rangle - c\|x - x_0\| \le h(x) - h(x_0)$$
$$\langle y, x - 1\rangle + c(x-1) \le (x+2) - h(1)$$
$$y(x-1) - c(1-x) \le (x+2) - 6$$
$$(x-1)(w+c) \le x - 4$$

Then $\partial^w h(1)$ for the case $-2 \le x \le 0$ obtained as:

$$\partial^w h(1) = \{(y,c) \in \mathbb{R} \times \mathbb{R}_+ : y + c \ge 4\}$$

We consider the case $0 < x \le 1$. We have the following from the definition (2.1) that,

$$\langle y, x - x_0\rangle - c\|x - x_0\| \le h(x) - h(x_0)$$
$$\langle y, x - 1\rangle - c|x-1| \le h(x) - h(1)$$
$$y(x-1) - c(1-x) \le 4x + 2 - 6$$
$$(x-1)(y+c) \le 4(x-1)$$

Then $\partial^w h(1)$ for the case $0 < x \le 1$ obtained as:

$$\partial^w h(1) = \{(y,c) \in \mathbb{R} \times \mathbb{R}_+ : y + c \geq 4\}$$

Now we consider the case when $1 < x < 2$. It follows from the definition (2.1) that,

$$\langle y, x-1\rangle - c|x-1| \leq h(x) - h(1)$$
$$y(x-1) - c(x-1) \leq 2|x-2| + 4 - 6,$$
$$(y-c)(x-1) \leq -2(x-1),$$

$\partial^w h(1)$ for the case $1 < x < 2$ is obtained as:

$$\partial^w h(1) = \{(y,c) \in \mathbb{R} \times \mathbb{R}_+ : y - c \leq -2\}$$

The last case is when $x \geq 2$. Then we have,

$$\langle y, x-1\rangle - c|x-1| \leq h(x) - h(1)$$
$$y(x-1) - c(x-1) \leq 2|x-2| + 4 - 6,$$
$$(y-c)(x-1) \leq 2(x-3),$$

$\partial^w h(1)$ for the case $x \geq 2$ is obtained as:

$$\partial^w h(1) = \{(y,c) \in \mathbb{R} \times \mathbb{R}_+ : y - c \leq -2\}$$

Then finally we obtained that

$$\partial^w h(1) = \{(y,c) \in \mathbb{R} \times \mathbb{R}_+ : 4 - c \leq y \leq c - 2\}$$

We give the normal cone and augmented normal cone definitions below. The augmented normal cone notion is introduced to the literature by Kasimbeyli and Mammadov and it is quite helpful for obtaining the optimality condition in nonconvex optimization [8].

Definition 5: Let $A \subseteq \mathbb{R}^n$ and $x_0 \in S$. The normal cone to A at x_0 defined as

$$N_A(x_0) = \{v \in \mathbb{R}^n : \langle v, x - x_0\rangle \leq 0 \text{ for all } x \in A\}.$$

It is clear that if $x_0 \in int(S)$ then the set $N_A(x_0)$ consists of a single element, that is the zero element $0 \in \mathbb{R}^n$. Such a normal cone is called trivial. If $x_0 \notin int\, S$ and S is convex then normal cone is called nontrivial, the zero of $\mathbb{R}^n$ may be the only element in this cone. A normal cone is called nontrivial if it contains non-zero elements.

Definition 6:
Let $x_0 \in A$ and $A\backslash\{x_0\} \neq \emptyset$. The augmented normal cone to A at x_0 is defined as:

$$N_A^a(x_0) = \{(v,c) \in \mathbb{R}^n \times \mathbb{R} : \langle v, x - x_0\rangle - c\|x - x_0\| \leq 0 \text{ for all } x \in A\}. \quad (3)$$

Below, we recall definition of the augmented normal cone (for nonconvex sets) earlier introduced in (3). Here we will use a slightly different but an equivalent formulation (in the definition we use $\langle v, x - x_0\rangle + c\|x - x_0\|$ instead of $\langle v, x - x_0\rangle + c\|x - x_0\|$).

Since, for pairs (v,c) with $\|v\| \leq c$, the inequality $\{(v,c) \in \mathbb{R}^n \times \mathbb{R} : \langle v, x - x_0\rangle - c\|x - x_0\| \leq 0$ is obviously satisfied for all x$\in \mathbb{R}^n$, an augmented normal cone consisting of only such elements is called trivial. The trivial augmented normal cone will be denoted by $N_A^{triv}(x_0)$ and defined as

$$N_A^a(x_0) = \{(v,c) \in \mathbb{R}^n \times \mathbb{R} : \|v\| \leq c\}$$

Remark 7: It follows from the definition of normal and augmented normal cone that, for a given set $A \subset \mathbb{R}^n$, if the normal cone $N_A(x_0)$ is not empty, then for the pair $v \in N_A(x_0)$ with $c \geq 0$ belongs to the augmented normal cone $N_A^a(x_0)$. Conversely, if $(v, c) \in N_A^a(x_0)$ with $c \leq 0$, then $v \in N_A(x_0)$. Therefore, we will use the following definition for the augmented normal cone in this paper:

$$N_A^a(x_0) = \{(v, c) \in \mathbb{R}^n \times \mathbb{R}: c \leq \|v\|,\ \langle v, x - x_0\rangle - c\|x - x_0\| \leq 0 \text{ for all } x \in A\}.$$

The following lemma was proved in [8, Lemma 4].

Lemma 8: If $x_0 \in int\ A$ then $N_A^a(x_0) = N_A^{triv}(x_0)$

Now we will establish a relationship between the augmented normal cone to the epigraph of a given function f at some point $(x_0, f(x_0))$ and the weak subdifferential of f at x_0.

Let $f: \mathbb{R}^n \to \mathbb{R}$ be a given function. The epigraph *epi*(f) of f is defined as follows:

$$epi(f) = \{(x, a) \in \mathbb{R}^n \times \mathbb{R}: f(x) \leq a\}.$$

Then the augmented normal cone to the set $epi(f) \in \mathbb{R}^n \times \mathbb{R}$ at the point $(x_0, f(x_0))$ can be rewritten as follows:

$$N_{epi(f)}^a\big(x_0, \mathrm{f}(x_0)\big) = \big\{\big((v, \beta), c\big) \in (\mathbb{R}^n \times \mathbb{R}) \times \mathbb{R}_+ :$$
$$\langle v, x - x_0\rangle + \beta\big(a - f(x_0)\big) - c\|(x - x_0), (a - f(x_0))\| \leq 0 \text{ for all } (x, a) \in epi(f).$$

where the set $\|(x - x_0), (a - f(x_0))\|_{\mathbb{R}^n \times \mathbb{R}} = \|x - x_0\|_{\mathbb{R}^n} + |a - f(x_0)|_{\mathbb{R}}$. Obviously, such a setting satisfies the definition of the norm, such that:

- $\|(x, a)\| = \|x\| + |\alpha| \geq 0$ for all $(x, a) \in \mathbb{R}^n \times \mathbb{R}$ and obviously $\|(x, a)\| = 0$ if and only if $(x, a) = (0_{\mathbb{R}^n}, 0)$;
- $\|\lambda(x, a)\| = \|(\lambda x, \lambda a)\| = \|\lambda x\| + |\lambda a| = |\lambda|(\|x\| + |a|) = |\lambda|\|(x, a)\|$ for all $(x, a) \in \mathbb{R}^n \times \mathbb{R}$ and $\lambda \in \mathbb{R}$;
- $\|(x_1, a_1) + (x_2, a_2)\| = \|(x_1, x_2) + (a_1 + a_2)\| = \|(x_1, x_2)\| + |a_1 + a_2| \leq \|x_1\| + \|x_2\| + |a_1| + |a_2|$=$\|(x_1, a_1)\| + \|(x_2, a_2)\|$ for all $(x_1, a_1) \in \mathbb{R}^n \times \mathbb{R}$ and $(x_2, a_2 \in \mathbb{R}^n \times \mathbb{R}$.

3. DUALITY IN NONCONVEX OPTIMIZATION

Suppose that *X* and *Y* are normed spaces and assume that X^* and Y^* are their dual spaces, respectively.

Taking the function $\boldsymbol{h}: \boldsymbol{X} \to \overline{\mathbb{R}}$ into account we consider a nonlinear problem in the following form:

$$(P) \quad \{\inf_{x \in X} \boldsymbol{f}(\boldsymbol{x}).$$

The problem *(P)* is referred to as the primal problem. Its infimum is denoted by *inf (P)*, and any $\boldsymbol{x} \in \boldsymbol{X}$ that satisfies $\boldsymbol{f}(\boldsymbol{x}) = \boldsymbol{inf}(\boldsymbol{P})$ is called an optimal solution of *(P)*. Problem *(P)* is considered nontrivial if there exists $\boldsymbol{x} \in \boldsymbol{X}$ such that $\boldsymbol{f}(\boldsymbol{x}) < +\infty$. .

$$\boldsymbol{X} = \{\boldsymbol{x} \in \boldsymbol{S}: \boldsymbol{g_j}(\boldsymbol{x}) \leq \boldsymbol{0}, \boldsymbol{j} = \boldsymbol{1}, \dots, \boldsymbol{m}\} \neq \emptyset.$$

For the problem (P) the associated dualizing parameterization function

$$\boldsymbol{\phi}(\boldsymbol{x}, \boldsymbol{y}) = \begin{cases} \boldsymbol{f}(\boldsymbol{x}) & \boldsymbol{if\ x \in S\ and\ g_j}(\boldsymbol{x}) \leq \boldsymbol{0}, \quad \boldsymbol{j} = \boldsymbol{1}, \dots, \boldsymbol{m}, \\ +\infty & \boldsymbol{otherwise}. \end{cases}$$

The function $\boldsymbol{\phi}: \boldsymbol{X} \times \boldsymbol{Y} \to \mathbb{R} \cup \{+\infty\}$ defined above satisfies that $\boldsymbol{\phi}(\boldsymbol{x}, \boldsymbol{0}) = \boldsymbol{f}(\boldsymbol{x})$. It is easy to check

$$\boldsymbol{inf}_{\boldsymbol{x}\in\boldsymbol{X}}\boldsymbol{\phi}(\boldsymbol{x}, \boldsymbol{0}) = \boldsymbol{inf}\ (\boldsymbol{P}).$$

Utilizing the classical method for constructing the dual of a minimization problem [6, 10] we can now define the corresponding dual problem. To formulate the dual problem based on the function $\boldsymbol{\phi}$, the weak conjugate function $\boldsymbol{\phi^w}$ must be calculated. By definition 2.1, the weak conjugate function $\boldsymbol{\phi^w}$ is from $(\boldsymbol{X}^* \times \mathbb{R}_+ \times \boldsymbol{X}) \times (\boldsymbol{Y}^* \times \mathbb{R}_+ \times \boldsymbol{Y})$ into $\overline{\mathbb{R}}$ and is given by the following definition:

$$\boldsymbol{\phi^w}((\boldsymbol{x}^*, \boldsymbol{c}, \boldsymbol{x_0}), (\boldsymbol{y}^*, \boldsymbol{\alpha}, \boldsymbol{y_0})) = \underset{(\boldsymbol{x},\boldsymbol{y})\in\boldsymbol{X}\times\boldsymbol{Y}}{\boldsymbol{sup}} \begin{cases} -\boldsymbol{c}\|\boldsymbol{x} - \boldsymbol{x_0}\| + \boldsymbol{c}\|\boldsymbol{x_0}\| + \langle \boldsymbol{x}^*, \boldsymbol{x}\rangle \\ -\boldsymbol{\alpha}\|\boldsymbol{y} - \boldsymbol{y_0}\| + \boldsymbol{\alpha}\|\boldsymbol{y_0}\| + \langle\ \boldsymbol{y}^*, \boldsymbol{y}\rangle - \boldsymbol{\phi}(\boldsymbol{x}, \boldsymbol{y})\} \end{cases}$$

is referred to as the dual problem of $(\boldsymbol{P})$ based on the dualizing parameterization $\boldsymbol{\phi}$.

When $(\boldsymbol{x}^*, \boldsymbol{c}) = (\boldsymbol{0}, \boldsymbol{0}), \boldsymbol{x_0} = \boldsymbol{0}, \boldsymbol{y_0} = \boldsymbol{0}$, the value of $\boldsymbol{\phi^w}$ will be referred to simply as:

$$\boldsymbol{\phi^w}(\boldsymbol{0}, \boldsymbol{y}^*, \boldsymbol{\alpha}) = \underset{(\boldsymbol{x},\boldsymbol{y})\in\boldsymbol{X}\times\boldsymbol{Y}}{\boldsymbol{sup}} \{-\boldsymbol{\alpha}\|\boldsymbol{y}\| + \langle \boldsymbol{y}, \boldsymbol{y}^*\rangle - \boldsymbol{\phi}(\boldsymbol{x}, \boldsymbol{y})\}$$

$$(\boldsymbol{P^w}) \qquad \underset{(\boldsymbol{y}^*,\boldsymbol{\alpha})\in\boldsymbol{Y}^*\times\mathbb{R}_+}{\boldsymbol{sup}} \{-\boldsymbol{\phi^w}(\boldsymbol{0}, \boldsymbol{y}^*, \boldsymbol{\alpha})\}$$

The supremum of problem $\boldsymbol{(P^w)}$ is represented by *sup* $\boldsymbol{(P^w)}$. Any element $(\boldsymbol{y}^*, \boldsymbol{\alpha}) \in \boldsymbol{Y}^* \times \mathbb{R}_+$ that satisfies $\boldsymbol{\phi^w}(\boldsymbol{0}, \boldsymbol{y}^*, \boldsymbol{\alpha})$= *sup* $\boldsymbol{(P^w)}$ is referred to as an optimal solution of $\boldsymbol{(P^w)}$.

Assume that $\boldsymbol{h}$ is a function from $\boldsymbol{Y}$ into $\overline{\mathbb{R}}$. We define the perturbation function associated with problem *(P)* as follows:

$$\boldsymbol{h}(\boldsymbol{y}) = \boldsymbol{inf}_{\boldsymbol{x}\in\boldsymbol{X}}\boldsymbol{\phi}(\boldsymbol{x}, \boldsymbol{y})$$

The perturbation function definition implies that

$$\boldsymbol{h}(\boldsymbol{y}) = \boldsymbol{inf}\ (\boldsymbol{P}).$$

The theorem below provides conditions for strong duality, based on the properties of the perturbation function $\boldsymbol{h}$.

Theorem 9: [1, Lemma 4.2] (i) $\boldsymbol{h^w}(\boldsymbol{y}^*, \boldsymbol{\alpha}, \boldsymbol{0}) = \boldsymbol{\phi^w}(\boldsymbol{0}, \boldsymbol{y}^*, \boldsymbol{\alpha})$;

(ii) $\boldsymbol{sup}(\boldsymbol{P^w}) = \boldsymbol{h^{ww}}$;

(iii) Suppose the perturbation function $\boldsymbol{h}$, defined by (10), is proper and weakly subdifferentiable at $\boldsymbol{0} \in \boldsymbol{Y}$. Then $\boldsymbol{inf}(\boldsymbol{P}) = \boldsymbol{sup}\ (\boldsymbol{P^w})$, and any weak subgradient of $\boldsymbol{h}$ at $\boldsymbol{0} \in \boldsymbol{Y}$ is an optimal solution of $(\boldsymbol{P^w})$.

Theorem 10: [10, Theorem 2.7] Let $\boldsymbol{h}$ be bounded from below on some neighborhood of zero and positively homogeneous function from $\boldsymbol{X}$ into $\mathbb{R}$. Then $\boldsymbol{h}$ is weakly subdifferentiable at $\boldsymbol{0_X}$.

In the following theorem, we show that if the objective and constraint functions defined on the conic set are positively homogeneous then the perturbation function is also positively homogeneous.

Theorem 11: Assume that $\boldsymbol{S}$ is a cone in $\mathbb{R}^{\boldsymbol{n}}$. Let $\boldsymbol{f}: \boldsymbol{S} \to \mathbb{R}$ be positively homogeneous and the mappings $\boldsymbol{g} = (\boldsymbol{g_1}, \boldsymbol{g_2}, \dots, \boldsymbol{g_m}): \boldsymbol{S} \to \mathbb{R}$ are positively homogeneous. Then the perturbation function $\boldsymbol{h}(\boldsymbol{y})$ is positively homogeneous.

Proof: We must show that $\boldsymbol{h}(\boldsymbol{\lambda y}) = \boldsymbol{\lambda h}(\boldsymbol{y})$. Now the definition of the perturbation function implies that:

$$\boldsymbol{h}(\boldsymbol{\lambda y}) = \boldsymbol{f}(\boldsymbol{x}) \text{ if } \boldsymbol{x} \in \boldsymbol{S \; and} \; \boldsymbol{g_j}(\boldsymbol{x}) \leq \boldsymbol{\lambda y}, \boldsymbol{j} = \boldsymbol{1}, \dots, \boldsymbol{m}.$$

Since $\boldsymbol{g_j's}$ are positively homogeneous we have that

$$\boldsymbol{h}(\boldsymbol{\lambda y}) = \boldsymbol{f}(\boldsymbol{x}) \text{ if } \boldsymbol{x} \in \boldsymbol{S \; and} \; \boldsymbol{g_j}\left(\frac{\boldsymbol{1}}{\boldsymbol{\lambda}}\boldsymbol{x}\right) = \frac{\boldsymbol{1}}{\boldsymbol{\lambda}}\boldsymbol{g_j}(\boldsymbol{x}) \leq \boldsymbol{y}, \boldsymbol{j} = \boldsymbol{1}, \dots, \boldsymbol{m}.$$

Now if we denote $\frac{\boldsymbol{1}}{\boldsymbol{\lambda}}\boldsymbol{x} = \boldsymbol{z}$ then we obtain:

$$\boldsymbol{h}(\boldsymbol{\lambda y}) = \boldsymbol{f}(\boldsymbol{\lambda z}) \text{ if } \boldsymbol{\lambda z} \in \boldsymbol{S \; and} \; \boldsymbol{g_j}(\boldsymbol{z}) \leq \boldsymbol{y}, \boldsymbol{j} = \boldsymbol{1}, \dots, \boldsymbol{m}.$$

By the assumption that $\boldsymbol{f}$ is positively homogeneous and $\boldsymbol{S}$ is a cone, then it yields that:

$$\boldsymbol{h}(\boldsymbol{\lambda y}) = \boldsymbol{\lambda f}(\boldsymbol{z}) \text{ if } \boldsymbol{z} \in \boldsymbol{S \; and} \; \boldsymbol{g_j}(\boldsymbol{z}) \leq \boldsymbol{y}, \boldsymbol{j} = \boldsymbol{1}, \dots, \boldsymbol{m}.$$

Hence

$$\boldsymbol{h}(\boldsymbol{\lambda y}) = \boldsymbol{\lambda h}(\boldsymbol{y}).$$

The proof is completed.

Based on the results of Theorem 9, Theorem 10 and Theorem 11 the following theorem can be stated.

Theorem 12: Assume that S is a cone in $\mathbb{R}^n$. Let $f: S \to \mathbb{R}$ be positively homogeneous and lower semicontinuous and the mappings $g = (g_1, g_2, \dots, g_m): S \to \mathbb{R}$ are positively homogeneous and lower semicontinuous. Then the zero duality gap satisfies.

Proof. If S is a cone in $\mathbb{R}^n$, the functions $f: S \to \mathbb{R}$ and $g = (g_1, g_2, \dots, g_m): S \to \mathbb{R}$ are positively homogeneous and lower semicontinuos then by Theorem 9 we know that the perturbation function h is positively homogeneous. Also, under the condition of lower semicontinuity of f and g, h is also lower semicontinuous. Thus, from Theorem 10 we obtain that h is weakly subdifferentiable at $\mathbf{0}$. Finally, Theorem 9 implies that the zero duality gap is satisfied. The proof is completed.

In convex analysis, the following proposition is well known that relates to normal cone and subdifferential.

Proposition 13: Let h be convex, proper function then

$$\partial f(\bar{x}) = \left\{v \in \mathbb{R}^n : (v, -1) \in N\left(\left(\bar{x}, f(\bar{x})\right), epi\, f\right)\right\}.$$

Theorem 14: Assume that $\boldsymbol{f}: \mathbb{R}^{\boldsymbol{n}} \to \mathbb{R}$ is a proper function.

i) If $\boldsymbol{f}$ is weakly subdifferentiable function at $\bar{\boldsymbol{x}} \in \mathbb{R}^{\boldsymbol{n}}$ and $(\boldsymbol{v}, \boldsymbol{c}) \in \boldsymbol{\partial^w f}(\bar{\boldsymbol{x}})$ then $((\boldsymbol{v}, -\boldsymbol{1}), \boldsymbol{c}) \in \boldsymbol{N^a_{epi(f)}}(\bar{\boldsymbol{x}}, \mathbf{f}(\bar{\boldsymbol{x}}))$.

ii) If $\boldsymbol{f}$ is Lipschitz function at $\overline{\boldsymbol{x}} \in \mathbb{R}^{\boldsymbol{n}}$ with Lipschitz constant $\boldsymbol{L}$ and $((\boldsymbol{v}, -\mathbf{1}), \boldsymbol{c}) \in \boldsymbol{N}^{\boldsymbol{a}}_{\boldsymbol{epi(f)}}(\overline{\boldsymbol{x}}, \mathbf{f}(\overline{\boldsymbol{x}}))$ with $\boldsymbol{c} \geq \mathbf{0}$ then $\boldsymbol{f}$ is weakly subdifferentiable function at $\overline{\boldsymbol{x}} \in \mathbb{R}^{\boldsymbol{n}}$ and $(\boldsymbol{v}, \boldsymbol{c} + \boldsymbol{cL}) \in \ \boldsymbol{\partial^w f}(\overline{\boldsymbol{x}})$.

Proof. (i)
Assume that $\boldsymbol{f}$ is Lipschitz at $\overline{\boldsymbol{x}} \in \mathbb{R}^{\boldsymbol{n}}$. Then clearly $\boldsymbol{f}$ is lower Lipschitz and hence weakly subdifferentiable at $\overline{\boldsymbol{x}} \in \mathbb{R}^{\boldsymbol{n}}$. Let $(\boldsymbol{v}, \boldsymbol{c}) \in \ \boldsymbol{\partial^w f}(\overline{\boldsymbol{x}})$. Then by definition of the weak subdifferential, we have:

$$f(x) - \mathrm{f}(\bar{x}) \geq \langle v, x - \bar{x} \rangle - c\|x - \bar{x}\| \ \text{ for all } x \in \mathbb{R}^{\boldsymbol{n}}.$$

Hence

$$\alpha - \mathrm{f}(\bar{x}) \geq \langle v, x - \bar{x} \rangle - c\|x - \bar{x}\| - c|\alpha - \mathrm{f}(\bar{x})| \ \text{ for all } (x, a) \in epi\ (f).$$

This can be written in the form:

$$\langle v, x - \bar{x} \rangle + (-1)(\alpha - \mathrm{f}(\bar{x})) - c\|(x - \bar{x}), (\alpha - \mathrm{f}(\bar{x}))\| \ \text{ for all } (x, a) \in epi\ (f).$$

which implies that $((\boldsymbol{v}, -\mathbf{1}), \boldsymbol{c}) \in \ \boldsymbol{N}^{\boldsymbol{a}}_{\boldsymbol{epi(f)}}(\overline{\boldsymbol{x}}, \mathbf{f}(\overline{\boldsymbol{x}}))$.

(ii) Now assume that $((\boldsymbol{v}, -\mathbf{1}), \boldsymbol{c}) \in \ \boldsymbol{N}^{\boldsymbol{a}}_{\boldsymbol{epi(f)}}(\overline{\boldsymbol{x}}, \mathbf{f}(\overline{\boldsymbol{x}}))$. This means that

$$\langle \boldsymbol{v}, \boldsymbol{x} - \overline{\boldsymbol{x}} \rangle + (-\mathbf{1})(\boldsymbol{\alpha} - \mathbf{f}(\overline{\boldsymbol{x}})) - \boldsymbol{c}\|(\boldsymbol{x} - \overline{\boldsymbol{x}}), (\boldsymbol{\alpha} - \mathbf{f}(\overline{\boldsymbol{x}}))\| \ \text{ for all } (\boldsymbol{x}, \boldsymbol{a}) \in \boldsymbol{epi}\ (\boldsymbol{f}). \tag{4}$$

Now by letting $\boldsymbol{\alpha} = \boldsymbol{f}(\boldsymbol{x})$ we obtain:

$$\langle \boldsymbol{v}, \boldsymbol{x} - \overline{\boldsymbol{x}} \rangle + (-\mathbf{1})(\boldsymbol{f}(\boldsymbol{x}) - \mathbf{f}(\overline{\boldsymbol{x}})) - \boldsymbol{c}\|(\boldsymbol{x} - \overline{\boldsymbol{x}}), (\boldsymbol{f}(\boldsymbol{x}) - \mathbf{f}(\overline{\boldsymbol{x}}))\| \ \text{ for all } \boldsymbol{x} \in \mathbb{R}^{\boldsymbol{n}}.$$

By the hypothesis, $\boldsymbol{f}$ is Lipschitz function at $\overline{\boldsymbol{x}}$ with Lipschitz constant $\boldsymbol{L}$. Hence,

$$\boldsymbol{f}(\boldsymbol{x}) - \mathbf{f}(\overline{\boldsymbol{x}}) \leq \boldsymbol{L}\|\boldsymbol{x} - \overline{\boldsymbol{x}}\| \text{ for all } \boldsymbol{x} \in \mathbb{R}^{\boldsymbol{n}}$$

Then it follows from (4) that

$$\boldsymbol{f}(\boldsymbol{x}) - \mathbf{f}(\overline{\boldsymbol{x}}) \geq \langle \boldsymbol{v}, \boldsymbol{x} - \overline{\boldsymbol{x}} \rangle - (\boldsymbol{c} + \boldsymbol{cL})\|\boldsymbol{x} - \overline{\boldsymbol{x}}\| \ \text{ for all } \boldsymbol{x} \in \mathbb{R}^{\boldsymbol{n}}.$$

which shows that the proof is completed.

4. CONCLUSION

In this work, we have presented a theorem relates the augmented normal cone when the set is epigraph and the weak subdifferential. We showed the existence of such a theorem in the nonconvex analysis. We additionally obtain a zero duality gap condition by imposing conditions on the objective function, constraint functions and the set S.

CONFLICT OF INTEREST

The authors stated that there are no conflicts of interest regarding the publication of this article.

CRediT AUTHOR STATEMENT

Samet Bila: Formal analysis, Writing - original draft, Investigation, Conceptualization.
Refail Kasımbeyli: Conceptualization, Visualization, Supervision.

REFERENCES

[1] Azimov AY, Gasimov RN. On weak conjugacy, weak subdifferentials and duality with zero gap in nonconvex optimization, International Journal of Applied Mathematics, 1, 1999, pp. 171–192.

[2] Bila S, Kasimbeyli R. On the some sum rule for the weak subdifferential and some properties of augmented normal cones, Journal of Nonlinear and Convex Analysis, 24(10), 2023, pp. 2239–2257.

[3] Borwein JM, Lewis AS. Convex Analysis and Nonlinear Optimization, CMS Books in Mathematics, Springer Science+Business Media, Inc., New York, 2006.

[4] Clarke FH. Necessary conditions for nonsmooth problems in optimal control and the calculus of variations, Thesis, University of Washington, Seattle, 1973.

[5] Clarke FH. Generalized gradients and applications, Trans. Amer. Math. Soc., 205, pp. 247–262, 1975.

[6] Ekeland I, Temam R. Convex Analysis and Variational Problems, Elsevier, 1976.

[7] Gasimov RN. Duality in nonconvex optimization, Ph.D. Dissertation, Department of Operations Research and Mathematical Modeling, Baku State University, Baku, 1992.

[8] Gasimov RN. Augmented Lagrangian duality and nondifferentiable optimization methods in nonconvex programming, J. Global Optimization, 24, 2002, pp. 187–203.

[9] Kasimbeyli R, Mammadov M. Optimality conditions in nonconvex opti-mization via weak subdifferentials, Nonlinear Analysis: Theory, Methods and Applications, 74, 2011, pp. 2534–2547.

[10] Rockafellar RT. Convex analysis, Princeton University Press, Princeton, 1970.

[11] Rockafeller RT. Convex analysis and dual extremum problems. Thesis, Harvard, 1963.